Supplementary Information

Discovery of the first genome-wide significant risk loci for ADHD

Table of Contents

Supplementary Methods and Results

Detailed description of individual Samples

A brief overview of the included samples can be found in Supplementary Table 1.

iPSYCH, Denmark

Since 1981 dried blood spot samples (Guthrie cards) from all newborn babies in Denmark have been stored in the Danish Newborn Screening Biobank (DNSB) at Statens Serum Institute (SSI). Samples from this nationwide biobank can be linked with the comprehensive Danish register system through the unique personal identification number (CPR-number), which is assigned to all live-born babies in Denmark. The CPR-number is stored in the Danish Civil Registration System (DCRS)[1] and is used in all contacts with the public sector, including all hospital contacts.

The iPSYCH-ADHD sample is a nationwide population based case-cohort sample selected from a baseline birth cohort comprising all singletons born in Denmark between May 1, 1981, and December 31, 2005, who were residents in Denmark on their first birthday and who have a known mother (N = 1,472,762). Cases were diagnosed by psychiatrists at psychiatric hospitals (in- or out-patient clinics) according to ICD10 (F90.0), identified using the Danish Psychiatric Central Research Register[2] (DPCRR). The DPCRR includes data on all people admitted to a psychiatric hospital for assessment, treatment, or both in Denmark since 1969 as well as people who attended psychiatric outpatient services since 1995. Diagnoses were given in 2013 or earlier for individuals at least 1 year old. Individuals with a diagnosis of moderate to severe mental retardation (ICD10 code F71-F79) were excluded. Controls were randomly selected from the same nationwide birth cohort and not diagnosed with ADHD (F90.0) or moderate-severe mental retardation (F71-F79).

DNA was extracted from dried blood spot samples and whole genome amplified in triplicates as described previously[3,4]. Genotyping was performed at the Broad Institute of Harvard and MIT

(Cambridge, MA, USA) using Illumina's Beadarrays (PsychChip; Illumina, CA, San Diego, USA) according to the manufacturer's protocols. Genotypes were a result of merging callsets from three different calling algorithms (GenCall, Birdseed and Zcall). GenCall[5] and Birdseed[6] was used to call genotypes with minor allele frequency (MAF) > 0.01 and zCall[7] was used to call genotypes with MAF < 0.01. The merging was done after pre-QC on individual call sets.

Processing of DNA, genotyping and genotype calling as well as imputing of genotypes of the iPSYCH-ADHD sample were carried out as a part of the genotyping of the full iPSYCH sample, which in total consists of around 79,492 individuals, including around 54,249 cases diagnosed with at least one of six mental disorders (schizophrenia, bipolar disorder, depression, ADHD, anorexia or autism spectrum disorder) and 26,248 randomly selected population controls (25,243 did not have any of the six psychiatric disorders investigated in iPSYCH). For the study of ADHD individuals with an ADHD diagnosis were exclude among the controls (N = 413). The data processing was done in 23 waves of approximately 3,500 individuals each. In order to control for potential batch effects we included "wave" as a covariate in the regression models of all downstream analyses when relevant. Following genotyping all data processing, quality control, and downstream analyses were performed at secured servers in Denmark at the GenomeDK high performance-computing cluster (http://genome.au.dk). Overview of number samples in the iPSYCH study in the various steps, from identification in the registers to high quality genotypes included in the meta-analysis, can be found in Supplementary Figure 1.

The study was approved by the Danish Data Protection Agency and the Scientific Ethics Committee in Denmark.

Samples from the Psychiatric Genomics Consortium (PGC)

Parent-offspring trio samples

CHOP, USA

The CHOP (Children's Hospital of Philadelphia) ADHD trio sample (2,064 trios) were recruited from pediatric and behavioral health clinics in the Philadelphia area[8] and included children aged 6–18 years from families of European with an ADHD diagnosis following the K-SADS (Schedule for Affective Disorders and Schizophrenia for School-Age Children; Epidemiologic Version) interview. Exclusion criteria were prematurity (<36 weeks), intellectual disability, major medical and neurological disorders, pervasive developmental disorder, psychoses and major mood disorders. Participants were assayed on the Illumina Infinium II HumanHap550 BeadChip (Illumina, San Diego, CA, USA) as previously described. The study was approved by The Children's Hospital of Philadelphia Institutional Review Board.

IMAGE-I, Europe

The IMAGE-I (International Multisite ADHD Genetics Project) trio samples[9,10] were collected using a common protocol with centralized training and reliability testing of raters and centralized data management. Family members were Caucasians of European origin from countries in and around Europe including Belgium, Germany, Ireland, the Netherlands, Spain, Switzerland, and the United Kingdom, and Israel. At the IMAGE sites, parents of children were interviewed with the Parental Account of Childhood Symptom (PACS), a semi-structured, standardized, investigator-based interview developed as an instrument to provide an objective measure of child behavior. Both parents and teachers completed the respective versions of the Conners ADHD rating scales and the Strengths and Difficulties Questionnaire (SDQ). Exclusion criteria were autism, epilepsy, IQ<70, brain disorders and any genetic or medical disorder associated with externalizing behaviors that might

mimic ADHD. Genotyping was conducted at Perlegen Sciences using their 600K genotyping platform, comprising approximately 600,000 tagging SNPs designed to be in high linkage disequilibrium with untyped SNPs for the three HapMap populations. The study was approved by the Institutional Review Board (IRB) or Ethical Committee at each site.

PUWMa, USA

The PUWMa (Pfizer-funded study from the University of California, Los Angeles (UCLA), Washington University, and Massachusetts General Hospital (MGH)) trio samples[11] were collected independently at those three sites using similar but slightly different methods.

309 families were recruited from clinics at MGH with children aged 6-17 years. Psychiatric assessments were made with the K-SADS-E. Exclusion criteria were major sensorimotor handicaps (deafness, blindness), psychosis/schizophrenia, autism, inadequate command of the English language, or a Full Scale IQ<80.

At Washington University, 272 families were selected from a population-representative sample identified through birth records of the state of Missouri, for a genetic epidemiologic study of the prevalence and heritability of ADHD. The original sample included 812 complete male and female twin pairs and six individual twins aged 7 to 19 years at the time of interview, identified from the Missouri Family Registry from 1996 to 2002. Families were invited into the study if at least one child exhibited three or more inattentive symptoms on a brief screening interview. Parents reported on their children and themselves, and the youths on themselves, using the Missouri Assessment of Genetics Interview for Children (MAGIC), a semi-structured psychiatric interview. DSM-IV diagnoses of ADHD were based upon parental reports (most of the time, maternal). Exclusion criteria were parent/guardian reported intellectual disability or if the parent/guardian and twins could not speak English.

At UCLA, 156 subjects were drawn from 540 children and adolescents aged 5 to 18 years and 519 of their parents ascertained from 370 families with ADHD-affected sibling pairs. Children and adolescents were assessed using the K-SADS-PL (Present and Lifetime version). Adult parents were assessed using the SADS-LA-IV (Lifetime version), supplemented with the K-SADS Behavioral Disorders module for diagnosis of ADHD and disruptive behavior disorders. Direct interviews were supplemented with parent and teacher versions of the Swanson, Nolan, and Pelham, version IV (SNAP-IV) rating scale, as well as a parent-completed Childhood Behavior Checklist (CBCL) and Teacher Report Form (TRF). Exclusion criteria were neurological disorder, head injury resulting in concussion, lifetime diagnoses of schizophrenia or autism, or estimated Full Scale IQ<70. For all sites DNA was extracted from blood at each participating institution and Genizon BioSciences Inc. conducted genotyping with funding from Pfizer Inc. Genomic DNA samples from MGH and WASH-U were genotyped using the Illumina Human1M BeadChip (N = 1,057,265 SNPs), whereas the UCLA samples were genotyped using the Illumina Human 1M-Duo array (N = 1,151,846 SNPs). The study was approved by the subcommittee for human subjects of each site.

Toronto, Canada

The Canadian ADHD trio sample[12] was drawn from an outpatient clinic in an urban pediatric hospital and included children aged 6-16 years who were referred for attention, learning and/or behavioral problems. ADHD diagnostic data was obtained from parents and teachers in semi-structured clinical interviews including the Parent Interview for Child Symptoms (PICS) and the Teacher Telephone Interview (TTI). Exclusion criteria were an IQ<80 on both the verbal and the performance subscales of the Wechsler Intelligence Scale for Children (WISC). Samples were genotyped on the Affymetrix Genome-Wide Human SNP Array 6.0 with standard protocols as provided by the manufacturer. The study was approved by the Research Ethics Board of the Hospital for Sick Children, Toronto.

Case-control samples

Barcelona, Spain

The Barcelona sample[13] comprised 607 ADHD cases. All patients were adults of Caucasian origin, recruited and evaluated at the Hospital Universitari Vall d'Hebron located in Barcelona (Spain). ADHD diagnostic criteria was assessed using the Structured Clinical Interview for DSM-IV and the Conner's Adult ADHD Diagnostic Interview for DSM-IV (CAADID). Impairment was measured with the Clinical Global Impression (CGI), included in the CAADID Part II, and the Sheehan Disability Inventory (SDI). Exclusion criteria were IQ<70, schizophrenia or other psychotic disorders, ADHD symptoms due to mood, anxiety, dissociative or personality disorders, adoption, sexual or physical abuse, birth weight <1.5 kg, and other neurological or systemic disorders that might explain ADHD symptoms. The control sample consisted of 584 unrelated blood donors frequency-matched for gender with the ADHD cases and screened to exclude those with lifetime ADHD symptoms or diagnosis.

Both cases and controls were genotyped on the Illumina HumanOmni1-Quad BeadChip platform. The study was approved by the relevant ethics committee.

Beijing, China

The Beijing, China sample[14] comprised 1,040 ADHD cases aged between 6-16 years of Han Chinese decent. Cases were recruited from the Child and Adolescent Psychiatric Outpatient Department of the Sixth Hospital, Peking University. Clinical diagnoses from a senior child and adolescent psychiatrist were confirmed using the Chinese version of the Clinical Diagnostic Interview Scale. Exclusion criteria were those with major neurological disorders (e.g. epilepsy), schizophrenia, pervasive development disorder, and IQ<70. The 963 control individuals were students from local elementary schools, healthy blood donors from the Blood Center of the First Hospital, Peking University, and healthy volunteers from the institute of Han Chinese decent, screened using the

ADHD Rating Scale-IV (ADHD RS-IV) to exclude ADHD. Additional exclusion criteria were major psychiatric disorders, family history of psychosis, severe physical diseases, and substance abuse. Both cases and controls were genotyped using the Affymetrix6.0 array at CapitalBio Ltd., Beijing, using the standard Affymetrix protocol.

The study was approved by the Institutional Review Board of the Peking University Health Science Center.

Bergen, Norway

The Bergen, Norway sample[15] consisted of 300 adults with ADHD. Patients recruited through a Norwegian national medical registry, as well as by psychologists and psychiatrists working at out-patient clinics. Information regarding ADHD was obtained following systematic assessment of ADHD diagnostic criteria, developmental history, physical examination, evaluation of comorbidity, and, where possible, information from collateral informants. All gathered information was then sent to one of the expert committees for a definitive diagnostic assessment. There were no formal exclusion criteria. The 205 controls were recruited through the Medical Birth Registry of Norway above the age of 18 years with no known intellectual disability. Cases and controls were genotyped using the Human OmniExpress-12v1-1_B (Illumina, San Diego, CA, USA) platform. Genotyping was performed according to the standard Illumina protocol at Decode facility (Reykjavik, Iceland). The study was approved by the Norwegian Regional Medical Research Ethics Committee West (IRB #3 FWA00009490, IRB00001872).

Cardiff, UK

The Cardiff sample[16] consisted of 727 Caucasian children aged 5-18 years old from Cardiff, Wales (N=510); St. Andrews, Scotland (N=35); and Dublin, Ireland (N=182). All children were recruited from community clinics and were assessed for ADHD using the Child and Adolescent Psychiatric

Assessment (CAPA) Parent Version, a semi-structured research diagnostic interview, to assess psychiatric diagnoses. Pervasiveness of ADHD symptoms (in school) was assessed using the Child ADHD Teacher Telephone Interview or the Conners Teacher Questionnaire. Exclusion criteria were intellectual disability (IQ <70), a major medical or neurological condition (e.g. epilepsy), autistic spectrum disorder, Tourette's syndrome, bipolar disorder, or known chromosomal abnormality. Control participants were obtained from the Wellcome Trust Case Control Consortium–Phase 2. They comprised 3,000 individuals born in the United Kingdom during 1 week in 1958 (the 1958 British Birth Cohort) and 3,000 individuals from the U.K. Blood Services collection (N=5,081 passed QC). The comparison subjects were not screened for psychiatric disorders. ADHD case subjects were genotyped on the Illumina (San Diego) Human660W-Quad BeadChip according to the manufacturer's instructions. Comparison subjects were genotyped by Wellcome Trust Case Control Consortium–Phase2 using the Illumina Human 1.2M BeadChip. The study was approved by the local research ethics committees at each site.

Germany

The German sample[17] comprised 495 patients with ADHD (aged 6–18 years) recruited and phenotypically characterized in six psychiatric outpatient units for children and adolescents (Aachen, Cologne, Essen, Marburg, Regensburg, and Wurzburg). ADHD was assessed using the K-SADS-PL and a German teacher rating scale for ADHD (FBB-HKS). Exclusion criteria were IQ≤75, potentially confounding psychiatric diagnoses such as schizophrenia, any pervasive developmental disorder, Tourette's disorder, and primary mood or anxiety disorder, neurological disorders such as epilepsy, a history of any acquired brain damage or evidence of the fetal alcohol syndrome, very preterm birth and/or (f) maternal reports of severe prenatal, perinatal or postnatal complications. The 1,300 adult controls were drawn from three population based epidemiological studies: (a) the Heinz Nixdorf Recall (Risk Factors, Evaluation of Coronary Calcification, and Lifestyle) study 3, (b) PopGen, (c)

KORA (Cooperative Health Research in the Region of Augsburg. Ethnicity was assigned to patients and controls according to self-reported ancestry (all German). The genome-wide genotyping was performed on HumanHap550v3 (Illumina; controls) and Human660W-Quadv1 BeadArrays (Illumina; cases). The study was approved by the ethics committees of all participating hospitals.

IMAGE-II, Europe & USA

The IMAGE-II ADHD case samples[18] included some samples from the original IMAGE project (see IMAGE-I details above) along with samples provided by colleagues at other sites (Cardiff; St. Andrews, Dublin; MGH; Germany; and the Netherlands), using similar but not identical methods. Samples from Dublin and MGH followed the procedures described above for Cardiff and PUWMa, respectively. Case collection for the German and Dutch sites are described below.

In Germany, 351 participants were recruited in order of clinical referral in the outpatient clinics in Wurzburg, Hamburg and Trier. Families were of German, Caucasian ancestry. All children were assessed by full semi-structured interview (Kiddie-Sads-PL-German Version or Kinder-DIPS) and parent and teacher ADHD DSM-IV based rating scales to ensure pervasiveness of symptoms. Exclusion criteria were IQ<80, comorbid autistic disorders or somatic disorders (hyperthyroidism, epilepsy, neurological diseases, severe head trauma etc.), primary affective disorders, Tourette's syndrome, psychotic disorders or other severe primary psychiatric disorders, and birth weight <2000 grams.

At the Dutch site, assessment data are available for 112 subjects aged 3-18 years with DSM-IV ADHD. Most of the sample was collected as part of a sib pair genome-wide linkage study in ADHD[19]. Subjects were assessed using the DSM-IV version of the Diagnostic Interview Schedule for Children (DISC-P) with both parents, supplemented by Conners Questionnaires (old versions), the CBCL and TRF. Exclusion criteria were autism, epilepsy, IQ <70, brain disorder, and any genetic or medical disorder associated with externalizing behaviors that might mimic ADHD.

Control samples (1,755 population controls of European ancestry) were assembled from an IRB approved genome-wide association study (GWAS) of myocardial infarction[20]. Controls were collected from multiple sites in the US and Europe, including Seattle, Washington; Boston, Massachusetts; Gerona, Spain; Malmo, Sweden; and the United Kingdom. Sampling procedures for each cohort have been described previously[20]. Control participants from the Wellcome Trust Case Control Consortium overlapping with the Cardiff, UK sample (described above) were removed.

Cases were genotyped using the Affymetrix 5.0 array at the State University of New York Upstate Medical University, Syracuse using the standard protocol issued by Affymetrix. Controls were genotyped using the Affymetrix 6.0 array. The study was approved by the Institutional Review Board (IRB) or Ethical Committee at each site.

Yale-Penn, USA

The Yale-Penn sample consists of small nuclear families and unrelated individuals (2020 individuals in 850 families and 6951 unrelated individuals), collected to study the genetics of substance dependence[21-23]. The case-control subjects were recruited from 2000 to 2013 from substance abuse treatment centers and through advertisements at the University of Connecticut Health Center, Yale University School of Medicine, the Medical University of South Carolina, the University of Pennsylvania, and McLean Hospital. The participants were identified through a family-based and a case-control protocol. Families were ascertained from treatment centers and advertisements that recruited affected sibling pairs (ASPs) meeting Diagnostic and Statistical Manual of Mental Disorders, 4th Edition (DSM-IV) criteria for cocaine or opioid dependence. Other family members of the ASPs were recruited when available, regardless of affection status and unaffected family members were included within the control subjects.

For this study, 182 individuals with ADHD and 1315 unrelated controls of European ancestry were included. Unrelated individuals with ADHD and controls were selected from the family-based

protocol, with a focus on maximizing the number of ADHD cases retained for the analysis. *DSM-IV* diagnoses of ADHD case status, as well as other major psychiatric traits, were derived from the Semi-Structured Assessment for Drug Dependence and Alcoholism for all participants. Exclusion criteria were a clinical diagnosis of a major psychotic illness (for example, schizophrenia or schizoaffective disorder).

The sample was genotyped using one of two genotyping arrays: (1) the Illumina HumanOmni1-Quad v1.0 microarray containing 988,306 autosomal SNPs (Yale- Penn.1: performed at the Center for Inherited Disease Research (CIDR) and the Yale Center for Genome Analysis), (2) the Illumina Infinium Human Core Exome microarray (Yale-Penn.2 and Yale-Penn.3: performed at the Yale Center for Genome Analysis). The study was approved by the relevant institutional review boards.

Replication samples

23andMe, self-reported ADHD diagnoses

The 23andMe sample consists of individuals who sent saliva samples (using the Oragene kit) to the genetic testing company 23andMe, Inc and agreed to take part in research and answered questions about their ADHD history as part of a longer survey. All participants provided informed consent and answered surveys online according to 23andMe's human subjects protocol, which was reviewed and approved by Ethical & Independent Review Services, an AAHRPP-accredited institutional review board. As part of the "Your Medical History" survey, they were asked: "Have you ever been diagnosed by a doctor with any of the following psychiatric conditions: Attention deficit disorder (ADD) or Attention deficit hyperactivity disorder (ADHD)?". The response options were: "Yes", "No", "I don't know". A second question asked independently as a "Research Snippet" was: "Have you ever been diagnosed with attention deficit disorder (ADD) or attention deficit hyperactive disorder (ADHD)?" with the response options: "Yes", "No", "I'm not sure". Individuals who gave a

positive response to these questions were classed as ADHD cases and controls were those who gave a negative response to these questions. Individuals with discordant responses were excluded.

Research participants were genotyped either on the Illumina HumanHap550k (13,030 controls, 840 cases) or HumanOmniExpress (57,363 controls, 5,017 cases) genotyping platforms by 23andMe. GWAS and imputation were performed separately for data generated by the two platforms. Within each platform, batches of 8,000-9,000 participants were imputed. Results were filtered for average and minimum imputation r^2 to exclude SNPs that showed batch effects. Covariates included in the GWAS were age, sex and the first four principal components to account for population stratification. For the current study, the GWAS summary statistics were then aligned to the genotyped samples. The 23andMe summary statistics were verified to be consistent with genome build hg19. They were then matched to the genotype data based on rsid, chromosome and base pair position. For SNPs, reported alleles were required to match the genotype data without a strand flip. For indels and multiallelic variants, alleles reported by 23andMe were evaluated heuristically for consistency with the genotype data and the alleles were matched accordingly (e.g. "I" or "D" alleles reported by 23andMe for indels were matched to the corresponding sequence of alleles for the insertion or deletion included in the genotype data). After alignment, the 23andMe GWAS results for the two platforms were combined in an inverse standard error-weighted meta-analysis to create a single 23andMe results set for use in the replication analyses. In total, 11,198,253 variants were matched from the 23andMe meta-analysis for inclusion in replication analyses.

EAGLE, ADHD symptom scores

The EArly Genetics and Lifecourse Epidemiology (EAGLE) consortium includes population-based birth cohorts from Europe, Australia, and the United States (http://www.wikigenes.org/e/art/e/348.html). The consortium focuses on a wide range of phenotypes

in childhood including traits related to cognition and behaviour e.g. aggression[24], astma allergy and atopy[25] and postnatal growth[26]. In the study of ADHD symptoms, nine EAGLE cohorts where included with available ADHD symptom scores in childhood (age at measurement <13 years). An overview of the nine cohorts included in the EAGLE meta-analysis is provided in Middeldorp et al.[27]. In order to assess ADHD symptoms different instruments were used across cohorts, including the Attention Problems scale of the Child Behavior Checklist (CBCL) and the Teacher Report Form (TRF), the Hyperactivity scale of the Strengths and Difficulties Questionnaire (SDQ), and the *DSM-IV* ADHD items as, for example, included in the Conners Rating Scale. For the meta-analysis, one phenotype was selected from each cohort. Based on the phenotype that was most available, school-age ratings were chosen over preschool-age ratings, parent ratings over teacher ratings, and the measurement instrument with the largest information density was preferred over the other instruments[27].

Each of the included cohorts went through their own optimal pre-imputation QC and imputation was done using the March 2012 release of the Genomes Project (phase 1)[28]. Detailed description of QC, imputation and the analysis procedures for the different cohorts can be found in Middeldorp et al.[27]. Association analyses were done using linear regression and relevant principal components and subsequently meta-analysed using METAL[29]. Summary statistics from the meta-analysis of N=17,666 individuals were provided for inclusion in the current study.

For the current study, summary statistics from the EAGLE meta-analysis were aligned to the genotyped ADHD samples based on rsid and chromosome and base pair location. SNP alleles were required to be concordant without a strand flip. No indels were included from the EAGLE meta-analysis. After alignment, 5,837,346 SNPs from the EAGLE meta-analysis were available for replication analyses.

Bioinformatic pipeline for quality control and association analyses

Quality control, imputation and primary association analyses were done using the bioinformatic pipeline "Ricopili", which has been developed by the Psychiatric Genomics Consortium (PGC) Statistical Analysis Group[30]. The pipeline generates high quality imputed data and performs GWAS and meta-analysis of large genetic data sets. In order to avoid potential study and "wave" effects the eleven PGC samples were processed separately and the iPSYCH sample was processed in 23 separate batches referred to as waves (see sample description above) unless otherwise is stated.

Pre-imputation quality control

Subjects and SNPs were included in the analyses based on the following quality control parameters: SNP call rate > 0.95 (before sample removal), subject call rate > 0.98 (> 0.95 for the iPSYCH samples), autosomal heterozygosity deviation ($| F_{het} | < 0.2$), SNP call rate > 0.98 (after sample removal), difference in SNP missingness between cases and controls < 0.02, and SNP Hardy-Weinberg equilibrium (HWE) ($P > 10^{-6}$ in controls or $P > 10^{-10}$ in cases).

Genotype imputation

In order to obtain information about non-genotyped markers, we used the pre-phasing software SHAPEIT[31] to estimate haplotypes and subsequently IMPUTE2[32] for imputing genotypes. Imputing was done in chunks of 3 Mb using default parameters. The imputation reference data consisted of 2,504 phased haplotypes from the 1000 Genomes Project, phase 3 (1KGP3)[33,34] data (October 2014, 81,706,022 variants, release 20130502). Trio imputation was done with a case-pseudocontrol setup,

where a pseudocontrol was defined to each affected offspring using the non-transmitted alleles from the two parents (estimated based on the haplotypes of the parents).

Relatedness and population stratification

Relatedness and population stratification were evaluated using a set of high quality markers (genotyped autosomal markers with minor allele frequency (MAF) > 0.05, HWE $p > 1x\ 10^{-4}$ and SNP call rate > 0.98), which were pruned for linkage disequilibrium (LD) resulting in a set of ~30,000 pruned markers (markers located in long range LD regions defined by Price et al.[35] were excluded). This was done separately for each of the PGC samples and on a merged set of genotypes from the 23 iPSYCH waves. In order to identify related individuals an identity by state analysis were performed using PLINK v1.9[36,37], and one individual was excluded in pairs of subjects with $\hat{\pi} > 0.2$ (cases preferred kept over controls).

In order to identify genetic outliers a principal component analysis (PCA) was performed using smartPCA incorporated in the software Eigensoft[38], and the same set of pruned autosomal markers as described above. For the iPSYCH sample a genetic homogenous sample was defined based on a subsample of individuals being Danes for three generations. This subsample was defined using register information about birth country of the individuals, their parents and grandparents, which was required to be Denmark in order to be included in the subsample. The subsample of Danes was used in order to define the center of an ellipsoid based on the mean values of principal component (PC) 1 and PC2. Subsequently PC1 and PC2 for all individuals in the iPSYCH sample were used to define a genetic homogenous population by excluding individuals with PC values greater than six standard deviations from the mean. For the PGC samples genetic outliers were removed based on visual inspection of the first six PCs. PCA including samples from the 1000 Genomes Project was also

performed to confirm that the selected individuals matched the ancestry of European reference populations.

PCA was redone after exclusion of genetic outliers. The first 20 principal components were tested for association with the phenotype using logistic regression and their impact on the genome-wide test statistics were evaluated using λ. In the iPSYCH GWAS PC1-4 and significant PCs were included as covariates. For PGC samples, the number of PCs was adjusted based on the cohort's sample size in order to avoid overfitting and to reflect the differential power to capture true population structure by PCA. Specifically, the first five principal components were included as covariates for samples with fewer than 1000 individuals, and the first ten PCs were included for larger samples. Trio samples did not include PCs in the analysis unless strong population structure was evident (i.e. PUWMa). Where necessary, study specific design covariates were also included (e.g. indicators variables for IMAGE-I sampling centres, alcohol dependence diagnosis for ascertainment in Yale-Penn).

GWAS and meta-analysis

Association analyses using the imputed marker dosages were performed separately for the 11 PGC samples and the 23 waves in iPSYCH by an additive logistic regression model using PLINK v1.9[36,37], with the derived principal components included as covariates as described above.

The meta-analysis included summary statistics from GWASs of the 23 waves in iPSYCH and 11 PGC samples, in total containing 20,183 cases and 35,191 controls. Only SNPs with imputation quality (INFO score) > 0.8 and MAF > 0.01 were included in the meta-analysis. Meta-analysis was performed using an inverse-weighted fixed effects model implemented in the software METAL (http://csg.sph.umich.edu//abecasis/Metal/)[29]. Finally we filtered the GWAS meta-analysis, so only

markers which were supported by an effective sample size (Neff = 2/(1/Ncases + 1/Ncontrols)[39] greater than 70% were included (8,047,421 markers).

In some of the secondary analyses (e.g. when using LD score regression[40] and MAGMA[41] (see below)), information about LD structure in a reference genome reflecting the ancestry of the analysed population is used. Such analyses therefore require results from a GWAS meta-analysis based on a genetic homogenous group reflecting the same ancestry. We therefore performed a GWAS of the iPSYCH samples and the PGC samples with European ancestry (subsequently referred to as European GWAS meta-analysis). In this GWAS meta-analysis the Chinese PGC sample was excluded and the PUWMa sample was replaced with the PUWMa (strict) sample, in which individuals with non-European genetic ancestry were excluded, resulting in 19,099 cases and 34,194 controls with European ancestry.

The GWAS meta-analysis identified 12 independent genome-wide significant (gws) loci (see Manhattan plot [Figure 1], forest plots [Supplementary Figure 3.A1 – 3.M1] and regional association plots [Supplementary Figure 3.A2 – 3.M2]). Independent loci were defined as described below. A more detailed description of potential risk genes located in the identified gws loci can be found in Supplementary Table 4.

In the European GWAS meta-analysis the number of independent gws loci decreased to 11. The gws locus on chromosome 2 (located in *SPAG16*) in the GWAS meta-analysis did not pass the significance threshold when only including individuals with European ancestry (see Manhattan plot, Supplementary Figure 2).

In addition, heterogeneity across studies/waves were tested with the Cochran's Q test and quantified with the I^2 heterogeneity index. No markers demonstrated significant heterogeneity (Supplementary Figure 6 and 7).

Defining independent genome-wide significant loci

303 variants reached genome-wide significance ($P < 5x10^{-8}$) in the meta-analysis. We then identified independent loci from these markers based on LD clumping (--clump in PLINK 1.9[36,37]). Beginning with the most significantly associated variant as the first index variant, we labelled variants as being part of the same locus if they were within 500 kb and correlated with an index variant ($r^2 > 0.2$). Variants not within 500 kb and not correlated with an existing index variant were labelled as a new index variant. Correlations were estimated from European-ancestry populations in the 1000 Genomes Phase 3 reference panel[34]. Clumping continued until all variants with $P < 5 \times 10^{-8}$ were either labelled as an index variant or assigned to a locus.

A gws locus was then defined as the physical region containing the identified LD independent index variants and their correlated variants ($r^2 > 0.6$) with $P < 0.001$. Associated loci located less than 400 kb apart were merged. The same process was applied to define independent genome-wide significant loci in subsequent meta-analyses.

Evaluating putative secondary signals

Correlation of secondary signals with their respective lead index variants

Two of the genome-wide significant loci defined by this process in the ADHD meta-analysis include more than one index variant (Supplementary Table 2). In other words, they contain two genome-wide significant variants that are within 500 kb but are not correlated ($r^2 < 0.1$). In this case, we label the less significantly associated index variant as a putative secondary signal and perform additional analyses to evaluate whether the second index variant can be confirmed as independent.

First, we confirmed that the putative secondary signals are not strongly correlated with their respective lead index variants in the current genotype data. The correlation with the index variant was evaluated in (1) imputed best-guess genotype data (hard-called genotypes derived from imputed

genotype probabilities, for all variants with an imputation info score > 0.8) from the 11 PGC cohorts, and (2) imputed best-guess genotype data from iPSYCH. For both putative secondary effects, the correlation between the index variant and secondary effect is ($r^2 < 0.1$) in both the PGC and iPSYCH imputed genotype data (Supplementary Table 2). This confirms that the putative secondary signal does not reflect LD structure in the ADHD cohorts that is not well captured by the 1000 Genomes Phase 3 European reference panel[34].

Conditional association analysis

The two putative secondary signals were then evaluated by considering analysis conditional on the lead index variant in each locus. In each cohort, logistic regression was performed with the imputed genotype dosage for the lead index variant included as a covariate. All covariates from the primary GWAS (e.g. principle components, site indicators) were also included. The conditional association results were then combined in an inverse-variance weighted meta-analysis.

Neither of the putative secondary signals achieve genome-wide significance in the conditional association analysis (Supplementary Table 2). The decreased significance observed in the conditional analysis reflects modestly attenuated estimates of the odds ratio and increased standard errors compared to the marginal association analysis in the primary GWAS.

Based on the non-significant results for the putative secondary variants in the conditional analyses, we conclude that there is not yet sufficient evidence to confidently label these as independent effects in their respective loci.

Bayesian credible set analysis

In order to refine the genome-wide significant loci, we defined a credible set of variants in each locus using the method described by Maller et al.[42]. Under the assumption that (a) there is one causal variant

in each locus, and (b) the causal variant is observed in the genotype data, the credible set can be considered to have a 99% probability of containing the causal variant.

Credible set estimation method

We summarize the method here following the description of Gormley et al.[43]. Briefly, let D be the data including the genotype matrix X with P variants and the vector Y of phenotypes, and let β be the regression model parameters. Define P models A_j where variant j is causal and the remaining variants are not causal, and define the null model A_0 where no variants are causal. Then by Bayes' rule the probability of model A_j is:

$$\Pr(A_j|D) = \int \Pr\left(D, \beta|A_j\right) \cdot \frac{\Pr(A_j)}{\Pr(D)} \cdot d\beta$$

Assuming a flat prior for the model parameters β, the integral can be approximated using the maximum likelihood estimates $\widehat{\beta_j}$, such that

$$\Pr(A_j|D) \approx \Pr(D|A_j, \widehat{\beta_j}) \cdot N^{-\frac{|\beta_j|}{2}} \cdot \frac{\Pr(A_j)}{\Pr(D)}$$

where N is the sample size and $|\beta_j|$ denotes the number of fitted parameters for model A_j. Given the assumption of one causal variant per locus, $|\beta_j|$ is a constant for all A_j. Next, note that the conventional likelihood ratio test of model $A_j$compared to the null model A_0 is defined as

$$\chi_j^2 \equiv -2 \log \frac{\Pr\left(D|A_0, \widehat{\beta_0}\right)}{\Pr\left(D|A_j, \widehat{\beta_j}\right)}.$$

Thus by substitution,

$$\Pr(A_j|D) \approx \exp\left(\frac{\chi_j^2}{2}\right) \cdot l_0 \cdot N^{-\frac{|\beta_j|}{2}} \cdot \frac{\Pr(A_j)}{\Pr(D)}$$

with $l_0 = \Pr(D|A_0, \widehat{\beta_0})$. Given a flat prior for models A_j the latter terms are constant, leaving

$$\Pr(A_j|D) \propto \exp\left(\frac{\chi_j^2}{2}\right).$$

Normalizing across all possible models A_j thus yields

$$\Pr(A_j) \equiv \Pr(A_j|D) / \sum_k \Pr(A_k|D).$$

Finally, the 99% credible set of variants is defined as the smallest set S of models such that

$$\sum_{A_j \in S} \Pr(A_j) \geq .99.$$

If the model assumptions are correctly specified, then this credible set S has a 99% probability of containing the true causal variant.

We implemented this approach using the published R script freely available online (https://github.com/hailianghuang/FM-summary).

Variants considered for credible set analysis

We applied the Bayesian credible set analysis to each of the 12 genome-wide significant loci identified in the primary meta-analysis of ADHD as described above. For each locus, variants within 1MB and in linkage disequilibrium (LD) with correlation $r^2 > 0.4$ to the index variant were considered for inclusion in the credible set.

Because the credible set estimation is conditioned on LD structure, we performed the credible set analysis using the European GWAS meta-analysis to ensure consistent LD structure in the analyzed cohorts. Credible sets were also estimated based on both (a) the observed LD in European ancestry PGC datasets, and (b) the observed LD in the iPSYCH dataset.

Observed LD with the index variant in each locus was computed using imputed best-guess genotype data (generated as described previously) with PLINK 1.9 (https://www.cog-genomics.org/plink2)[37]. For the European ancestry PGC datasets, imputed genotype data was merged across cohorts prior to

computed LD. For the iPSYCH dataset, imputed genotyped data for the 23 genotying waves were similarly merged before computing LD.

Credible set results in PGC and iPSYCH data

Bayesian credible sets for each of the 12 genome-wide significant loci are reported in Supplementary eTable 1 (A-L). For the majority of the loci (7 of 12), there is no difference between the credible set results based on LD structure in the PGC datasets versus LD from the iPSYCH dataset (Supplementary Table 3). Differences between the credible sets for the remaining loci are modest, with no more than six non-overlapping variants between the two sets for each locus. The non-overlapping variants also tend to have weak evidence for inclusion in the 99% credible set; of the 19 non-overlapping variants, only six would be included in an 90% credible set (i.e. the smallest set of variants with an 90% probability of containing the true causal variant under the Bayesian model), and only one would be included in an 80% credible set. To be conservative, we define the final credible set as the union of the credible sets estimated from the PGC and iPSYCH LD structure.

Functional annotation of variants in credible set

To evaluate the potential impact of the variants in the credible set for each locus, we consider annotations of predicted functional consequences for those variants based on external reference data. In particular we evaluate:

- Functional consequences: Coding and regulatory consequences of each variant were annotated using the Ensembl Variant Effect Predictor (VEP[44]) for genome build GRch37 (hg19). Annotated consequences for transcripts without a HGNC gene symbol (e.g. clone-based vega genes) were excluded. Gene names were updated to the current HGNC gene symbol where applicable. For each variant, we summarize (a) annotated genes, excluding

"upstream" and "downstream" annotations; (b) genes with an annotated consequence (i.e. excluding intronic annotations); and (c) annotated regulatory regions.

- Transcription start site (TSS): We annotate variants within 2kb upstream of the TSS of at least one gene isoform based on Gencode v19[45].
- Hi-C interactions: Variants annotated as physically interacting with a given gene were identified based on Hi-C data from samples of developing human cerebral cortex during neurogenesis and migration[46]. Annotations are considered for both the germinal zone (GZ), primarily consisting of actively dividing neural progenitors, and the cortical and subcortical plate (CP), primarily consisting of post-mitotic neurons.
- Expression quantitative trait loci (eQTLs): SNPs associated with gene expression were annotated using FUMA (http://fuma.ctglab.nl/). Annotated eQTLs were identified from GTEx v6[47] and BIOS[48], and filtered for false discovery fate (FDR) < $1x\ 10^{-3}$ within each dataset. Annotations were updated to current HGNC gene symbols where applicable. For variants with multiple eQTL associations, we summarize the strongest eQTL association (i.e. the association with the lowest P-value) from each dataset.
- Chromatin state: Chromatin states for each variant were annotated based on the 15-state chromHMM analysis of epigenomics data from Roadmap[49]. For each SNP, the most common chromatin state across 127 cell types was annotated using FUMA (http://fuma.ctglab.nl/). For all variants, we also annotate the predicted chromatin state in fetal brain. The 15 states are summarized to annotations of active chromatin marks (i.e. Active TSS, Flanking Active TSS, Flanking Transcription, Strong Transcription, Weak Transcription, Genic Enhancer, Enhancer, or Zinc Finger [ZNF] gene), repressive chromatin marks (Heterochromatin, Bivalent TSS, Flanking Bivalent TSS, Bivalent Enhancer, Repressed Polycomb, or Weak Repressed Polycomb), or quiescent.

- CADD: Combined Annotation Dependent Depletion (CADD v1.3[50]) scores were annotated for each SNP using FUMA (http://fuma.ctglab.nl/).

Supplementary eTable 2 summarizes the observed annotations for the credible set at each locus (see also Supplementary eTable 3 for variant-level annotations).

Gene-based association analysis

Exome-wide association of single genes with ADHD

Gene-based association with ADHD was estimated by MAGMA 1.05[41] using the summary statistics from the European GWAS meta-analysis (N_{cases} = 19,099; $N_{controls}$ = 34,194; Supplementary Table 1) and summary statistics from the GWAS meta-analysis including the EAGLE sample (N_{total} = 70,959). We annotated SNPs to genes within their transcribed regions using the NCBI 37.3 gene definitions provided with MAGMA. We then calculated gene P-values using the SNP-wise mean model in which the sum of –log(SNP P-value) is used as a test statistic. The gene P-value was calculated using a known approximation of the sampling distribution[51]. MAGMA accounts for gene-size, number of SNPs in a gene and LD between markers. When using summary statistics in estimating gene-based P-values, MAGMA corrects for LD based on estimates from reference data with similar ancestry; for this we used the 1KGP3, European ancestry samples, as the reference[34].

In total 20 genes demonstrated significant gene-wise association with ADHD after Bonferroni correction (correction for 17,877 genes; Supplementary Table 5). 11 genes were located in the complex region on chromosome 1 demonstrating strong gws association with ADHD in the single marker GWAS meta-analysis (see regional association plot for this region, Supplementary Figure 3.A2). Additional five genes overlapped with loci with gws single markers (*MEF2C*, *FOXP2*, *SORCS3*, *DUSP6* and *SEMA6D*). Four genes (*MANBA, CUBN, PIDD1, CDH8)* not located in single marker gws loci showed significant association (Supplementary Table 5). The LD region around three

of the genes (*MANBA, CUBN, CDH8)* contains only the respective genes, indicating that the gene-based association signals were driven by markers in the genes and were unlikely to be caused by extended LD with markers in neighbouring gene loci (see regional association plots for the four new genes; Supplementary Figure 4.A. – 4.D.).

Gene-wise association of candidate genes for ADHD

Prior to the availability of large-scale whole-genome methods and technologies, many candidate genes have been examined in relation to ADHD. Such candidate gene studies frequently fail to replicate[52] and are likely to have been affected by publication bias, so it is unclear how many of the reported candidate genes are actually robustly associated with ADHD. As such, we set out to examine what the evidence for association is for the most highly studied candidate genes for ADHD, obtained from a recent review[53], in the current GWAS dataset. Annotated ADHD SNP results were tested for enrichment in each of these candidate genes using MAGMA to obtain overall gene P-values. The results do not show any support for the majority of the candidate genes that have been historically studied in relation to ADHD (Supplementary Table 6). The only exception is *SLC9A9* which shows nominal enrichment.

Gene-set analyses

Hypothesis free gene set analyses

For gene set analyses, we applied MAGMA[41]. The analyses were based on the gene-based *P*-values generated as described above under "Gene-based association analysis", based on summary statistics from the European GWAS meta-analysis. Those P-values were used to analyse sets of genes in order to test for enrichment in association signals in genes belong to specific to biological pathways or

processes. MAGMA applies a competitive test to analyse if the genes of a gene set are more strongly associated with the trait than other genes, while correcting for a series of confounding effects such as gene length and size of the gene-set. In the analysis only genes on autosomes, and genes located outside the broad MHC region (hg19:chr6:25-35M) were included in the analysis. We applied no padding around genes. We used the gene names/locations and the European genotype reference panel provided with the program. For gene sets we used the Gene Ontology[54] sets curated in MsigDB 6.0[55] keeping only gene sets with 10-1000 genes. No gene-sets remained significant after correction for multiple testing (Supplementary eTable 4).

FOXP2 downstream target gene set analysis

Targeted gene set analyses were run in MAGMA to determine whether *FOXP2* downstream target gene sets are enriched in ADHD. Three sets of genes were examined: 1) Putative target genes of *FOXP2* that were enriched in wild type compared to control *FOXP2* knockout mouse brains in ChIP-chip experiments, 2) Genes showing differential expression in wild type compared to *FOXP2* knockout mouse brains, and 3) *FOXP2* target genes that were enriched in either or both basal ganglia (BG) and inferior frontal cortex (IFC) from human fetal brain samples in ChIP-chip experiments. Curated lists of high-confidence genes were obtained from Vernes et al.[56] and Spiteri et al[57]. Mouse genes were mapped to human orthologues using MGI and NCBI. *FOXP2* was excluded, only 8 genes were present on more than one list and only one gene was present on all three lists (*NRN1*). ADHD SNP results were annotated using MAGMA and used for gene set analyses. Competitive P-values, using a conditional model to correct for confounding due to gene size and gene density were obtained for each gene set. The results showed no evidence of enrichment for any of these gene sets (Supplementary Table 7).

Highly constrained gene set analysis

We assessed whether genes that are intolerant to loss of function and thereby highly evolutionarily constrained are enriched in ADHD. The set of highly constrained genes was defined using a metric for probability of being loss-of-function (LoF) intolerant (pLI) based on the observed and expected protein-truncating variant (PTV) counts within each gene in a very large study of exome data (the Exome Aggregation Consortium; ExAC)[58]. Genes with observed <10% of expected PTVs were deemed haploinsufficient or highly constrained. Publically available results based on the full ExAC dataset were downloaded from:

ftp://ftp.broadinstitute.org/pub/ExAC_release/release0.3.1/functional_gene_constraint

Genes with pLI ≥0.9 were selected as the set of highly constrained genes. Annotated ADHD SNP results were tested for enrichment in this gene set in MAGMA using a competitive gene set analysis. Results showed a significant enrichment of this set of genes (see Supplementary Table 8).

LD Score intercept evaluation

A strong deviation from null was observed in the distribution of the test statistics in the quantile-quantile plot (Q-Q plot) of the results from the GWAS meta-analyses (Supplementary Figure 5.A - 5.B.). When using LD score regression it is possible to distinguish the contribution of polygenicity from other confounding factors such as cryptic relatedness and population stratification to the deviation in the distribution of the test statistics[40]. Under this model when regressing the chi-square statistics from GWAS against LD scores (pre-computed LD-scores downloaded from https://github.com/bulik/ldsc) for each SNP, the intercept minus one is an estimator for the mean contribution of confounding bias to the inflation in the test statistics. LD score regression analysis of the European GWAS meta-analysis estimated that the intercept was close to one (intercept = 1.04 (SE = 0.01)). Additionally, the ratio (ratio = (intercept-1)/(mean(chi^2)-1)), which estimate of the

proportion of the inflation in the mean chi-square that the LD Score regression intercept ascribes to causes other than polygenic heritability was estimated to ratio = 0.12 (SE = 0.03), indicating that the strong inflation in the distribution of the test statistics is caused primarily by polygenicity rather than confounding.

Genetic correlations between PGC and iPSYCH ADHD samples

In order to estimate the overlap in shared genetic risk factors between samples, genetic correlations r_g were calculated using LD Score regression[40]. Pre-computed LD scores for HapMap3 SNPs calculated based on 378 phased European-ancestry individuals from the 1000 Genomes Project were used in the analysis (LD scores available on https://github.com/bulik/ldsc) and the summary statistics from European GWAS meta-analysis (iPSYCH + PGC European samples) and the PGC European samples[27]. The r_g estimate was left unbounded in order to obtain unbiased estimates of SE. Only results for markers with an imputation INFO score > 0.90 were included in the analysis. The estimated genetic correlation between iPSYCH and PGC European GWAS was highly significant (r_g = 1.17; SE = 0.2; P = 7.98 x10^{-9}) and did not suggest imperfect correlation (i.e. r_g < 1) of common genetic risk factors between the studies.

Genetic correlation between PGC case-control and trio samples

The PGC European ancestry dataset consisted of two kinds of association study designs: case-control (Bergen, Cardiff, Germany, IMAGE-II, Spain, Yale-Penn) and trios (CHOP, Canada, IMAGE-I, PUWMa). A previous analysis of the PGC samples showed a genetic correlation of 0.71 (SE=0.17) across case-control and trio studies[59]. We repeated this analysis within this newer set of PGC ADHD data.

For each of the PGC studies, best guess genotype data were generated using Ricopili and strictly filtered (MAF>0.05, in addition to previous frequency, imputation quality and other filters). Genotypes were merged together across studies using PLINK. Asymmetric/ambiguous (AT, TA, CG, GC) and duplicate position SNPs were excluded. GCTA[60] was used to calculate a genomic relationship matrix for all individuals in this merged PGC sample for HapMap-3 SNPs. Analyses were based on 191,466 SNPs. One of each pair of individuals related at the level of 2nd cousins (pi-hat>0.05) was excluded, preferentially keeping cases; this excluded: N=16 cases and N=91 controls. PCA was performed on the merged, unrelated samples using PLINK. The first 10 principal components as well as binary study/wave indicators were used as covariates for subsequent analyses. Univariate GREML analyses in GCTA were used to estimate SNP-h^2 on the liability scale (assuming a population prevalence of 5%) in the case-control samples and the trio samples separately. The GREML method was used for consistency with the previously published comparison of trio and case-control ADHD cohorts, and to accommodate the smaller sample sizes of the PGC subsets. As in the primary GWAS, trio studies were analysed using a case/pseudo-control design, where the pseudo-control is composed of the un-transmitted chromosomes from the parents of the proband. Bivariate GREML was then used to estimate the genetic correlation across these sub-cohorts.

The genetic correlation between the trio and case-control cohorts was strong and indistinguishable from 1 (r_g=1.02, SE=0.32), though the standard error remains quite large (Supplementary Table 10). The observed SNP-h^2 estimates were somewhat lower than the overall SNP-h^2 estimated in the primary analyses for the full meta-analysed results, consistent with the somewhat lower SNP-h^2 estimated from the PGC samples compared to iPSYCH (see SNP heritability analysis below).

Polygenic risk scores for ADHD

In addition to the genetic correlation analyses, we performed analyses of polygenic risk scores (PRS) to evaluate the consistency of common genetic effects and their predictive power across cohorts. We specifically considered PRS prediction within the iPSYCH samples, within the PGC cohorts, and in leave-one-out analysis across all cohorts.

Polygenic risk score prediction in iPSYCH samples

For analysis with the iPSYCH sample as the target cohort, the 23 genotyping-waves within the iPSYCH sample were split into five groups, aiming for approximately equal numbers of ADHD cases within each group. We then conducted two sets of five leave-one-out analyses, with each leave-one-out analysis using four out of five iPSYCH groups as training datasets for estimation of SNP weights and then applying those weights to estimate PRS for the remaining target group[61]. One set of leave-one-out analyses was performed with PGC European samples among the training datasets, while the other was without (only iPSYCH). The meta-analysis of the training samples was conducted using a SNP list filtered for minor allele frequency > 0.01 and an imputation threshold score above 0.8 intersecting across waves. Indels and variants in the extended MHC region (chromosome 6: 25-34 Mb) were also removed. Meta-analysis and "clumping" of significant SNPs was conducted using the Ricopili pipeline[30]. PRS were then estimated for each target sample using a range of meta-analysis P-value thresholds ($5x10^{-8}$, $1x10^{-6}$, $1x10^{-4}$, $1x10^{-3}$, 0.01, 0.05, 0.1, 0.2, 0.5, 1.0), multiplying the natural log of the odds ratio of each variant by the allele-dosage (imputation probability) of each variant. Whole genome PRS were obtained by summing values over variants for each individual.

For each of the five groups of target samples PRS were normalized (subtracting the mean and dividing by the standard deviation), and the significance of the case-control score difference was tested by standard logistic regression including the first six principal components and a dummy variable indicating genotyping wave as covariates (using the glm() function of *R* 3.2.2). For each target group and for each P-value threshold the proportion of variance explained (i.e. Nagelkerke's R^2) was

estimated, comparing the full model to a reduced model without PRS and covariates only. The mean of the maximum Nagelkerke's R^2 across P-value thresholds for each group was R^2 = 0.055 (SE = 0.055, range 0.047 – 0.06). For the P-value threshold with the highest Nagelkerke's R^2, odds ratios for PRS decile groups compared to the lowest decile were estimated for each target group (Supplementary Figure 8) and for the normalized score pooled across groups (Figure 2). Odds ratios were also estimated using logistic regression on the continuous scores for each target group separately and finally an OR based on all samples was estimated by using the normalized PRS across all groups (Supplementary Figure 9).

Polygenic risk score prediction in PGC samples

Next the predictive utility of PRS was evaluated in the PGC samples. All European ancestry PGC best guess genotype data were merged together and iPSYCH-only summary statistics were used to calculate PRS in the PGC samples, using the approach described above. PRS in the PGC dataset were based on 9,323 clumped SNPs with P < 0.1 in the iPSYCH sample. The association between ADHD PRS and case status was significant in the merged PGC sample (OR=1.26 (1.22-1.31), variance explained on the liability scale (R^2) = 0.0103, P = 2.4E-35). Figure 2 displays odds ratios for ADHD case status by ADHD PRS decile for the PGC datasets. In the merged dataset, PRS were converted to deciles (where 1 was the lowest decile and 10 was the highest). Deciles 2-10 were then compared to the lowest decile using logistic regression including PCs as covariates. There is a clear pattern of increasing ORs with increasing decile.

To examine variation that could be related to differences in ascertainment of cases and controls within the PGC sample, mean PRS (residualised for PC covariates) were plotted stratified by case status and study (see Supplementary Figure 11). PGC cases had consistently higher PRS than PGC controls in the same study. There is some variation in PRS z-score across cases in different studies, for example

with ADHD cases from the Cardiff (UK) sample having particularly high scores. Within controls, individuals within the Yale-Penn study have particularly high PRS; this may be due to this sample's ascertainment for the primary phenotype of substance abuse, with high levels of these problems in both the cases and controls[21-23,62] . Variation in PRS in controls from different studies may be due to differences in ascertainment (e.g. pseudo-controls, screened or unscreened controls).

Leave-one-out analysis across cohorts

The odds ratio based on PRS over all PGC and iPSYCH waves/studies was also evaluated using a leave-one-study/wave-out approach. First, GWAS analyses of imputed dosage data were run for all samples in each PGC study and iPSYCH wave separately, as described previously, co-varying for relevant PCs. Meta-analyses using METAL[29] (with the STDERR scheme) were run excluding one set of summary results at a time, for each combination of studies. For each set of discovery results, LD-clumping was run to obtain a relatively independent set of SNPs, while retaining the most significant SNP in each LD block. The following parameters were applied in PLINK: --clump-kb 500 --clump-r2 0.3 --clump-p1 0.5 --clump-p2 0.5. Asymmetric/ambiguous (AT, TA, CG, GC) SNPs, indels and duplicate position SNPs were excluded. The SNP selection P-value threshold used was $P < 0.1$. The number of clumped SNPs for each study/wave varied from 20596-43427. Polygenic risk scores were calculated for each individual as described above. Scores were derived in best guess genotype data after filtering out SNPs with MAF < 0.05 and INFO < 0.8. The polygenic risk scores were standardized using z-score transformations. Logistic regression analyses including PCs tested for association of polygenic risk scores with case status. Finally, overall meta-analyses of the leave-one-out analyses were performed (Supplementary Figure 10).

SNP heritability

SNP heritability was estimated using LD score regression[40] in order to evaluate how much of the variation in the phenotypic trait could be ascribed to common additive genetic variation. Summary statistics from GWAS meta-analyses and pre-computed LD scores (available from https://github.com/bulik/ldsc) were used in the analyses. The SNP heritability for ADHD was calculated on the liability scale when using summary statistics from analyses of diagnosed ADHD and assuming a 5% prevalence of ADHD in the population[63]. The SNP heritability (h^2_{SNP}) was estimated to be 0.216 (SE = 0.014) based on the summary statistics from the European GWAS meta-analysis (Supplementary Table 9).

Partitioning heritability by functional annotation and cell type

Partitioning of the heritability by functional categories was done using LD score regression and 53 functional overlapping annotations described in Finucane et al.[64] and the baseline model LD scores, regression weights and allele frequencies based on the 1KGP3 European ancestry samples were downloaded from https://data.broadinstitute.org/alkesgroup/LDSCORE/. The summary statistics from the European GWAS meta-analysis were used in the analysis. Enrichment in the heritability of a functional category was defined as the proportion of SNP heritability explained divided by the proportion of SNPs[64]. Results from analysis of the 24 main annotations (no window around the functional categories) are displayed in Supplementary Figure 12. The analysis revealed significant enrichment in the heritability by SNPs located in conserved regions ($P = 8.49 \times 10^{-10}$; Supplementary Figure 12).

Test for enrichment in the heritability of SNPs located in cell-type-specific regulatory elements was evaluated in two ways. One by using the 220 cell-type-specific annotations that have been grouped into 10 cell-type groups as described in Finucane et al.[65]. These annotations are based on cell-specific histone markers, related to H3K4me1[66], H3K4me3[66], H3K9ac[66] and H3K27ac[67]. The test was done

using the summary statistics from the European GWAS meta-analysis and cell-type specific LD scores, baseline model LD scores, regression weights and allele frequencies based on 1KGP3 European ancestry samples available for download at: https://data.broadinstitute.org/alkesgroup/LDSCORE/. In the analyses, it was tested if the cell-group specific annotations contributed significantly to the SNP heritability when controlling for the annotations in the full baseline model (the coefficient P-value). The analysis revealed a significant enrichment in the heritability by SNPs located in central nervous system specific enhancers and promoters (enrichment = 2.44, SE=0.35, P = 5.81 x 10^{-5}; Supplementary Figure 13).

Additionally we expanded the cell-type specific heritability analysis by including an annotation based on information about H3K4Me1 imputed gapped peaks excluding the broad MHC-region (chr6:25-35MB), generated by the Roadmap Epigenomics Mapping Consortium[67,68]. This mark has previously been used with success in identifying significant enrichments in tissues/cells and often in a biologically plausible manner[66,67]. This analysis identified enrichment in the heritability of SNPs located in specific regulatory elements of nine brain tissues as well as three stem-cell line (Supplementary Figure 14).

Genetic correlations of ADHD with other traits

The genetic correlation of ADHD with other traits were evaluated using LD Score regression[40]. Correlations were tested for 219 phenotypes with publically available GWAS summary statistics using LD Hub (http://ldsc.broadinstitute.org/ldhub/)[69]. This estimation was based on summary statistics from the European GWAS meta-analysis and summary statistics from published GWASs. In addition, correlation with Major Depressive Disorder was tested using GWAS results from an updated analysis of 130,664 cases and 330,470 controls from the Psychiatric Genomics Consortium (submitted). In total 220 phenotypes were tested for genetic overlap with ADHD and 38 demonstrated

significant correlation after Bonferroni correction ($P < 2.27 \times 10^{-4}$). Detailed information about significant genetic correlations can be found in Supplementary Table 11 and extended results for all phenotypes tested can be found in Supplementary eTable 5.

Replication analysis in 23andMe and EAGLE cohorts

To replicate the results of the ADHD GWAS meta-analysis we compared the results to analyses from 23andMe and EAGLE. The sample design of these cohorts and the process for matching their GWAS results to the ADHD GWAS are described under the sample description section. We evaluated replication based on: (a) sign tests of concordance between the ADHD GWAS meta-analysis and each replication cohort; (b) genetic correlation between the ADHD GWAS and each replication cohort; (c) meta-analysis of the ADHD GWAS meta-analysis results with the results from analyses of the replication cohorts; and (d) tests of heterogeneity in the meta-analyses of the ADHD GWAS meta-analysis with the replication cohorts.

Genetic correlation analyses were performed using LD score regression[40] with the same procedure as described above. Methods for the remaining analyses are additionally described below.

Sign test

To evaluate concordance of the direction of effect between the ADHD GWAS and the replication cohorts, we first identified the 5,636,243 SNPs present in all three analyses (i.e. ADHD GWAS meta-analysis, 23andMe meta-analysis, and EAGLE meta-analysis). The ADHD GWAS meta-analysis for these SNPs were then clumped to define independent loci using PLINK 1.9[37]. Given that the previous conditional analysis was unable to conclusively confirm putative independent signals in the loci defined with LD $r^2 > 0.1$ within 500 kb of the index variant, we apply more conservative clumping parameters to ensure independence for the sign test ($r^2 > 0.05$ within 1 Mb) and merge index variants

within 1 Mb. This clumping was performed for all variants with $P < 1 \times 10^{-4}$ in the ADHD GWAS using 1000 Genomes Phase 3 data on European ancestry populations as reference.

After clumping, sign tests were performed to compare the loci from the ADHD GWAS meta-analysis to 23andMe and EAGLE results. Specifically, for loci passing a given P-value threshold in the ADHD GWAS meta-analysis, we tested the proportion with a concordant direction of effect in the replication cohort (π) using a one sample test of the proportion with Yates' continuity correction[70] against a null hypothesis of $\pi = 0.50$ (i.e. the signs are concordant between the two analyses by chance) in R[71]. This test was evaluated separately for concordance in the 23andMe results and the EAGLE results for loci passing P-value thresholds of $P < 5 \times 10^{-8}$ (i.e. genome-wide significant loci), $P < 1 \times 10^{-7}$, $P < 1 \times 10^{-6}$, $P < 1 \times 10^{-5}$, and $P < 1 \times 10^{-4}$ in the ADHD GWAS meta-analysis. We note that only 11 of the 12 genome-wide significant loci from the ADHD GWAS are present in all data sets; the significant variants from the chromosome 4 locus (index variant: rs28411770) are all absent in the 23andMe and EAGLE results.

Replication meta-analyses and heterogeneity tests

For the replication analysis, we considered three meta-analyses based on the ADHD GWAS meta-analysis result and the results from the two replication cohorts.

First, we performed an inverse variance-weighted meta-analysis of the ADHD GWAS meta-analysis with the 23andMe GWAS. This analysis focused on the case/control diagnosis of ADHD, combining the analysis of clinically ascertained ADHD cases in the ADHD GWAS meta-analysis with the analysis of self-reported ADHD case status in 23andMe data. We refer to this analysis as ADHD+23andMe.

Second, we meta-analyzed the ADHD GWAS meta-analysis with the EAGLE GWAS results using a modified sample size-based weighting method (see detailed description of methods below). This

analysis focuses on concordant results between clinical diagnosed ADHD and continuous measures of ADHD-related behavior in childhood population samples. We refer to this analysis as ADHD+EAGLE.

Finally, we applied the modified sample size-based weighting method to meta-analyze the EAGLE GWAS with the ADHD+23andMe analysis. Although this analysis does not account for imperfect correlation between the clinical ADHD GWAS and the self-report 23andMe GWAS, is does allow joint consideration of the ADHD GWAS meta-analysis with both replication cohorts. We refer to this analysis as ADHD+23andMe+EAGLE.

For each of these three meta-analyses, we evaluated results for the genome-wide significant loci from the ADHD GWAS and identified new loci reaching genome-wide significance. In addition, for the first two replication meta-analyses we considered Cochran's *Q* test of heterogeneity. Specifically, we focus on the 1 degree of freedom test for heterogeneity between the ADHD GWAS and the replication cohort.

Results for replication in 23andMe

We observed moderate concordance of genome-wide significant results between the ADHD GWAS meta-analysis and 23andMe. Of 94 clumped loci with $P < 1 \times 10^{-5}$ in the ADHD GWAS meta-analysis, 71 had effects in the same direction in the 23andMe GWAS, significantly greater than expected by chance ($P = 1.25 \times 10^{-6}$). The direction of effect from 23andMe was also concordant for 8 of the 11 genome-wide significant loci in the ADHD GWAS meta-analysis included in the sign test, though that concordance rate was not statistically significant (P = 0.228; see Supplementary Table 12). Of the genome-wide significant loci, the estimated direction of effect in 23andMe was discordant for loci on chromosome 1 (rs112984125), chromosome 15 (rs281320) and chromosome 16 (rs212178; Supplementary Table 13).

Genetic correlation analysis using LD score regression similarly indicated significant but incomplete genome-wide correlation between the two analyses. The estimated genetic correlation between the 23andMe and the ADHD GWAS was large and significant ($r_g = 0.653$, SE = 0.114, $P = 1.11 \times 10^{-8}$), but also significantly less than 1 (one-sided $P = 1.17 \times 10^{-3}$).

The ADHD+23andMe meta-analysis identified 11 genome-wide significant loci (Supplementary eTable 6, Supplementary Figure 15). Three of these loci were novel: rs30266 (chr5, Refseq gene *LOC105379109*), rs62250537 (chr3, *CADM2*), and rs2243638 (chr13, *RNF219-AS1*). Conversely, 4 of the 12 genome-wide significant loci from the ADHD GWAS meta-analysis were no longer significant after meta-analyzing with 23andMe: rs281324 (chr15, *SEMA6D*), rs212178 (chr16, *LINC01572*), rs4916723 (chr5, *LINC00461*), rs74760947 (chr8, *LINC01288*). Two additional loci are only significant in the ADHD+23andMe meta-analysis for variants that are not present in the 23andMe results: rs11420276 (chr1, *ST3GAL3*) and rs28411770 (chr4, *PCDH7*).

Cochran's *Q* test of heterogeneity identified genome-wide significant heterogeneity between the ADHD GWAS and the 23andMe GWAS in the top locus on chromosome 1 from the ADHD GWAS (Supplementary Figure 16-17). The strongest evidence for discordance was at rs12410155 (*ST3GAL3*), with an estimated odds ratio of 1.111 ($P = 3.63 \times 10^{-13}$) in the ADHD GWAS, compared to an odds ratio of 0.954 (P = 0.0244) in the 23andMe analysis (heterogeneity $P = 2.28 \times 10^{-9}$, $I^2 = 97.2$).

Results for replication in EAGLE

For the most strongly associated loci in the ADHD GWAS meta-analysis, the direction of effect observed in EAGLE was strongly concordant. The estimated effects had the same sign in 10 of the 11 genome-wide significance loci from the ADHD GWAS meta-analysis (P = 0.0159), and for 65 of the 94 loci with $P < 1 \times 10^{-5}$ for the index variant in the ADHD GWAS ($P = 3.06 \times 10^{-4}$; Supplementary

Table 12). Genetic correlation analysis of the EAGLE and ADHD GWAS similarly suggests significant overlap between the two studies (r_g = 0.943, SE = 0.204, P = 3.65 x 10^{-6}). This genetic correlation was not significantly less than 1 (one-sided P = 0.389).

The one genome-wide significant locus from the ADHD GWAS that is not sign concordant between the two studies is on chromosome 12 (index SNP rs1427829; Supplementary Table 13). The A allele for this SNP was associated with higher ADHD risk in the ADHD GWAS meta-analysis (OR = 1.083, P = 1.8x10^{-9}), but slightly favours lower levels of ADHD-related behaviour in EAGLE (z = -0.110, P = 0.91). On the other hand, other SNPs in this locus were sign concordant between the EAGLE and ADHD GWAS results (e.g. rs704067; Supplementary eTable 6).

Using the adjusted sample size-based weighting method described above, we meta-analyzed the EAGLE and ADHD GWAS meta-analysis results. The ADHD+EAGLE meta-analysis identified 15 independent genome-wide significant loci (Supplementary eTable 6, Supplementary Figure 18). All 12 genome-wide significant loci from the ADHD GWAS meta-analysis are significant in the ADHD+EAGLE meta-analysis, as well as new loci on chromosomes 10 (rs2483936, intergenic), 11 (rs4275621, Refseq gene *LOC105376602*), and 13 (rs7997529, *RNF219-AS1*). The chromosome 13 locus is the same one identified by the ADHD+23andMe meta-analysis above. Two of the loci – rs1222063 (chr1, intergenic) and rs9677504 (chr2, *SPAG16*) – are only significant for variants that are not present in the EAGLE results. No significant heterogeneity was observed between the EAGLE and ADHD GWAS meta-analysis (Supplementary Figure 19-20), consistent with the strong genetic correlation between the two studies.

Results for ADHD+23andMe+EAGLE meta-analysis

Meta-analysis of EAGLE and ADHD+23andMe using adjusted sample size-based weights identified 16 independent genome-wide significant loci (Supplementary eTable 6, Supplementary Figure 21).

The genome-wide significant loci included 10 of the 12 loci that are significant in the ADHD GWAS; rs281324 (chr15, *SEMA6D*) and rs212178 (chr16, *LINC01572*) were no longer significant. The genome-wide significant loci also included three loci not identified in the ADHD, ADHD+23andMe, or ADHD+EAGLE meta-analyses: rs62444906 (chr7, *MAD1L1*), rs7459616 (chr8, *DLGAP2*), and rs10419998 (chr19, *TM6SF2*).

Method for meta-analysis of continuous and dichotomous ADHD measures

In order to integrate the EAGLE data with the current analysis, we need to define a framework for comparing the GWAS of (continuous) measures of ADHD-related behavior to the ADHD GWAS meta-analysis of (dichotomous) clinical diagnosis of ADHD.

As a starting point, motivated by the strong genetic correlation between the EAGLE results and the ADHD GWAS meta-analysis, we could consider a conventional sample size-weighted meta-analysis of Z scores. Such an analysis however would not account for: (a) differences in power for continuous vs. dichotomous phenotypes, (b) differences in power from ascertainment on the dichotomous phenotype, (c) differences in the relative strength of overall genetic association (e.g. SNP heritability) for the phenotype measures, or (d) imperfect correlation between the continuous ADHD-related behaviours measured in EAGLE and clinical diagnosis of ADHD, with the matter being the phenotype of interest for the current study.

Therefore, we instead define a basic model for the genetic relationship between clinical diagnosis of ADHD and continuous ADHD-related behaviours that allows us to derive modified sample size-based weights that account for these factors. These weights should be better calibrated to provide a statistically efficient meta-analysis of the EAGLE results with the ADHD GWAS.

Basic genetic model for latent-scale phenotypes

We begin by defining a joint model for the genetics of the two phenotypes. Let Y_1 be the observed dichotomous phenotype and Y_2 be the observed continuous phenotype. For dichotomous phenotype Y_1, we assume there exists some latent continuous liability θ_1 such that

$$Y_1 = \begin{cases} 0, & \theta_1 < \tau_1 \\ 1, & \theta_1 \geq \tau_1 \end{cases}$$

where τ_1 is a threshold corresponding to the population prevalence K of Y_1 consistent with the standard liability threshold model[72]. For convenience, assume that θ_1 is standardized with mean zero and unit variance. Similarly, let θ_2 denote the continuous phenotype Y_2 normalized to have mean 0 and unit variance in the population.

We describe a model for the genetics of the latent continuous phenotypes θ_1 and θ_2 before returning to the impact of the observed scale for each phenotype. Let g_1 and e_1 be genetic and environment components of θ_1, respectively, and let g_2 and e_2 be corresponding components of θ_2 such that

$$\begin{bmatrix} \theta_1 \\ \theta_2 \end{bmatrix} = \begin{bmatrix} g_1 \\ g_2 \end{bmatrix} + \begin{bmatrix} e_1 \\ e_2 \end{bmatrix}$$

$$E\left(\begin{bmatrix} \theta_1 \\ \theta_2 \end{bmatrix}\right) = \mathrm{E}\left(\begin{bmatrix} \mathrm{g}_1 \\ \mathrm{g}_2 \end{bmatrix}\right) = \mathrm{E}\left(\begin{bmatrix} \mathrm{e}_1 \\ \mathrm{e}_2 \end{bmatrix}\right) = \begin{bmatrix} 0 \\ 0 \end{bmatrix}$$

$$Cov\left(\begin{bmatrix} g_1 \\ g_2 \\ e_1 \\ e_2 \end{bmatrix}\right) = \begin{bmatrix} h_1^2 & \rho_g & 0 & 0 \\ \rho_g & h_2^2 & 0 & 0 \\ 0 & 0 & \epsilon_1^2 & \rho_e \\ 0 & 0 & \rho_e & \epsilon_2^2 \end{bmatrix}$$

Note that we assume that not only are genetics and environment uncorrelated within phenotype (i.e. $Cov(g_1, e_1) = Cov(g_2, e_2) = 0$), but also between phenotypes ($Cov(g_1, e_2) = Cov(g_2, e_1) = 0$). Since θ_1 and Y_2^* are each defined to have unit variance, it follows that $\epsilon_1^2 = 1 - h_1^2$, $\epsilon_2^2 = 1 - h_2^2$, and

ρ_g and ρ_e are the genetic and environmental covariances, respectively. The genetic correlation between the latent phenotypes $\theta_1$and θ_2 can then be defined as $r_g \equiv cor(g_1, g_2) = \rho_g / \sqrt{h_1^2 h_2^2}$.

Defining independent genetic factors

We next seek to specify the covariance of g_1 and g_2 in terms of two independent factors f_1 and f_2. This transformation serves two purposes. First, for modeling the effects of individual SNPs it will allow us to define independent effects on f_1 and f_2. Second, if we specify that g_1 depends only on f_1 while g_2 may depend on both f_1 and f_2, then it will be possible to focus on the factor f_1 that determines the genetic component g_1 for Y_1 separate from any independent factors f_2 that contribute to Y_2 only. Separating these factors therefore allows us to move towards the goal of defining a scheme for meta-analysis that focuses only on genetic effects for the dichotomous phenotype (i.e. clinical ADHD diagnosis) while discounting any independent genetic effects that are only relevant to the continuous phenotype (i.e. ADHD-related behaviours).

The desired transformation is given by the inverse of the Cholesky decomposition of the covariance matrix for g_1 and g_2, which yields

$$\begin{bmatrix} f_1 \\ f_2 \end{bmatrix} \equiv \begin{bmatrix} \frac{1}{\sqrt{h_1^2}} & 0 \\ \frac{-r_g}{\sqrt{1-r_g^2}\sqrt{h_1^2}} & \frac{1}{\sqrt{1-r_g^2}\sqrt{h_2^2}} \end{bmatrix} \begin{bmatrix} g_1 \\ g_2 \end{bmatrix}.$$

It can then be shown that

$$Cov\left(\begin{bmatrix} f_1 \\ f_2 \end{bmatrix}\right) = \begin{bmatrix} 1 & 0 \\ 0 & 1 \end{bmatrix},$$

and $E(f_1) = E(f_2) = 0$. By substitution for g_1 and g_2, the latent phenotypes are related to these factors by

$$\theta_1 = \left(\sqrt{h_1^2}\right) f_1 + e_1$$

$$\theta_2 = \left(r_g\sqrt{h_2^2}\right) f_1 + \left(\sqrt{1-r_g^2}\sqrt{h_2^2}\right) f_2 + e_2\,.$$

Effects of individual variants

The above model fully specifies the overall genetic components of the two phenotypes, but does not model the contribution of any specific variant. We now define the effects of individual variants so that we can work towards describing the GWAS results for each phenotype and the desired meta-analysis in terms of parameters for a given variant.

To consider effects for a given variant, let γ_{1j}^* be the causal effect of variant j on f_1, and let γ_{2j}^* be the corresponding effect on f_2. Then

$$f_1 = \sum_j \gamma_{1j}^* x_j$$

$$f_2 = \sum_j \gamma_{2j}^* x_j,$$

where x_j is the standardized genotype of variant j. We denote these causal effects as γ to distinguish them from marginal effects β, and use the * superscript here to indicate that these as effect sizes on the latent genetic components f_1 and f_2 as opposed to the standardized phenotypes. The corresponding causal effects on θ_1 and θ_2 are

$$\gamma_{1j} = \sqrt{h_1^2}\gamma_{1j}^*$$

$$\gamma_{2j} = \left(r_g\sqrt{h_2^2}\right)\gamma_{1j}^* + \left(\sqrt{1-r_g^2}\sqrt{h_2^2}\right)\gamma_{2j}^*$$

respectively.

The marginal effect on f_1 and f_2 will depend not only on the variant's causal effect, but on the causal effect of other variants in LD with x_j. We define the corresponding marginal effects β_j^* as

$$\beta_{1j}^* = \left(X_j' X_j\right)^{-1} X_j' \boldsymbol{X} \boldsymbol{\gamma_1^*} = \sum_k \gamma_{1k}^* r_{jk}$$

$$\beta_{2j}^* = \left(X_j' X_j\right)^{-1} X_j' \boldsymbol{X} \boldsymbol{\gamma_2^*} = \sum_k \gamma_{2k}^* r_{jk}$$

where $r_{jk} = cov(x_j, x_k)$ and $\boldsymbol{\gamma_1^*}$ and $\boldsymbol{\gamma_2^*}$ are column vectors with elements γ_k^* for all k. As with γ^*, the superscript denotes these β_j^* as effect sizes on the latent genetic components f_1 and f_2.

To get marginal effect sizes on the phenotypes, we can denote

$$f_{1,-j} = f_1 - \beta_{1j}^* x_j$$

$$f_{2,-j} = f_2 - \beta_{2j}^* x_j$$

to indicate f_1 and f_2 with the full marginal effect of x_j removed, so that we can then express the phenotypes in terms of the marginal effect of variant j as

$$\theta_1 = (f_{1,-j} + \beta_{1j}^* x_j)\sqrt{h_1^2} + e_1$$

$$= \left(\beta_{1j}^* \sqrt{h_1^2}\right) x_j + \left(\sqrt{h_1^2}\right) f_{1,-j} + e_1$$

$$\theta_2 = \left(r_g \sqrt{h_2^2}\right)(f_{1,-j} + \beta_{1j}^* x_j) + \left(\sqrt{h_2^2\left(1 - r_g^2\right)}\right)(f_{2,-j} + \beta_{2j}^* x_j) + e_2$$

$$= \left[\beta_{1j}^* \left(r_g \sqrt{h_2^2}\right) + \beta_{2j}^* \left(\sqrt{h_2^2\left(1 - r_g^2\right)}\right)\right] x_j + \left(r_g \sqrt{h_2^2}\right) f_{1,-j} + \left(\sqrt{h_2^2\left(1 - r_g^2\right)}\right) f_{2,-j} + e_2$$

Therefore, given θ_1, θ_2 and x_j are all standardized and x_j, $f_{1,-j}$, $f_{2,-j}$, e_1, and e_2 are all independent except for $cov(e_1, e_2) = \rho_e$,

$$\beta_{1j} = cor(x_j, \theta_1) = \beta_{1j}^* \sqrt{h_1^2}$$

$$\beta_{2j} = cor(x_j, \theta_2) = \beta^*_{1j}\left(r_g\sqrt{h_2^2}\right) + \beta^*_{2j}\left(\sqrt{h_2^2(1-r_g^2)}\right)$$

These are the standardized marginal effect of variant j on each phenotype (defined on the latent liability scale in the case of the dichotomous phenotype Y_1). We denote them as β_j because they are the effects of interest for the GWASs of θ_1 and θ_2.

GWAS test statistics for ß$_j$

Given the above parameterization, we can now focus on the behavior of the test statistics from the GWAS of each phenotype. These test statistics are of primary interest since they are the intended input for the desired meta-analysis across the two phenotypes. In particular, we are focused on defining the relationship between these test statistics and β_{1j}, the effect of variant j on the dichotomous phenotype, so that we can calibrate meta-analysis of the observed Z scores to test the null hypothesis $\beta_{1j} = 0$.

Before discussing the test statistics for the observed phenotypes however, it is instructive to describe test statistics for a hypothetical GWAS of the latent phenotypes (θ_1 and θ_2), as a foundation evaluating the impact of e.g. dichotomizing θ_1 to a case/control phenotype. If both θ_1 and θ_2 were observed, we could define Z scores for the standardized effects β_j as

$$\begin{aligned} Z_{\theta,1j} &= \sqrt{N_1}\hat{\beta}_{1j} \\ &= \sqrt{N_{1j}}\beta_{1j} + \sqrt{N_{1j}}\delta_{1j} \\ Z_{\theta,2j} &= \sqrt{N_2}\hat{\beta}_{2j} \\ &= \sqrt{N_{2j}}\beta_{2j} + \sqrt{N_{2j}}\delta_{2j} \end{aligned}$$

where $\hat{\beta}_j$ is the observed GWAS estimate of β_j, N_j is the sample size of the data used to estimate $\hat{\beta}_j$, and δ_j is the corresponding sampling error of the estimate.

$$\delta_{1j} \sim N\left(0, \frac{1}{N_{1j}} var\left[\left(\sqrt{h_1^2}\right) f_{1,-j} + e_1\right]\right)$$

$$\delta_{2j} \sim N\left(0, \frac{1}{N_{2j}} var\left[\left(r_g\sqrt{h_2^2}\right) f_{1,-j} + \left(\sqrt{h_2^2\left(1 - r_g^2\right)}\right) f_{2,-j} + e_2\right]\right)$$

Assuming the marginal effect of any given variant is small, we can approximate $f_{1,-j} \approx f_1$ and $f_{2,-j} \approx f_2$, giving

$$\delta_{1j} \sim N\left(0, \frac{1}{N_{1j}}\left[h_1^2 + \epsilon_1^2\right]\right)$$

$$\sim N\left(0, \frac{1}{N_{1j}}\right)$$

$$\delta_{2j} \sim N\left(0, \frac{1}{N_{2j}}\left[r_g^2 h_2^2 + \left(1 - r_g^2\right)h_2^2 + \epsilon_2^2\right]\right)$$

$$\sim N\left(0, \frac{1}{N_{2j}}\left[h_2^2 + \epsilon_2^2\right]\right)$$

$$\sim N\left(0, \frac{1}{N_{2j}}\right)$$

based on f and e being independent, $var(f) = 1$, $var(e) = \epsilon^2$, and $h^2 + \epsilon^2 = 1$. To the extent that $f \neq f_{-j}$, then this is an overestimate of the variance of δ_j since $var\left(f_{-j}\right) \leq 1$. Returning to the Z scores defined previously, this gives

$$Z_{\theta,1j} \sim N(\sqrt{N_{1j}}\beta_{1j}, 1)$$

$$Z_{\theta,2j} \sim N\left(\sqrt{N_{2j}}\beta_{2j}, 1\right)$$

which have the desired standard normal distribution when $\beta_j = 0$. We can also express these in terms of the latent effects β_j^*

$$Z_{\theta,1j} \sim N(\sqrt{N_{1j}h_1^2}\beta_{1j}^*, 1)$$

$$Z_{\theta,2j} \sim N\left(r_g\sqrt{N_{2j}h_2^2}\beta_{1j}^* + \sqrt{N_{2j}h_2^2\left(1 - r_g^2\right)}\beta_{2j}^*, 1\right)$$

$$\sim N\left(\sqrt{N_{2j}h_2^2}\left[r_g\beta_{1j}^* + \sqrt{1-r_g^2}\beta_{2j}^*\right], 1\right)$$

We now consider how the actual observed Z statistics for each phenotype will differ from these idealized tests of association with the latent phenotypes.

Test of ß$_{ij}$ in GWAS of dichotomous Y$_1$

For the dichotomous phenotype (i.e. ADHD diagnosis) we do not observe the latent liability θ_1, and thus we cannot compute $Z_{\theta,1j}$. Instead the GWAS results come from logistic regression of the observed phenotype Y_1. The statistical properties of Z_{2j} will be affected by two key features of GWAS with case/control phenotypes: dichotomization and ascertainment. For dichotomization, recall that

$$\beta_{1j} = cor(x_j, \theta_1)$$

It has been shown that dichotomizing one variable attenuates the correlation such that if x and Y are approximated as bivariate normal

$$cor(x_j, Y_1) \approx \frac{\phi(\Phi^{-1}[K])}{\sqrt{K(1-K)}} cor(x_j, \theta_1)$$

where K is the prevalence of $Y_1 = 1$ after dichotomization, and $\phi(\cdot)$ and $\Phi^{-1}(\cdot)$ are the density function and inverse of the cumulative density function of the standard normal distribution, respectively[73,74].

With respect to case/control ascertainment, we note that the power of logistic regression is approximately proportional to $\sqrt{P^*(1-P^*)}$, where P^* is the probability $Y = 1$ at the mean liability in the sample[75]. Given a symmetric distribution of liability, $P^* \approx P$ where P is the sample proportion of cases. Therefore, power for the analysis in an ascertained sample differs from power in a population sample with the sample size by a factor of $\sqrt{P(1-P)}/\sqrt{K(1-K)}$.

Putting together these adjustments for dichotomization and ascertainment, we adopt the approximation

$$Z_{1j} \sim N\left(\frac{\phi(\Phi^{-1}[K])}{\sqrt{K(1-K)}}\frac{\sqrt{P(1-P)}}{\sqrt{K(1-K)}}\sqrt{N_{1j}}\beta_{1j}, 1\right)$$

Importantly, we note that this adjustment mirrors the conversion between observed scale heritability and liability scale heritability derived by Lee at al[76].

$$h^2_{obs} = h^2_{liab}\frac{(\Phi^{-1}[K])^2}{K(1-K)}\frac{P(1-P)}{K(1-K)}$$

Indeed, noting that

$$\beta_{1j} = \beta^*_{1j}\sqrt{h^2_1}$$

we can equate

$$\begin{aligned} E(Z_{1j}) &= \frac{\phi(\Phi^{-1}[K])}{\sqrt{K(1-K)}}\frac{\sqrt{P(1-P)}}{\sqrt{K(1-K)}}\sqrt{N_{1j}}\beta_{1j} \\ &= \frac{\phi(\Phi^{-1}[K])}{\sqrt{K(1-K)}}\frac{\sqrt{P(1-P)}}{\sqrt{K(1-K)}}\sqrt{N_{1j}}\beta^*_{1j}\sqrt{h^2_1} \\ &= \sqrt{N_{1j}}\sqrt{h^2_1\frac{(\Phi^{-1}[K])^2}{K(1-K)}\frac{P(1-P)}{K(1-K)}}\beta^*_{1j} \\ &= \sqrt{N_{1j}}\sqrt{h^2_{1,obs}}\beta^*_{1j} \end{aligned}$$

which highlights the parallel between the observed Z_{1j}, the test the effect of variant j on the observed scale, and the corresponding $Z_{\theta,1j}$ testing on the latent scale.

Finally, we can define an effective sample size adjustment for N_1

$$\widetilde{N}_{1j} \equiv N_{1j}\frac{P(1-P)\,\phi(\Phi^{-1}[K])^2}{[K(1-K)]^2}$$

so that the approximate distribution of Z_{1j} from logistic regression of the dichotomous phenotype can be expressed as

$$Z_{1j} \sim N\left(\sqrt{\tilde{N}_{1j}}\beta_{1j}, 1\right)$$

This formulation, with Z_{1j} following a standard normal distribution conditional on (adjusted) sample size and the effect of interest (β_{1j}), is central to allowing the desired meta-analysis.

Test of ß$_{1j}$ in GWAS of continuous Y$_2$

For the continuous phenotype Y_2, the observed Z scores are computed from conventional linear regression of the observed phenotype. The observed phenotype only differs from the latent θ_2 by a linear transformation to center and scale to unit variance. Thus since Z scores are invariant linear transformations of the phenotype,

$$Z_{2j} = Z_{\theta,2j}$$

But unlike the dichotomous phenotype analysis, the GWAS of Y_2 is a test of $\beta_{2j} = 0$ rather than $\beta_{1j} = 0$. For the current analysis, our primary interest is in the latter test to identify effects β_{1j} of each variant on the dichotomous phenotype of ADHD diagnosis. The residual effects from f_2 in β^*_{2j} that are unique to the continuous trait (population measures of ADHD-related behavior) are of less relevance, and given a high r_g are anticipated to have a limited contribution even to the continuous measure (proportional to $\sqrt{1 - r_g^2}$).

For that reason, we adopt a random effects framework for β^*_{2j}, and treat them as nuisance parameters. Specifically, we assume that the causal effect sizes

$$\gamma^*_{2j} \sim N\left(0, \frac{1}{M}\right)$$

where M is the total number of variants j. This is equivalent to the standard infinitesimal random effects model used by[40,77], but specified here in terms of γ_{2j}^* on the latent scale of f_2 prior to scaling by h_2^2 for the phenotype. For the marginal effects

$$\beta_{2j}^* = \sum_k \gamma_{2k}^* r_{jk}$$

we additionally assume that γ_{2k}^* and r_{jk} are independent, meaning that the causal effect size of variant k is independent of its LD with other variants. This leads to

$$\beta_{2j}^* \sim N\left(0, \sum_k \frac{1}{M} r_{jk}^2\right)$$

$$\beta_{2j}^* \sim N\left(0, \frac{1}{M} l_j\right)$$

where we note that

$$l_j = \sum_k r_{jk}^2$$

is the LD score of variant j as defined by Bulik-Sullivan et al[40].

Returning to the Z score, we note that the previous expression for Z_{2j}^* is now a conditional distribution given a particular value of β_{2j}^*.

$$Z_{2j} | \beta_{2j}^* \sim N\left(\sqrt{N_{2j} h_2^2}\left[r_g \beta_{1j}^* + \sqrt{1 - r_g^2}\beta_{2j}^*\right], 1\right)$$

Substituting $\beta_{1j} = \beta_{1j}^* \sqrt{h_1^2}$ as the actual parameter of interest and marginalizing over β_{2j}^* as a random effect yields

$$Z_{2j} \sim N\left(r_g \sqrt{N_{2j} h_1^2 h_2^2}\beta_{1j}, 1 + \left(1 - r_g^2\right)\frac{N_{2j} h_2^2}{M} l_j\right)$$

To construct the intended meta-analysis for genetics effects on the diagnosis of ADHD, we want to have a test statistic that has a standard normal distribution under the null hypothesis $\beta_{1j} = 0$.

Although Z_{2j} is normally distributed with mean zero under that null hypothesis, it's variance is inflated if Y_2 is heritable (i.e. $h_2^2 > 0$) and is not completely genetically correlated with Y_1 (i.e. $r_g < 1$). We note that inflation proportional to $N_{2j}h_2^2 l_j/M$ is consistent the expected values derived by Bulik-Sullivan et al.[40] To obtain a statistic with the desired distribution, we define a new modified Z score

$$\tilde{Z}_{2j} = \frac{Z_{2j}}{\sqrt{1 + \left(1 - r_g^2\right)\frac{N_{2j}h_2^2}{M} l_j}}$$

which is distributed as

$$\tilde{Z}_{2j} \sim N\left(\frac{r_g\sqrt{N_{2j}h_2^2/h_1^2}}{\sqrt{1 + \left(1 - r_g^2\right)\frac{N_{2j}h_2^2}{M} l_j}}\beta_{1j}, 1\right)$$

We note that $\left|\tilde{Z}_{2j}\right| \leq \left|Z_{2j}\right|$ since $\left[1 + \left(1 - r_g^2\right) N_{2j}h_2^2 l_j/M\right] \geq 1$ by definition for the involved quantities. Therefore $\tilde{Z}_{2j}$ can be interpreted as a more conservative estimate for inference about β_{1j} that has been attenuated from the raw observation proportional to the potential for genetic effects on the continuous phenotype to be unique to that phenotype rather than shared with the dichotomous outcome (i.e. $\left[1 - r_g^2\right]h_2^2$).

Lastly, if we define adjusted N_2 as

$$\widetilde{N}_{2j} \equiv N_{2j}\frac{r_g^2 h_2^2/h_1^2}{1 + (1 - r_g^2) N_{2j}h_2^2 l_j/M}$$

then the distribution of the modified test statistic can be expressed as

$$\tilde{Z}_{2j} \sim N\left(\sqrt{\widetilde{N}_{2j}}\beta_{1j}, 1\right)$$

This provides a clear parallel to Z_{1j} for the dichotomous phenotype, and sets up the meta-analysis of the two Z scores.

Meta-analysis for ß$_{1j}$ from GWAS of dichotomous Y$_1$ and continuous Y$_2$

Summarizing the above derivations, we have now established a framework for the GWAS results of dichotomous phenotype Y_1 and continuous phenotype Y_2, respectively, where we can approximate

$$Z_{1j} \sim N\left(\sqrt{\widetilde{N}_{1j}}\beta_{1j}, 1\right)$$

$$\tilde{Z}_{2j} \sim N\left(\sqrt{\widetilde{N}_{2j}}\beta_{1j}, 1\right)$$

where

$$\tilde{Z}_{2j} = \frac{Z_{2j}}{\sqrt{1 + \left(1 - r_g^2\right)N_{2j}h_2^2\, l_j/M}}$$

$$\widetilde{N}_{1j} = N_{1j}\frac{P(1-P)\,\phi(\Phi^{-1}[K])^2}{[K(1-K)]^2}$$

$$\widetilde{N}_{2j} = N_{2j}\frac{r_g^2 h_2^2/h_1^2}{1 + (1 - r_g^2)\,N_{2j}h_2^2 l_j/M}$$

From this form, we have a pair of Z statistics for β_{1j} with corresponding (adjusted) sample sizes. This is sufficient to then proceed with a conventional sample size-weighted meta-analysis[78].

$$Z_{j,meta} = \frac{\sqrt{\widetilde{N}_{1j}}Z_{1j} + \sqrt{\widetilde{N}_{2j}}\tilde{Z}_{2j}}{\sqrt{\widetilde{N}_{1j} + \widetilde{N}_{2j}}}$$

Expanding the numerator makes it clear that the adjusted sample size weights corresponds to weighting each Z proportional to the observed heritability and then balancing by genetic correlation.

$$Z_{j,meta} = \frac{\sqrt{N_{1j}\frac{P(1-P)\,\phi(\Phi^{-1}[K])^2}{[K(1-K)]^2}}Z_{1j} + \sqrt{N_{2j}\frac{r_g^2 h_2^2/h_1^2}{1+(1-r_g^2)\,N_{2j}h_2^2 l_j/M}}\tilde{Z}_{2j}}{\sqrt{\widetilde{N}_{1j}+\widetilde{N}_{2j}}}$$

$$Z_{j,meta} \propto \sqrt{h_{1,obs}^2}\sqrt{N_{1j}}Z_{1j} + r_g\sqrt{h_2^2}\sqrt{N_{2j}}\frac{\tilde{Z}_{2j}}{\sqrt{1+(1-r_g^2)\,N_{2j}h_2^2 l_j/M}}$$

We use these weights to implement the meta-analysis of the GWAS of ADHD-related behavior from EAGLE with the ADHD GWAS.

Notes on Implementation

It may be noted that $\tilde{Z}_{2j}$, $\widetilde{N}_{1j}$, and $\widetilde{N}_{2j}$ are computed from both observed values (Z_{1j}, Z_{2j}, N_{1j}, N_{2j}, and P) and unknown population parameters (K, r_g^2, h_1^2, h_2^2, l_j, and M). Sensible estimates for each of these population parameters can be obtained as described below and plugged into the expression for the weights. Importantly, estimation error in K, r_g^2, h_1^2, h_2^2, l_j, and M is only expected to affect the efficiency (i.e. power) of the meta-analysis. For a fully null variant (i.e. $\beta_{1j}^* = \beta_{2j}^* = 0$), Z_{1j} and Z_{2j} both have standard normal distributions, and since they are independent any weighted combination of these Z scores will also follow the null distribution. Suboptimal weights will only affect the power of the meta-analysis when the null hypothesis does not hold. In addition, since we use $\tilde{Z}_{2j}$ in place of $\tilde{Z}_{2j}$ and $|\tilde{Z}_{2j}| \leq |Z_{2j}|$, the test of $Z_{j,meta}$ will be conservative when there is no genetic effect specific to the continuous phenotype (i.e. $\beta_{2j}^* = 0$).

With this reassurance, we obtain estimates of K, r_g^2, h_1^2, h_2^2, l_j, and M as follows:

- Estimates of K can be derived from the literature. We use $K = .05$ for the prevelance of ADHD here and throughout this paper[79].

- Estimates of r_g^2, h_1^2 and h_2^2 are computed from the GWAS results using LD score regression[40]. For meta-analysis with the ADHD GWAS, we use the European ADHD GWAS to estimate these parameters in order to ensure that the population ancestry is matched between the input GWAS for ADHD, EAGLE, and the European reference panel used for computing LD scores.
- For M, we utilize the value $M = 5{,}961{,}159$ corresponding to LD scores computed from 1000 Genomes Project Phase 3 data on individuals of European ancestry[34]. These LD scores have been described previously[64] and are publically available for download at: http://data.broadinstitute.org/alkesgroup/LDSCORE/
- We estimate $l_j = 124.718$, the mean LD score of common HapMap3 SNPs as computed from 1000 Genomes Project Phase 3 data on individuals of European ancestry (as above). We use this value for two reasons: (a) using a single value is convenient and allows meta-analysis for all variants in the GWAS, including variants that may not be present in the precomputed LD scores from the 1000 Genomes Project reference data; and (b) we can demonstrate that the value of l_j has a trivial impact on the derived meta-analysis weights when the sample sizes, heritabilities, and genetic correlation are at the levels observed in the current study.

To demonstrate this final point, we consider the relative difference in $\tilde{Z}_{2j}$ and $\tilde{N}_{2j}$ conditional on a range of possible values of l_j with fixed values of N_{1j}, N_{2j}, and P and fixed estimates of K, r_g^2, h_1^2, h_2^2, and M. First, we observe that the >99.5% of 1000 Genomes LD scores have values between 0 and 1000 (Supplementary Figure 22); variants with higher LD scores are predominantly from known regions of long-range LD (e.g. the MHC region[35]). Then we show that for LD scores in this range the value of $\sqrt{1 + (1 - r_g^2) N_{2j} h_2^2 \, l_j / M}$, the term used to adjust the magnitude of Z_{2j} to account for polygenic effects specific to the second phenotype, is minimally affected by the value of l_j

conditional on the estimates of r_g^2, N_{2j}, and h_2^2, observed in the current study (Supplementary Figure 23). The impact of l_j on the relative effective sample size $\widetilde{N}_{2j}$ is also limited, with the weight effectively unchanged for values of l_j between 0 and 1000 (Supplementary Figure 24).

We note however that the limited effect of l_j on the shrinkage parameter and the relative effective sample size is conditional on the estimated values for the other parameters in the current study. Specifically, l_j contributes to the meta-analysis weights through the term $\sqrt{1 + \left(1 - r_g^2\right) N_{2j} h_2^2 \, l_j / M}$. When r_g is large (e.g. $r_g = .94$ for the ADHD GWAS and EAGLE) and N_{2j} and h_2^2 are modest (e.g. $N_{2j} = 17{,}666$ and $h_2^2 = .078$ for EAGLE) the potential contribution of l_j to the value of this term is limited. On the other hand, if the genetic correlation is further from 1 (e.g. r_g =.7) or the GWAS of the continuous phenotype is better powered (e.g. $N_{2j} = 40{,}000$ and $h_2^2 = .40$) then the influence of l_j on the meta-analysis weights becomes non-negligible (Supplementary Figures 23-24). Thus although the parameters for the current study enable the convenient use of mean l_j for all variants, this simplification cannot be expected to hold for all studies.

Supplementary Tables

Supplementary Table 1. Samples included in the GWAS meta-analyses of diagnosed ADHD

Samples marked in bold are included in the GWAS meta-analysis. The European GWAS meta-analysis excludes samples marked with "*" and PUWMa (strict) is used in place of PUWMa. "% F" reports the percentages of females among cases and controls. "Children/Adults" indicates the age range of the participants with ADHD. "Literature" lists previously published studies including the ADHD cohort.

Sample	Cases	% F cases	Controls	% F controls	Children/Adults	Sample design	Ancestry	Genotyping chip	Literature
Lundbeck Foundation Initiative for Integrative Psychiatric Research (iPSYCH)									
iPSYCH-ADHD, Denmark	14584	26.6%	22492	49.2%	Children & adults	Case-control	European	PsychChip	New
Psychiatric Genomics Consortium (PGC)									
Barcelona, Spain	572	30.20%	425	23.50%	Adults	Case-control	European	Illumina Omni1-Quad	Ribases et al.[80], Sanchez-Mora et al.[13]
Beijing, China*	1012	15.70%	925	37.80%	Children	Case-control	Han Chinese	Affymetrix 6.0	Yang et al.[14]
Bergen, Norway	295	53.60%	202	60.90%	Adults	Case-control	European	Illumina OmniExpress-12v1	Zayats et al.[15]
Cardiff, UK	721	12.90%	5081	49.40%	Children	Case-control	European	Illumina 660K (cases) & Illumina 1.2M (controls)	Stergiakouli et al.[16]
CHOP, USA	262	24.40%	262	24.40%	Children	Trios	European	Illumina 550K	Elia et al.[8], Neale et al.[10]
Germany	487	19.30%	1290	49.10%	Children	Case-control	European	Illumina 660K (cases) & Illumina 550v3 (controls)	Hinney et al.[17]
IMAGE-I	700	12.10%	700	12.10%	Children	Trios	European	Perlegen 600K	Neale et al.[9,10]
IMAGE-II	624	18.60%	1755	50.00%	Children	Case-control	European	Affymetrix 5.0 & Affymetrix 6.0	Neale et al.[10]
PUWMa*	635	35.70%	635	35.70%	Children	Trios	Diverse (USA)	Illumina 1M-Duo	Mick et al.[11], Neale et al.[10]
PUWMa (strict)	563	35.90%	563	35.90%	Children	Trios	European	Illumina 1M-Duo	
Toronto, Canada	109	24.80%	109	24.80%	Children	Trios	European	Affymetrix 6.0	Lionel et al.[12]
Yale-Penn	182	30.20%	1315	42.20%	Adults	Case-control	European	Illumina HumanOmni1-Quad & Illumina Infinium Human Core Exome	Gelernter et al.[21-23] (studies of substance use disorders)

Supplementary Table 2. Conditional Analysis of Secondary GWAS Signals

Linkage disequilibrium (r^2) computed between the putative secondary effect variant and the index variant in individuals of European ancestry from the 1000 Genomes Project (1KG), and imputed genotypes in the merged PGC and iPSYCH cohorts. Odds ratio (OR) and standard error (SE) of the secondary variant reported for the primary GWAS and conditional on the corresponding index variant.

				r^2 with Index Variant			**Marginal Association**			**Conditional Association**		
Variant	CHR	BP	Index Var.	1KG	PGC	iPSYCH	OR	SE	P	OR	SE	P
rs3952787	1	44323244	rs11420276	0.054	0.046	0.064	1.085	0.015	3.49×10^{-8}	1.063	0.015	6.02×10^{-5}
rs304132	5	88215594	rs4916723	0.051	0.059	0.091	0.925	0.014	4.23×10^{-8}	0.939	0.015	2.03×10^{-5}

Supplementary Table 3. Summary of Bayesian Credible Set Results

For each genome-wide significant locus (denoted with the chromosome [CHR] and base pair [BP] position of the index variant), the number of variants that are the in the 99% credible set computed based on linkage disequilibrium (LD) in the PGC cohorts, the 99% credible set computed based on LD in the iPSYCH data, and their overlap.

			Number of Variants in Credible Set		
CHR	**Index Variant**	**BP**	**PGC only**	**iPSYCH only**	**Both sets**
1	rs11420276	44184192	0	0	96
12	rs1427829	89760744	0	0	13
16	rs212178	72578131	0	3	21
4	rs28411770	31151456	0	0	53
10	rs11591402	106747354	0	0	87
8	rs74760947	34352610	0	1	13
2	rs9677504	215181889	0	0	23
5	rs4916723	87854395	0	0	67
7	rs5886709	114086133	5	0	63
3	rs4858241	20669071	1	5	44
15	rs281324	47754018	0	0	43
1	rs1222063	96602440	0	4	4

Supplementary Table 4. Biological function of potential ADHD risk genes located in genome-wide significantly associated loci

Literature review of biological function, mutational constraint, tissue-specific expression, and relevant phenotypic associations for genes affiliated with the 12 loci significantly associated with ADHD. Mutational constraint is indexed by the estimated probability of loss-of-function intolerance (pLI) reported by the Exome Aggregation Consortium (ExAC; release 0.3.1)[58].

Chr	Gene	Index SNP	P-value	Function of encoded product	pLI	Tissue specificity	ADHD-related phenotype associations
1	*ST3GAL3*	rs11420276	2.14×10^{-13}	ST3 Beta-Galactoside Alpha-2,3-Sialyltransferase 3 (*ST3GAL3*), encodes a membrane protein (ST3Gal III) that adds sialic acid to the terminal site of glycolipids or glycoproteins. ST3Gal III may play an important role in brain development as the human brain is especially enriched in sialic acid-containing glycolipids (termed gangliosides)[81-83] and in mice *St3gal2* and *St3gal3* were found to be responsible for nearly all the terminal sialylation of brain gangliosides[84] as well as playing an important role for normal cognition[82]. Gangliosides are known to modulate Ca(2+) homeostasis and signal transduction in neurons[85,86].	0.57	This gene is expressed in several tissues including neurons[82].	Mutations in this gene have been associated with autosomal recessive mental retardation[83] and early infantile epileptic encephalopathy[87]. DNA methylation at sites annotated to *ST3GAL3* were reported capable to differentiate individuals with high and low ADHD symptomatology ratings[88]. Variants in *ST3GAL3* have also been associated with educational attainment[89].
1	*PTPRF*	rs3001723	3.62×10^{-10}	Homo sapiens protein tyrosine phosphatase, receptor type, F (*PTPRF*). *PTPRF* encodes the leukocyte common antigen-related (LAR) receptor PTP which is present in neurons expressing TrkB, and LAR is associated with caveolae and regulates survival and	1.00	This gene is expressed in several tissues including neurons[91].	Gws association of genetic markers in *PTPRF* with schizophrenia has been found[30]. Gws association of genetic markers in *PTPRF* with educational attainment has been found in a study of individuals from the UK Biobank (*N*=112,151)[92]. Overexpression of the

				neurite outgrowth [90]. The LAR receptor is present in neurons expressing TrkB, which is receptor for the brain-derived neurotrophic factor (BDNF), and it has been demonstrated that LAR, through its interaction with TrkB can affect the neurotrophic activity of BDNF[91].			LAR receptor encoded by *PTPRF* may contribute to insulin resistance[93].
1	Intergenic	rs1222063	3.07×10^{-8}	Not applicable.	n/a	Not applicable.	Not applicable.
2	*SPAG16*	rs9677504	1.39×10^{-8}	Homo sapiens sperm associated antigen 16 (*SPAG16*). *SPAG16* encodes two major proteins that associate with the microtubular backbone of sperm tails and the nucleus of postmeiotic germ cells [94,95].	0.00	Highly expressed in testis, but also detected throughout many tissues including brain, spinal cord, pituitary ovary, esophagus, thyroid, vagina, tibial nerve, bladder (http://www.gtexportal.org/home/gene/ENSG00000144451.14)	Studies have suggested that SPAG16 may play a role in multiple sclerosis[96,97].
3	Intergenic	rs4858241	1.74×10^{-8}	Not applicable.	n/a	Not applicable.	Not applicable.
4	*PCDH7*	rs28411770	1.15×10^{-8}	Homo sapiens protocadherin 7 (*PCDH7*). This gene belongs to the protocadherin gene family, a subfamily of the cadherin superfamily. It encodes an integral membrane protein that is thought to function in cell-cell recognition and calcium-dependent adhesion[98,99] and plays an important role in neuron development[100].	n/a	The gene is expressed in several brain regions especially the thalamus, cerebral cortex and brainstem circuits[101].	Variants in *PCDH7* have been significantly associated with generalised epilepsy in GWAS[102]. *PCDH7* is a target gene for *MECP2*[103] and *MECP2* mutations causes Rett syndrome, which is a is a neurodevelopmental disorder characterized by loss of speech, microcephaly, seizures, and mental retardation (http://omim.org/entry/312750).
5	*LINC00461*	rs4916723	1.58×10^{-8}	Homo sapiens long intergenic noncoding RNA 461 (*LINC00461*), also known as visual cortex-expressed gene (Visc). The locus is conserved across	n/a	Primarily expressed in the brain[47] (https://www.gtexportal.org/home/gene/LINC00461).	Variants in *LINC00461* have been associated with educational attainment[89].

				diverse mammals, but mouse knockouts of the Visc-2 transcript do no exhibit any clear anatomical phenotype[104].		In mice, it's strongly localized in the cortex and sites of neurogenesis during neurodevelopment and continuing into adulthood[104].	
5	*MEF2C / MEF2C−AS1*	rs304132	4.22×10^{-8}	Homo sapiens myocyte enhancer factor 2C (*MEF2C*). *MEF2C* encodes a member of the MADS box transcription factors, which binds to the conserved MADS box sequence motif[105]. *MEF2C* is important for normal neuronal function by regulating neuronal proliferation, differentiation, survival and synapse development[106-108]. Plays a role in hippocampal-dependent learning and memory, possibly by controlling the number of excitatory synapses[107,109].	0.00	*MEF2C* is expressed in brain especially the frontal cortex, cortex and skeletal muscle (http://www.gtexportal.org/home/gene/MEF2)	Mutations and deletions in *MEF2C* have been associated with severe mental retardation, stereotypic movements, epilepsy, lack of speech and cerebral malformation (http://omim.org/entry/613443). GWAS studies have identified genome-wide significant association of variants in loci implicating *MEF2C* with Alzheimer´s disease[110], depression[111] and schizophrenia[30]. *Mef2c* knockout mice have demonstrated autism like behaviours[106,108], and individuals with *MEF2C* deletions have been found to display autism like traits [112,113].
7	*FOXP2*	rs5886709	1.66×10^{-8}	Homo sapiens forkhead box P2 (*FOXP2*). This gene encodes a member of the forkhead/winged-helix (FOX) family of transcription factors. *FOXP2* is involved in e.g. synapse formation and neural mechanisms mediating the development of speech and language and learning related to linguistic issues [114-116]. It influences a large number of downstream gene targets[57,114,117] with potential regional or tissue-specific differences in activity[57].	1.00	*FOXP2* is expressed in both fetal and adult human brain[118,119].	Deletions in *FOXP2* may cause speech-language disorder 1 (SPCH1) inherited in an autosomal dominant manner. The disorder is characterized by abnormal development of several brain areas critical for both orofacial movements and sequential articulation[117,120] (http://omim.org/entry/602081). Candidate gene analysis previously suggested tentative evidence for association between *FOXP2* and ADHD[121]. Variants in FOXP2 have also been associated with educational attainment[89], and age of having a child[122].

8	*LINC01288*	rs74760947	1.35×10^{-8}	Homo sapiens long intergenic non-protein coding RNA 1288 (*LINC01288*). No additional information available.	n/a	No information available.	No information available.
10	*SORCS3*	rs11591402	1.34×10^{-8}	Homo sapiens sortilin-related VPS10 domain containing receptor 3 (*SORCS3*). This gene encodes a transmembrane receptor that is a member of the vacuolar protein sorting 10 receptor family[123]. *SORCS3* is involved in signalling and intracellular sorting[124] important for neuronal development and synaptic plasticity[125,126].	0.33	Expressed in both the prenatal and adult brain regions [126] (http://www.gtexportal.org/home/gene/SORCS3)	Rare CNVs overlapping *SORCS3* have been suggested to be involved in ADHD[12]. Decreased expression of *SORCS3* in brains from patients with Alzheimer´s disease compared to controls has been found[127]. GWAS studies have demonstrated strong association of variants in *SORCS3* with schizophrenia (however not gws)[30] and gws association with depression[111].
12	*DUSP6*	rs1427829	1.82×10^{-9}	Homo sapiens dual specificity phosphatase 6 (*DUSP6*). The protein encoded by *DUSP6* is a member of the dual specificity protein phosphatase subfamily[128]. *DUSP6* (also referred to as mitogen kinase phosphatase 3 (*MKP-3*)) is involved in negative regulation of mitogen-activated protein kinases (MAPKs) by acting as a dual phosphatase that dephosphorylate MAPKs at both threonine and tyrosine residues and thereby inactivate them[129]. *DUSP6* is a cytoplasmic enzyme which has preference for extracellular signal-regulated MAPKs[129-131]. MAPKs are components of highly conserved signal transduction pathways, responding to a wide variety of extracellular and intracellular stimuli, and they are involved in e.g. embryogenesis, cellular proliferation and differentiation[132-134]. Additionally *MKP-3* has been suggested to play a role in regulating	0.91	Generally expressed at low levels in the brain (http://gtexportal.org/home/gene/DUSP6) and is strongly regulated during development[134].	Rare mutations in *DUSP6* may lead to congenital hypogonadotropic hypogonadism[138] (http://omim.org/entry/602748). *DUSP6* may play a role in Hirschsprung´s disease, due to decreased expression [139]. *DUSP6* have been found in reduced levels in Alzheimer brains[140]. Additionally, *MKP-3* may play a critical role in cancer development[141,142].

				neurotransmitter homeostasis, as increased *MKP-3* was found to reduce depolarization-dependent release of dopamine in rat PC12 cells, possibly through a down regulation of *Cacna1c*[135]. It has been suggested that *MKP-3* stabilizes the dopamine transporter in the presynaptic dopaminergic neuron[136]. *MKP-3* is upregulated by methamphetamine[137].			
15	*SEMA6D*	rs281324	2.68×10^{-8}	Homo sapiens sema domain, transmembrane domain (TM), and cytoplasmic domain, (semaphorin) 6D (*SEMA6D*). The product encoded by this gene is a transmembrane semaphoring which play role in maintenance and remodeling of neuronal connections[143]. *Sema6D* acts as ligand for PlexinA1 which is involved in critical steps of neuronal development in the spinal cord[144] as well as cardiac development[145,146].	1.00	Expressed in adult brain, spinal cord, and fetal brains[143].	Variants in *SEMA6D* have been associated with educational attainment[89].
16	*LINC01572*	rs212178	7.68×10^{-9}	Homo sapiens long intergenic non-protein coding RNA 1572 (*LINC01572*). No additional information available.	n/a	No information available.	No information available.

Supplementary Table 5. Results from MAGMA gene-based association with ADHD

Genes demonstrating significant gene-wise association with ADHD after Bonferroni correction in the MAGMA[41] analysis. Chromosome (CHR), number of SNPs in the genes (N SNPS) and number of relevant parameters used in the model (N PARAM) are shown. Chromosome band location of the associated gene and the chromosome band location of the nearest gws single marker are shown. Genes marked in bold are not overlapping with loci with gws single markers.

Gene	CHR	N SNPS	N PARAM	P	Location of Gene	Location of nearest gws marker
ST3GAL3	1	483	57	7.38×10^{-12}	1p34.1	1p34.1
KDM4A	1	71	28	2.15×10^{-11}	1p34.1	1p34.1
PTPRF	1	226	60	5.68×10^{-10}	1p34.2	1p34.2
SZT2	1	87	25	8.47×10^{-9}	1p34.2	1p34.2
TIE1	1	30	15	2.01×10^{-8}	1p34.2	1p34.2
MPL	1	13	6	3.33×10^{-8}	1p34.2	1p34.2
CDC20	1	5	5	6.34×10^{-8}	1p34.2	1p34.2
HYI	1	5	4	3.28×10^{-7}	1p34.2	1p34.2
SLC6A9	1	60	31	7.58×10^{-7}	1p34.1	1p34.1
ELOVL1	1	3	3	1.26×10^{-6}	1p34.2	1p34.2
CCDC24	1	6	5	2.12×10^{-6}	1p34.1	1p34.1
MANBA	**4**	**203**	**55**	**6.00×10^{-8}**	**4q24**	**4p15.1(*PCDH7*)**
MEF2C	5	320	54	3.19×10^{-8}	5q14.3	5q14.3
FOXP2	7	812	110	5.50×10^{-7}	7q31.1	7q31.1
SORCS3	10	1823	106	2.18×10^{-9}	10q25.1	10q25.1
CUBN	**10**	**1172**	**167**	**1.59×10^{-7}**	**10p13**	**10q25.1 (*SORCS3*)**
PIDD1	**11**	**27**	**12**	**5.30×10^{-7}**	**11p15.5**	**NA**
DUSP6	12	20	8	2.24×10^{-9}	12q21.33	12q21.33
SEMA6D	15	1458	138	2.63×10^{-10}	15q21.1	15q21.1
CDH8	**16**	**764**	**79**	**4.67×10^{-8}**	**16q21**	**16q22.2 (*LINC01572*)**

Supplementary Table 6. Results from MAGMA gene-based association of ADHD candidate genes

MAGMA[41] analysis of previously reported candidate genes for ADHD from a recent review[53]. Number of SNPs in the genes (N SNPS), number of relevant parameters used in the model (N PARAM) are shown.

Gene symbol	Entrez ID	N SNPS	N PARAM	Z	P
SLC9A9	285195	1609	129	3.395	3.40×10^{-4}
DRD5	1816	4	2	-1.374	0.92
SLC6A3	6531	101	12	-0.975	0.84
HTR1B	3351	3	1	2.246	0.012
DRD4	1815	5	2	-0.192	0.58
NOS1	4842	410	30	1.088	0.14
GIT1	28964	21	5	0.77	0.22
SLC6A4	6532	67	12	-0.021	0.51
SNAP25	6616	180	25	-0.512	0.7

Supplementary Table 7. Enrichment analysis of gene sets related to *FOXP2* downstream target genes

Competitive gene set analysis of each set of *FOXP2* target genes performed using MAGMA[41]. For each gene set, the number of genes (N Genes), raw and semi-standardized (Std.) regression coefficients, and corresponding standard error (SE) are reported.

Gene Set	N Genes	Beta	Beta (Std.)	SE	P
Mouse brain (ChIP-chip)	219	0.016	0.002	0.06	0.39
Mouse brain (knockout)	243	0.034	0.004	0.055	0.27
Human brain (ChIP-chip)	258	-0.094	-0.011	0.053	0.96

Supplementary Table 8. Enrichment analysis for a set of highly constrained genes

Competitive gene set analysis of highly constrained genes (pLI > 0.9) performed using MAGMA[41]. The number of genes (N Genes), raw and semi-standardized (Std.) regression coefficients, and corresponding standard error (SE) are reported.

Gene Set	N Genes	Beta	Beta (Std.)	SE	P
Highly constrained genes	2932	0.062	0.023	0.018	2.60×10^{-4}

Supplementary Table 9. SNP heritability of ADHD

SNP heritability estimated (h^2) and standard error (SE) using LD score regression and summary statistics from GWAS meta-analyses. Estimates are reported on the liability scale assuming a 5% population prevalence of ADHD. Only PGC European samples (Eur samples) were included.

Sample	h^2 (liability scale)	SE
iPSYCH	0.26	0.02
PGC (Eur samples)	0.12	0.03
iPSYCH+PGC (Eur samples)	0.22	0.01

Supplementary Table 10. Heritability and genetic correlations for PGC ADHD samples

Univariate and bivariate heritability estimates for PGC ADHD samples stratified by study design type (case-control vs. parent-offspring trios). The estimated SNP heritability (SNP-h^2) of each subset and the genetic correlation (r_g) between the two sets are reported with their respective standard errors (SE). Heritability estimates are reported on the liability scale assuming a 5% population prevalence of ADHD.

Cohort	N cases	N controls	SNP-h^2 (SE)	r_g (SE)
PGC case-control	2871	9983	0.138 (0.019)	1.02 (0.32)
PGC trios	1628	1629	0.081 (0.045)	

Supplementary Table 11. Genetic correlations of ADHD with other selected traits

Genetic correlation (r_g) and its standard error (SE) is estimated using LD score regression and summary statistics from the European GWAS meta-analysis (iPSYCH + PGC European samples (Eur samples)) and summary statistics from published GWASs of other selected traits available at LDhub (http://ldsc.broadinstitute.org/ldhub/). Genetic correlations (based on analyses of European populations) significant after Bonferroni correction are presented in the table (correction for 220 tests). Extended table with results for all 220 phenotypes can be found in Supplementary eTable 5). Four significant results are omitted here as they were based on analyses of populations with mixed ancestry (Body fat and Coronary artery disease) and large overlap in samples already represented in other analyses (Years of schooling 2013 and 2014), results for correlation with these traits can be found in supplementary eTable 5.

Trait	Trait type	N	r_g	SE	P-value
Childhood IQ[147]	Cognition/education	17,989	-0.411	0.082	5.09×10^{-7}
Years of schooling[89]	Cognition/education	328,917	-0.535	0.028	1.44×10^{-80}
College completion[148]	Cognition/education	126,559	-0.538	0.046	3.30×10^{-31}
Neuroticism[149]	Personality	170,911	0.264	0.046	1.02×10^{-8}
Depressive symptoms[149]	Psychiatric	161,460	0.446	0.050	7.00×10^{-19}
Subjective well being[149]	Psychiatric	298,420	-0.283	0.048	3.73×10^{-9}
Major depressive disorder (submitted)	Psychiatric	461,134	0.424	0.033	7.38×10^{-38}
PGC cross-disorder analysis[150]	Psychiatric	61,220	0.266	0.046	5.58×10^{-9}
Body mass index[151]	Weight related	123,865	0.258	0.032	1.68×10^{-15}
Waist circumference[152]	Weight related	224,459	0.269	0.034	2.20×10^{-15}
Hip circumference[152]	Weight related	254,459	0.160	0.034	2.13×10^{-6}
Waist-to-hip ratio[153]	Weight related	254,459	0.304	0.036	1.16×10^{-17}
Overweight[152]	Weight related	158,855	0.275	0.036	1.73×10^{-14}
Obesity class 1[152]	Weight related	98,697	0.285	0.036	1.81×10^{-15}
Obesity class 2[152]	Weight related	75,729	0.320	0.046	5.10×10^{-12}
Obesity class 3[152]	Weight related	50,364	0.338	0.067	4.05×10^{-7}
Extreme BMI[152]	Weight related	16,068	0.254	0.052	9.31×10^{-7}
Childhood obesity[154]	Weight related	13,848	0.216	0.046	3.29×10^{-6}
Type 2 Diabetes[155]	Glycemic	149,821	0.185	0.047	7.80×10^{-5}
HDL cholesterol[156]	Lipids	99,900	-0.217	0.042	2.44×10^{-7}
Triglycerides[156]	Lipids	96,598	0.159	0.040	6.49×10^{-5}
Ever vs never smoked[157]	Smoking behaviour	74,035	0.478	0.059	4.33×10^{-16}

Cigarettes smoked per day[157]	Smoking behaviour	68,028	0.451	0.103	1.07×10^{-5}
Former vs Current smoker[157]	Smoking behaviour	41,969	-0.344	0.086	6.74×10^{-5}
Lung cancer[158]	Cancer	56,697	0.390	0.063	6.35×10^{-10}
Lung cancer (all)[159]	Cancer	27,209	0.368	0.071	2.53×10^{-7}
Squamous cell lung cancer[158]	Cancer	56,697	0.549	0.135	4.57×10^{-5}
Age of first birth[122]	Reproductive	251,151	-0.612	0.037	3.70×10^{-61}
Number of children ever born[122]	Reproductive	343,072	0.421	0.051	8.51×10^{-17}
Age at Menopause[54]	Reproductive	69,360	-0.161	0.042	1.50×10^{-4}
Mothers age at death[160]	Aging	52,776	-0.432	0.087	6.48×10^{-7}
Fathers age at death[160]	Aging	63,775	-0.298	0.066	7.19×10^{-6}
Parents age at death[160]	Aging	45,627	-0.376	0.091	3.51×10^{-5}
Rheumatoid Arthritis[161]	Autoimmune	103,638	0.162	0.042	1.32×10^{-4}

Supplementary Table 12. Sign test results in 23andMe and EAGLE replication cohorts

Test of whether the proportion of loci with estimated effects in the same direction as the ADHD GWAS (π) is greater than expected by chance. Values in bold are nominally significant after Bonferroni correction for testing in 2 replication cohorts ($P < 0.025$).

		23andMe Concordance		EAGLE Concordance	
P Threshold	Number of Loci	π	*P*	π	*P*
5.00×10^{-8}	11	0.727	2.28×10^{-1}	0.909	**1.59×10^{-2}**
1.00×10^{-7}	13	0.615	5.79×10^{-1}	0.846	2.65×10^{-2}
1.00×10^{-6}	34	0.735	**1.01×10^{-2}**	0.765	**3.55×10^{-3}**
1.00×10^{-5}	94	0.755	**1.25×10^{-6}**	0.691	**3.06×10^{-4}**
1.00×10^{-4}	288	0.622	**4.79×10^{-5}**	0.670	**5.42×10^{-9}**

Supplementary Table 13. Replication of significant ADHD loci in 23andMe and EAGLE

GWAS results from EAGLE and 23andMe for the genome-wide significant loci identified in the ADHD GWAS. Replication is tested for the index variant from the ADHD GWAS, or for a proxy variant when the index variant is not present in the replication cohort. Proxy variants are identified by linkage disequilibrium (LD) clumping of the ADHD GWAS results using European ancestry samples from the 1000 Genomes Project after restricting to variants present in EAGLE and 23andMe results. No proxy variant is available for rs28411770. Effects (Z or odds ratio [OR]) that are sign concordant with the ADHD GWAS are indicated in bold. Genome-wide significant p-values from meta-analysis of the ADHD GWAS and replication cohorts are indicated in bold.

Variant				EAGLE		23andMe		Meta-Analysis P-values		
Index	Proxy	Effect Allele	LD to Index	Z	p	OR	p	ADHD +EAGLE	ADHD +23andMe	ADHD +EAGLE+23andMe
rs11420276	rs112984125	A	0.980	**-2.248**	2.5×10^{-02}	1.044	4.0×10^{-02}	**2.76×10^{-14}**	1.69×10^{-06}	1.58×10^{-07}
rs1222063	rs2391769	A	0.093	**-0.248**	8.0×10^{-01}	**0.957**	3.2×10^{-02}	9.89×10^{-08}	**7.76×10^{-09}**	**2.45×10^{-08}**
rs9677504	--	A	--	**0.030**	9.8×10^{-01}	**1.068**	3.5×10^{-02}	5.33×10^{-08}	**3.64×10^{-09}**	**1.79×10^{-08}**
rs4858241	--	T	--	**0.842**	4.0×10^{-01}	**1.016**	4.4×10^{-01}	**1.77×10^{-08}**	3.78×10^{-07}	**1.56×10^{-08}**
rs4916723	--	A	--	**-2.816**	4.9×10^{-03}	**0.989**	5.9×10^{-01}	**4.80×10^{-10}**	5.60×10^{-07}	**1.90×10^{-08}**
rs5886709	rs10262192	A	0.955	**1.540**	1.2×10^{-01}	**1.045**	2.6×10^{-02}	**4.91×10^{-09}**	**8.63×10^{-09}**	**1.53×10^{-09}**
rs74760947	--	A	--	**-1.168**	2.4×10^{-01}	**0.955**	3.9×10^{-01}	**7.89×10^{-09}**	1.08×10^{-07}	6.18×10^{-08}
rs11591402	--	A	--	**-1.540**	1.2×10^{-01}	**0.957**	6.3×10^{-02}	**4.10×10^{-09}**	**1.10×10^{-08}**	**3.30×10^{-09}**
rs1427829	--	A	--	-0.110	9.1×10^{-01}	**1.036**	7.0×10^{-02}	**1.05×10^{-08}**	**2.15×10^{-09}**	**1.42×10^{-08}**
rs281324	rs281320	T	0.992	**-0.995**	3.2×10^{-01}	1.010	6.1×10^{-01}	**2.21×10^{-08}**	1.77×10^{-05}	1.10×10^{-05}
rs212178	--	A	--	**-1.216**	2.2×10^{-01}	1.030	3.8×10^{-01}	**4.00×10^{-09}**	6.80×10^{-06}	3.20×10^{-06}

Supplementary Figures

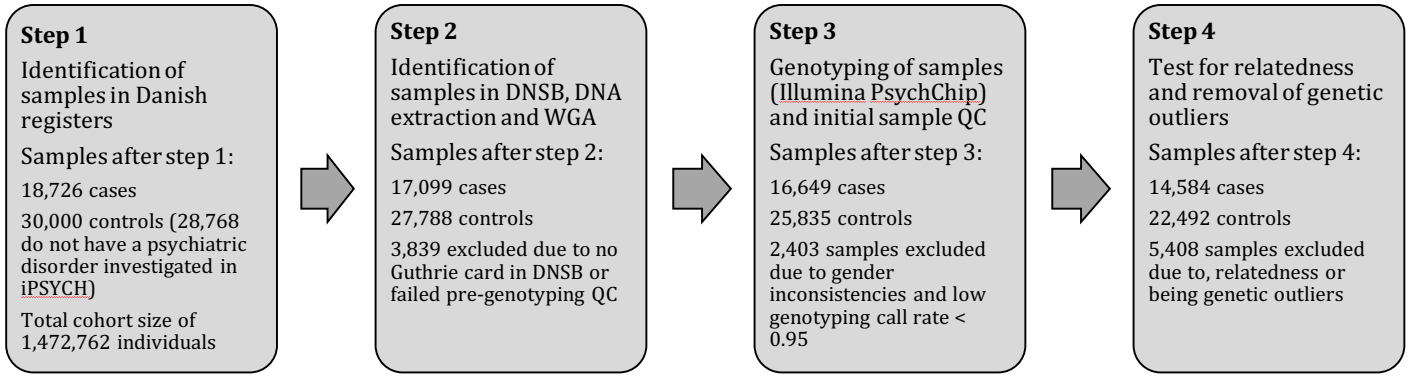

Supplementary Figure 1. Genotyping iPSYCH-ADHD sample, main steps and sample loss

Flowchart demonstrating the main steps and sample loss during the process of obtaining high quality genotypes for the iPSYCH sample. Detailed description of the Danish registers, DNA generation, genotyping and QC is described under the detailed description of the iPSYCH sample.

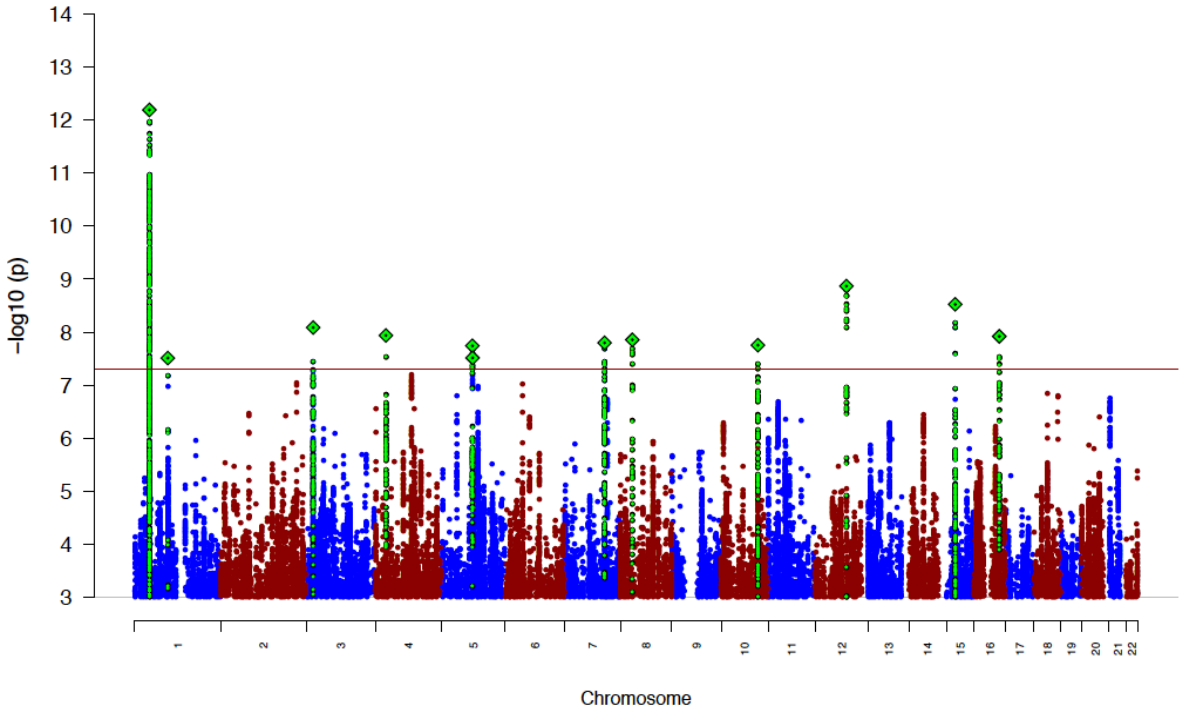

Supplementary Figure 2. Manhattan plot from ADHD European GWAS meta-analysis

Results from GWAS meta-analysis of iPSYCH and PGC European samples.

Supplementary Figure 3.A1 - M1. Forest plots for index SNPs in gws loci

Forest plots for the index SNP in each of the gws associated regions in the GWAS meta-analysis. Each plot provides a visualization of the effect size estimates for each wave in the iPSYCH sample and each PGC sample and for the summary meta-analysis in addition the 95% confidence intervals are included for the estimates.

Supplementary Figure 3.A2 - M2. Regional association plots for index SNPs in gws loci

Regional association plots of the local association results. Each plot includes information about the gws locus, the location and orientation of the genes in the region, LD estimates of surrounding SNPs with the index SNP (r^2 values estimated based on 1KGP3) is indicated by colour (colour bar in upper left corner indicates r^2 values), if multiple index SNPs then different colour scheme for each index SNP. Additionally the local estimates of recombination rate. Detailed SNP info in upper right corner (blue letters): snp-name, P, OR, MAF, imputation INFO score, directions in the analysed samples/waves (left - right - missing). Gene lists were downloaded from ftp://hgdownload.cse.ucsc.edu/goldenPath/hg19/database/refGene.txt.gz. Previously reported gws regions were downloaded from the NHGRI GWAS catalogue available from http://www.ebi.ac.uk/gwas.

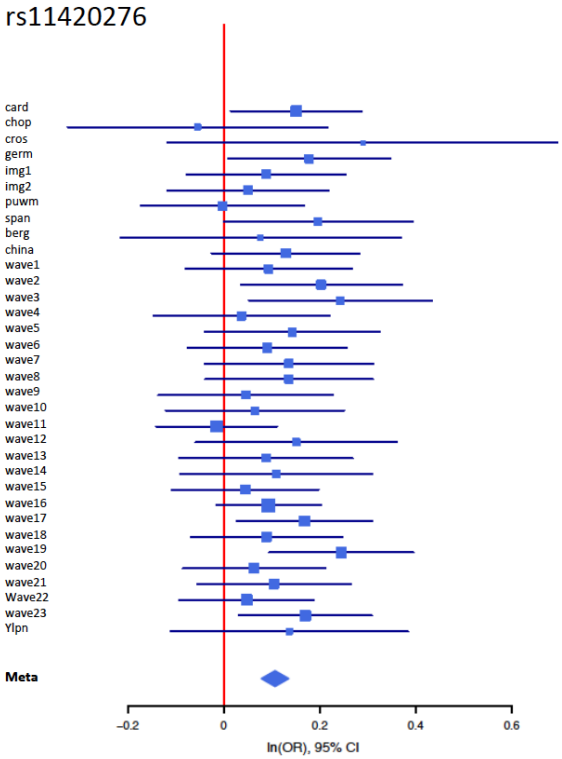

Figure 3.A1. Forest plot for rs11420276

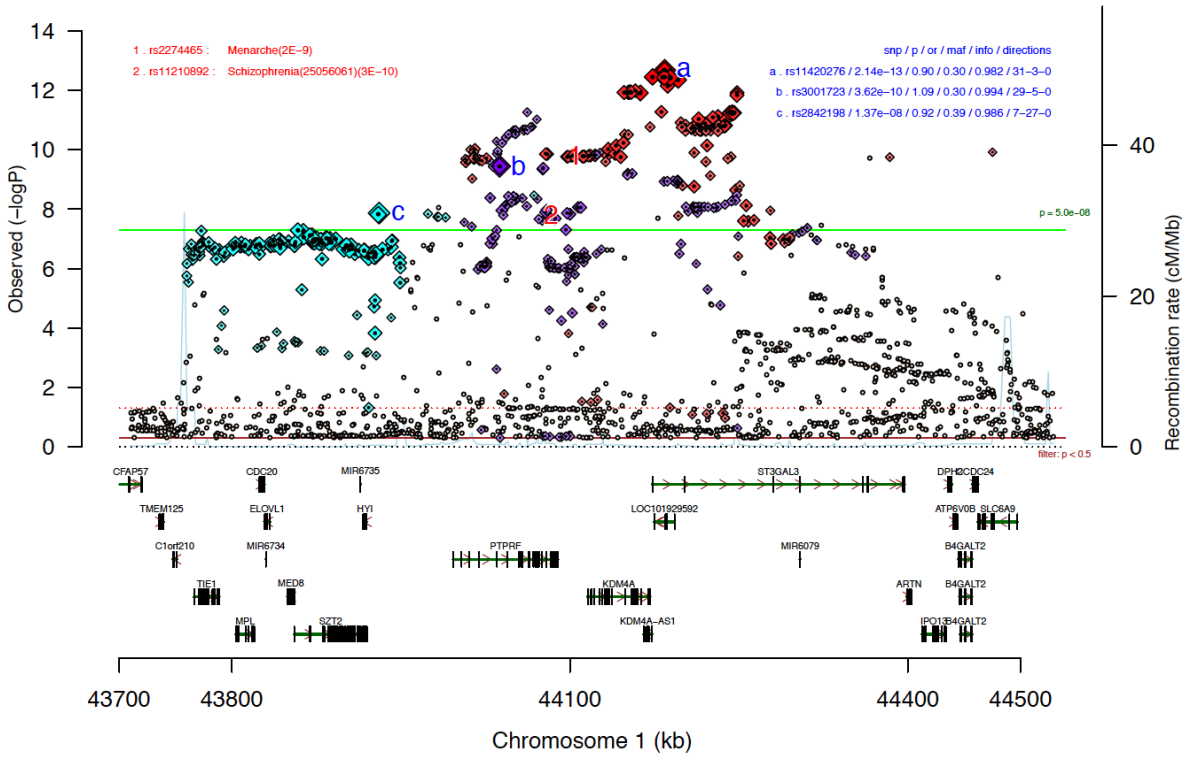

Figure 3.A2. Regional association plot for rs11420076

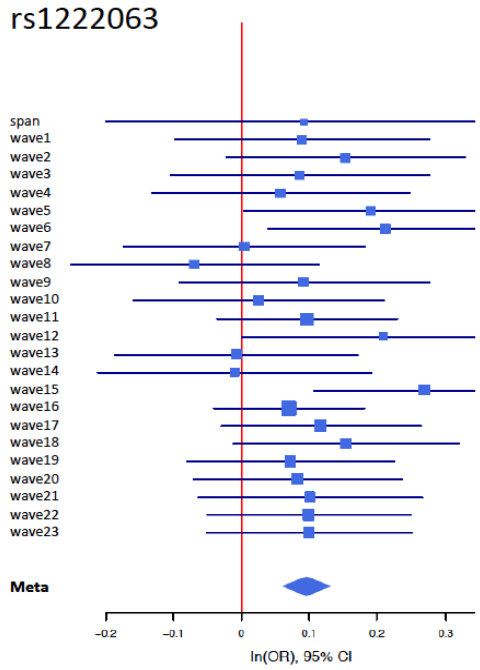

Figure 3.B1. Forest plot for rs1222063

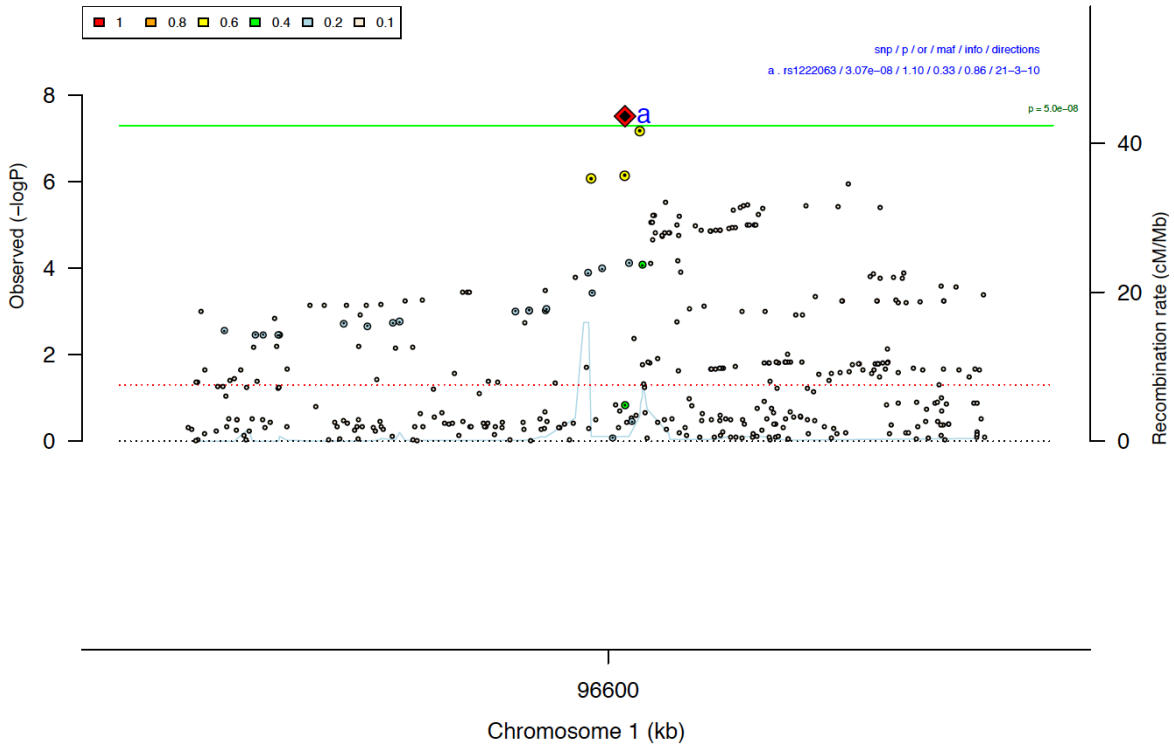

Figure 3.B2. Regional association plot for rs1222063

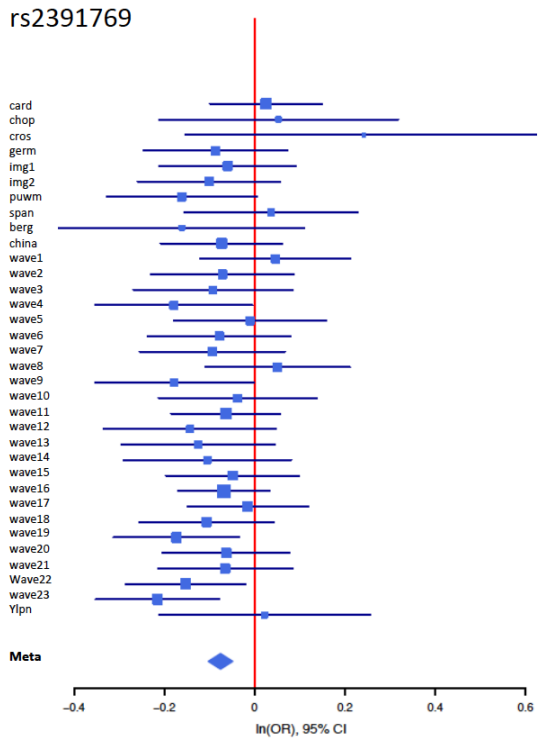

Figure 3.C1. Forest plot for rs2391769

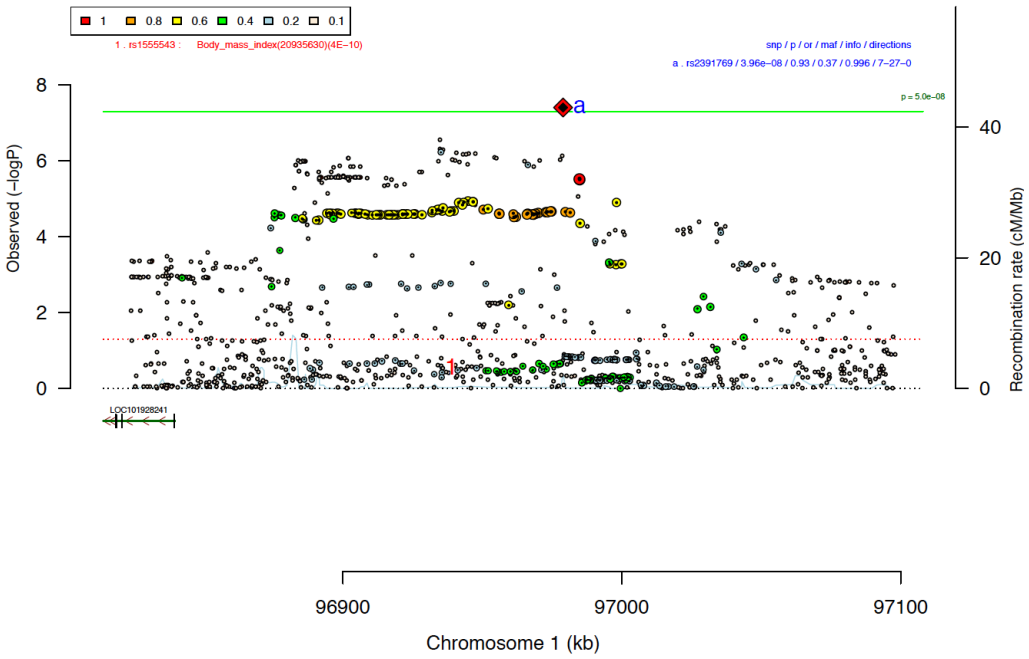

Figure 3.C2. Regional association plot for rs2391769

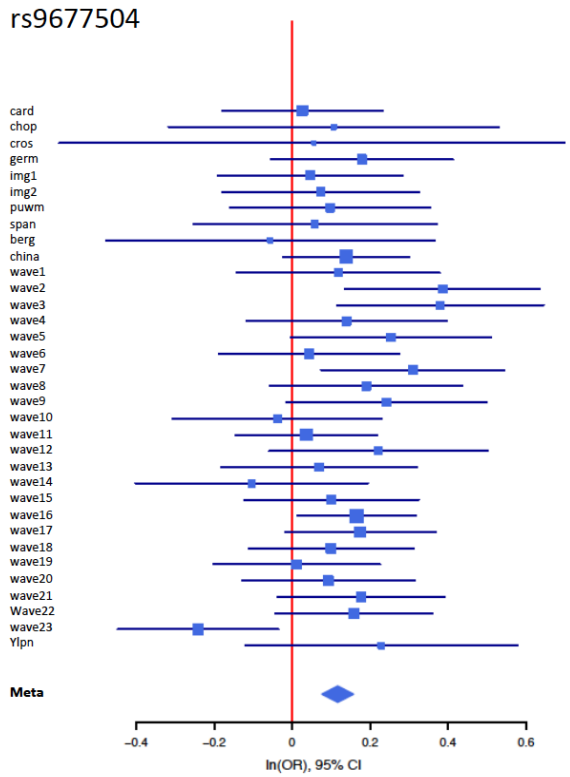

Figure 3.D1. Forest plot for rs9677504

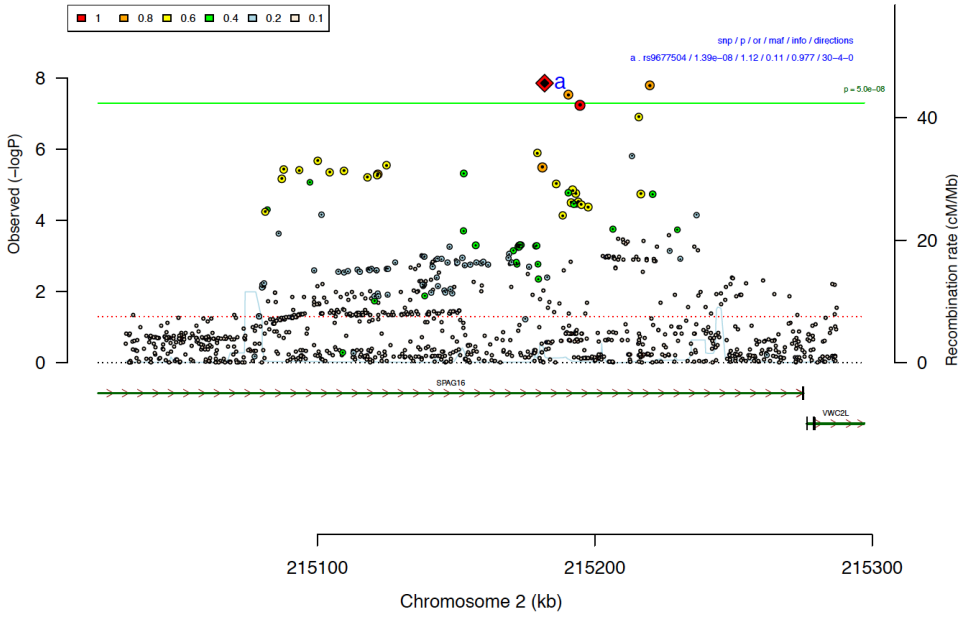

Figure 3.D2. Regional association plot for rs9677504

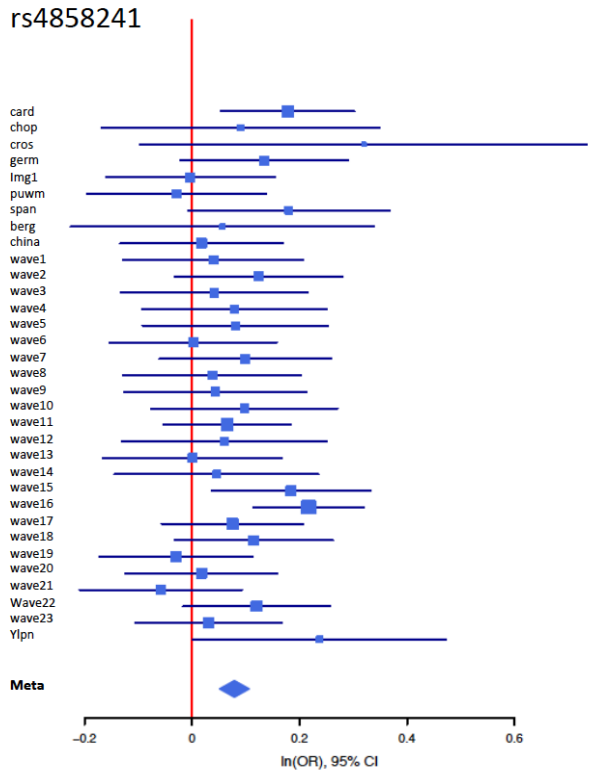

Figure 3.E1. Forest plot for rs4858241

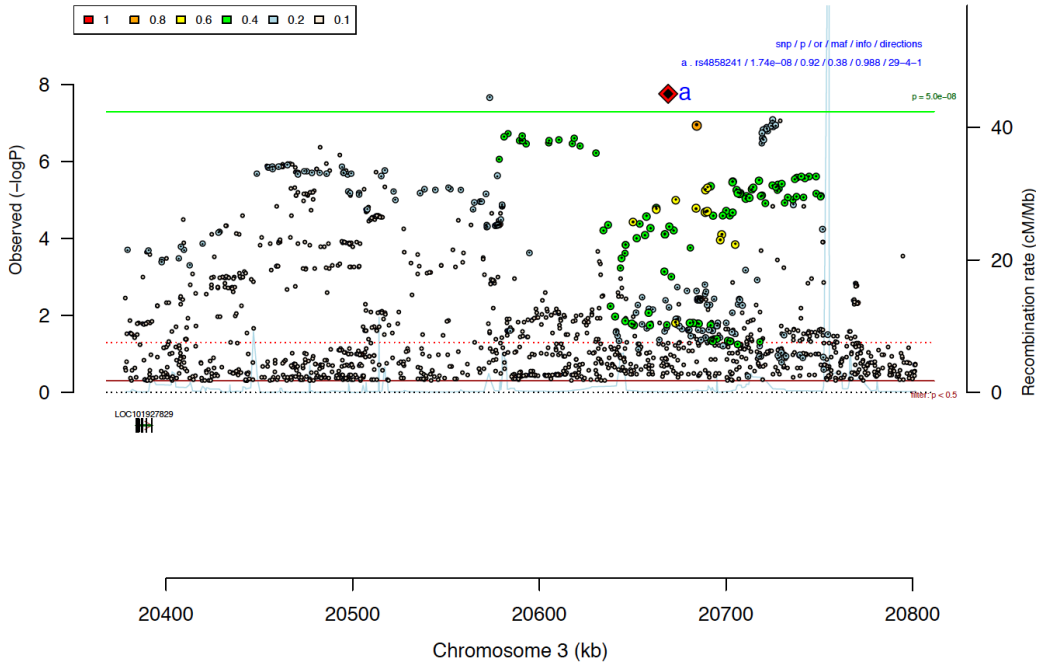

Figure 3.E2. Regional association plot for rs4858241

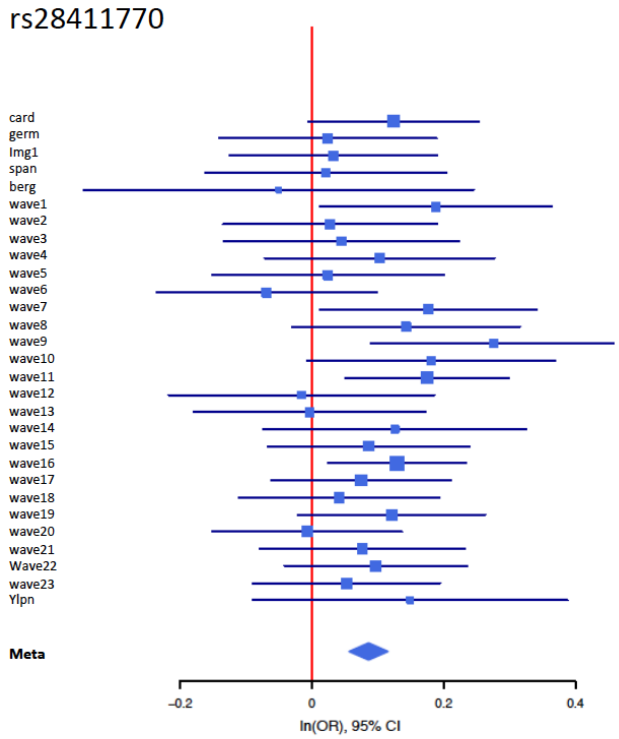

Figure 3.F1. Forest plot for rs28411770

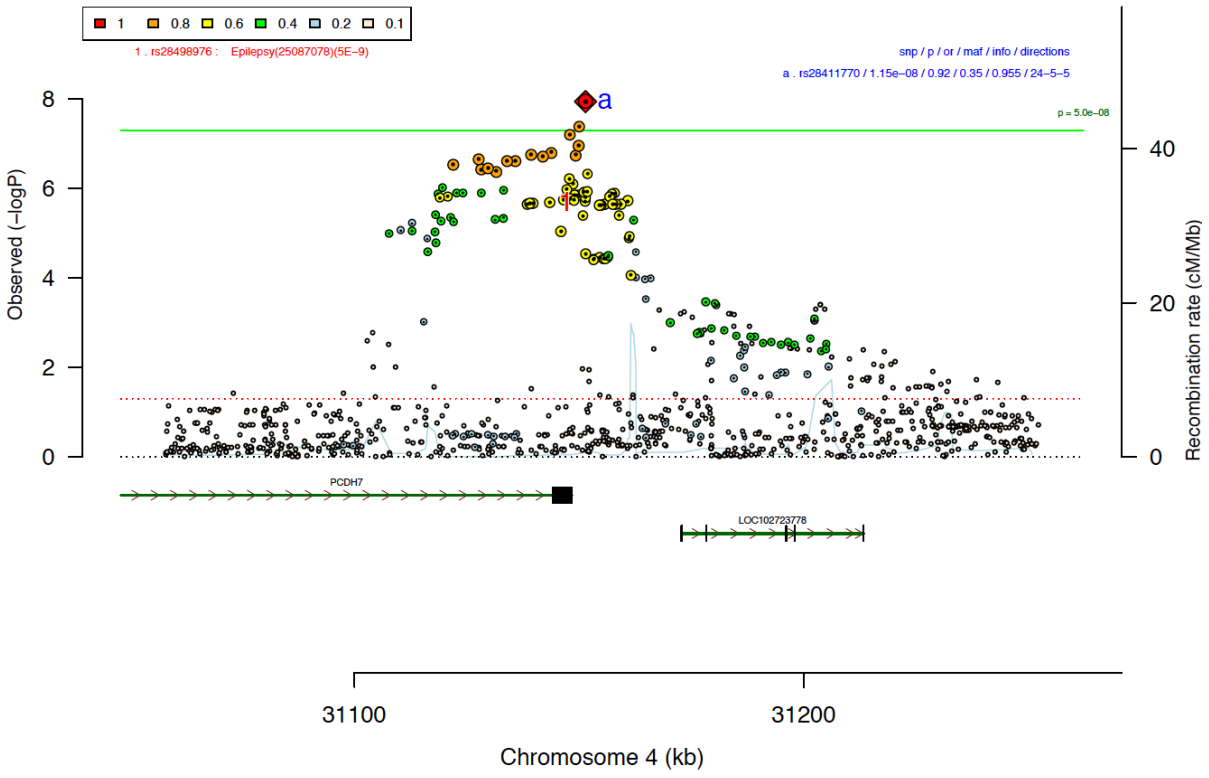

Figure 3.F2. Regional association plot for rs2811770

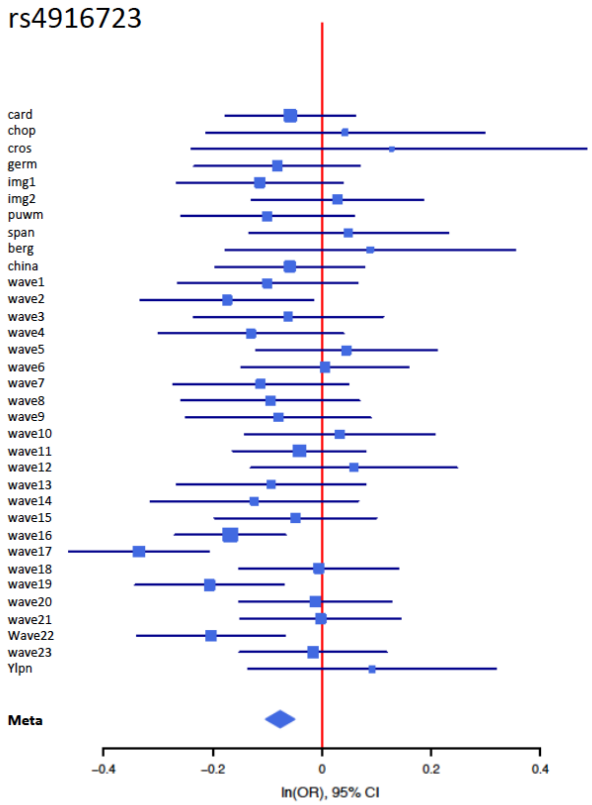

Figure 3.G1. Forest plot for rs4916723

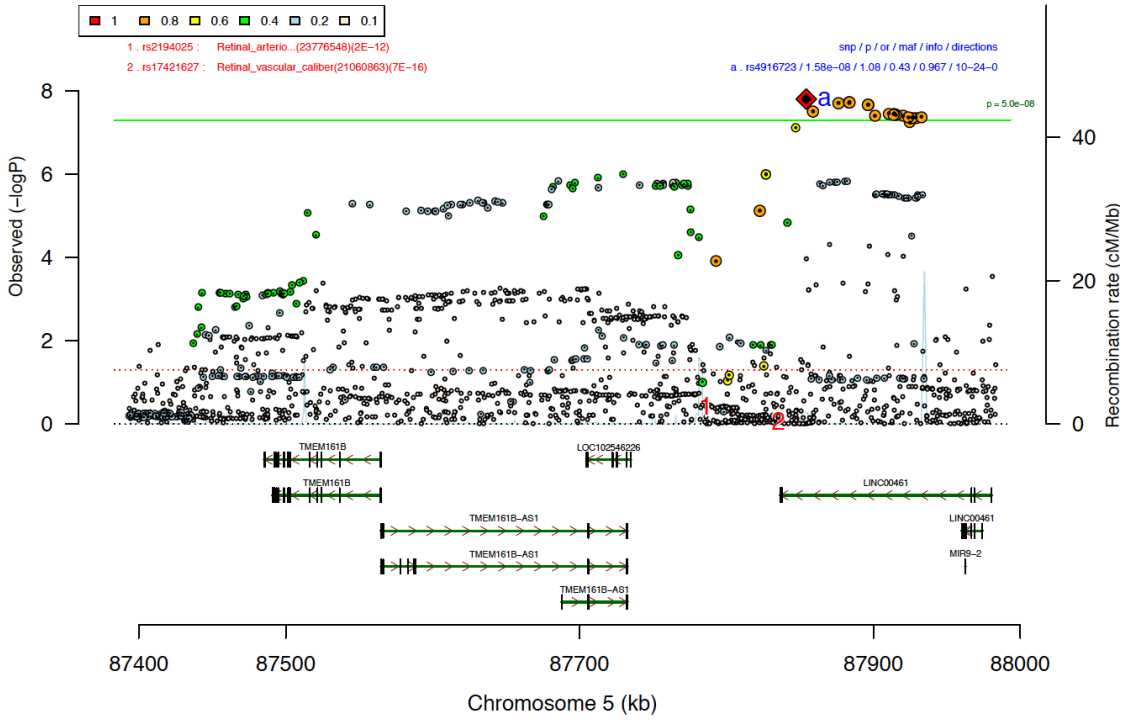

Figure 3.G2. Regional association plot for rs4916723

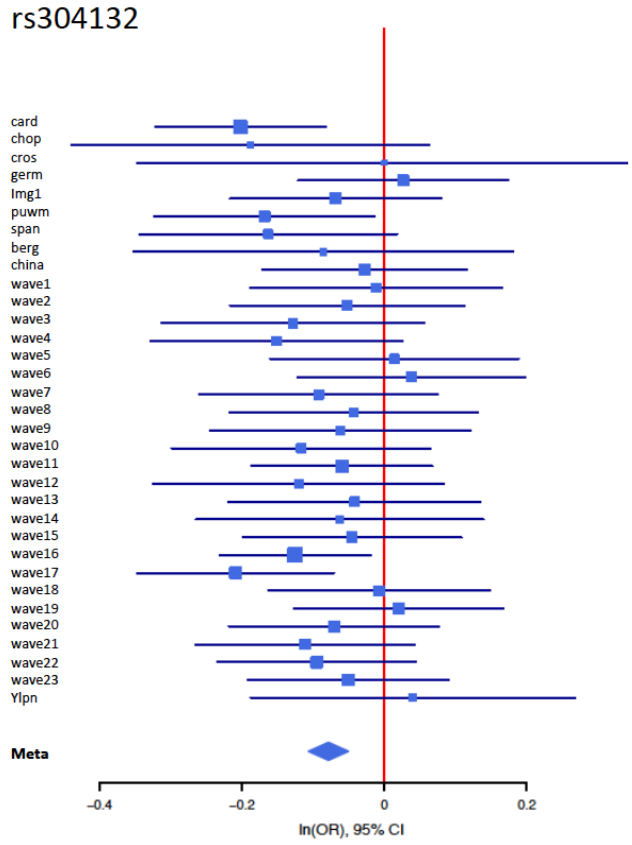

Figure 3.H1. Forest plot for rs304132

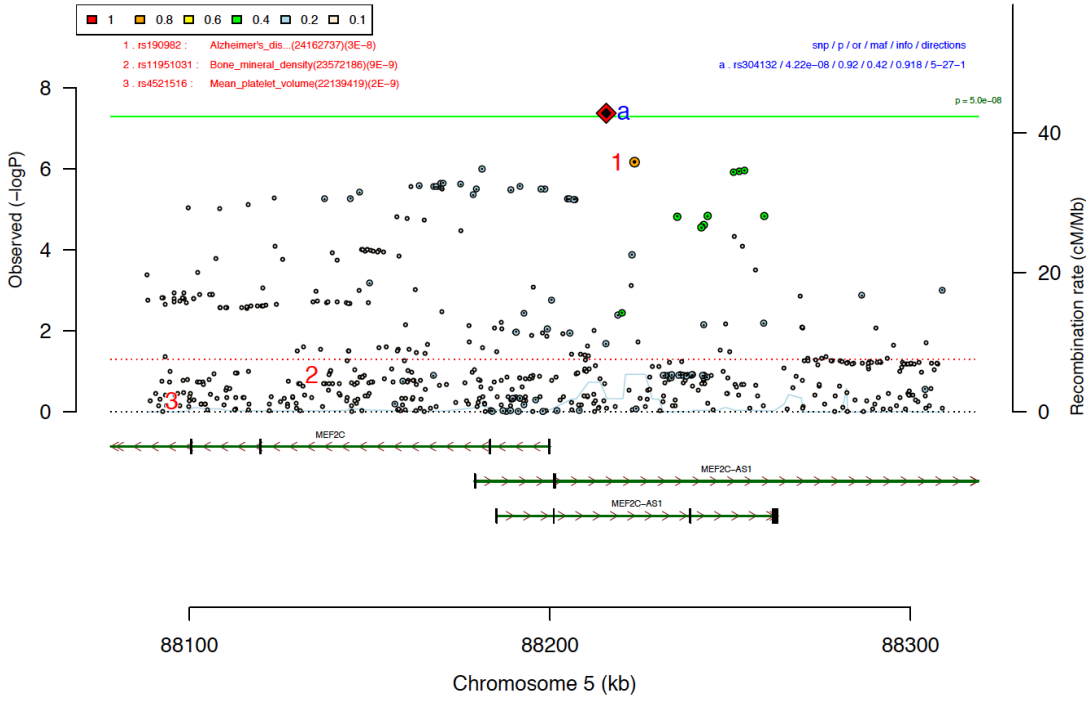

Figure 3.H2. Regional association plot for rs304132

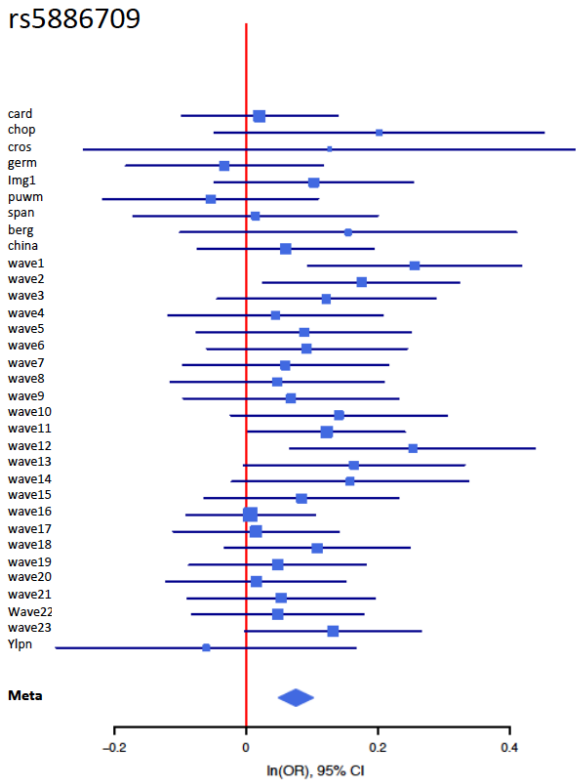

Figure 3.I1. Forest plot for rs5886709

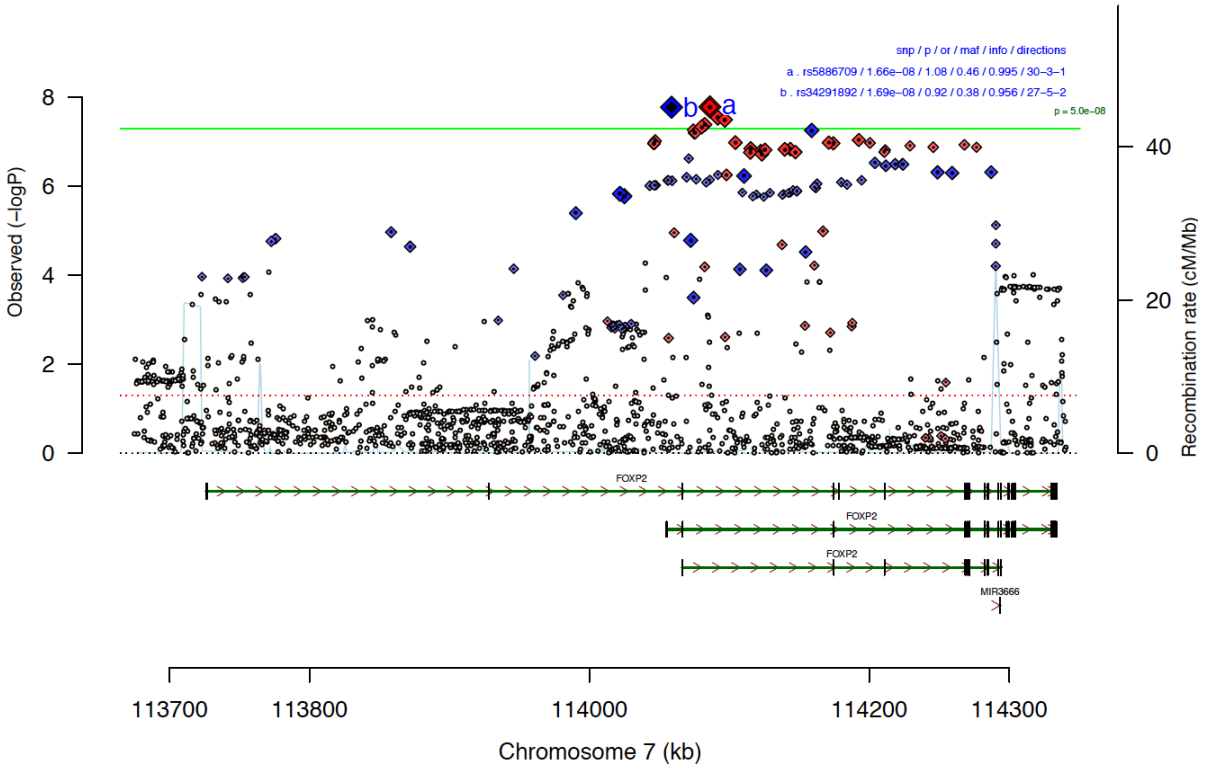

Figuren 3.I2. Regional association plot for rs5886709

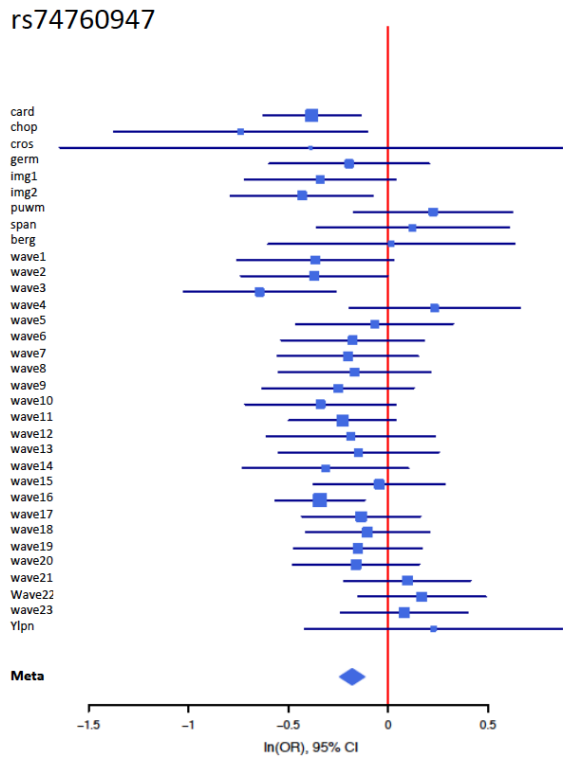

Figure 3.J1. Forest plot for rs74760947

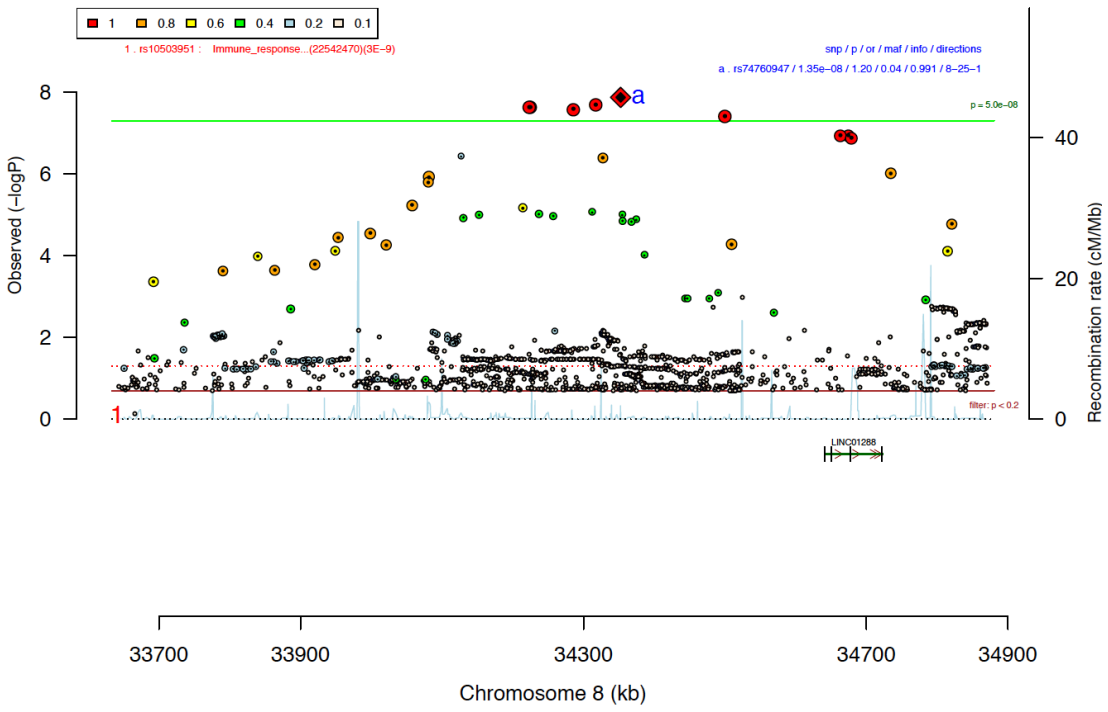

Figure 3.J2. Regional association plot for rs74760947

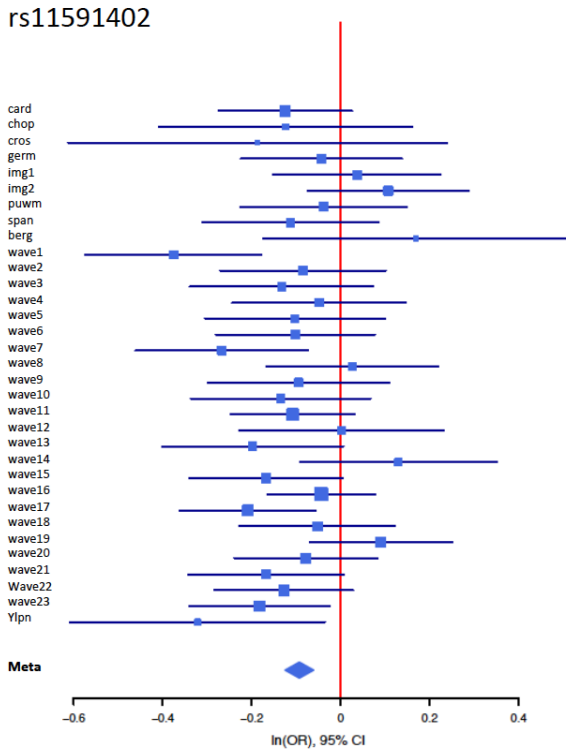

Figure 3.K1. Forest plot for rs11591402

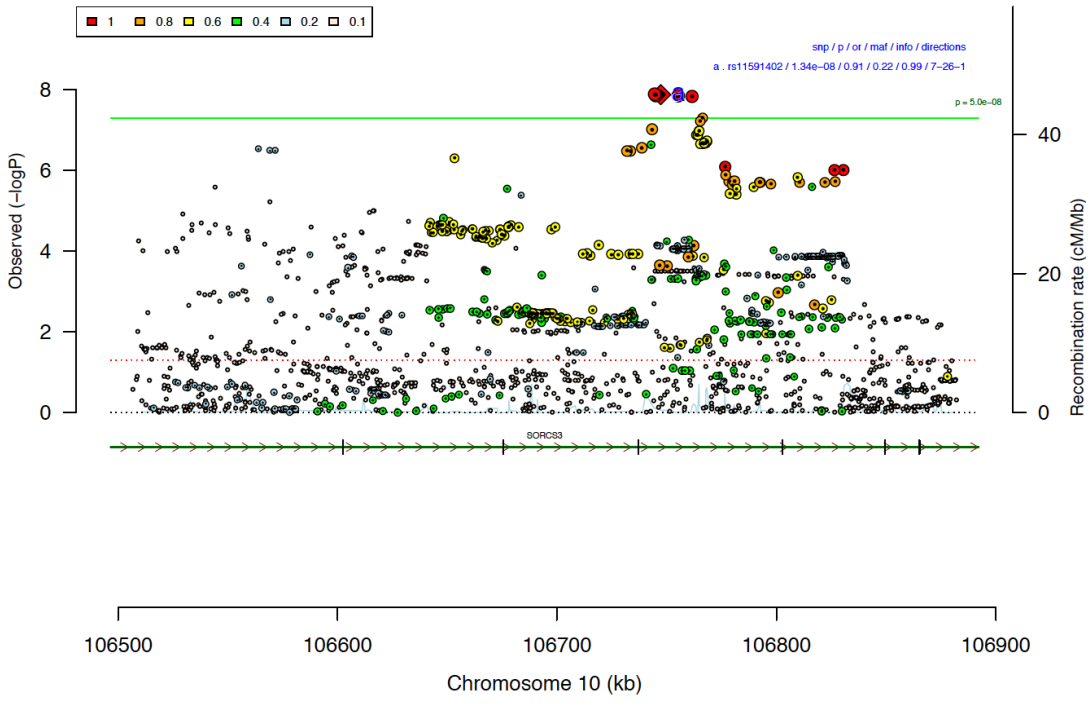

Figure 3.K2. Regional association plot for rs11591402

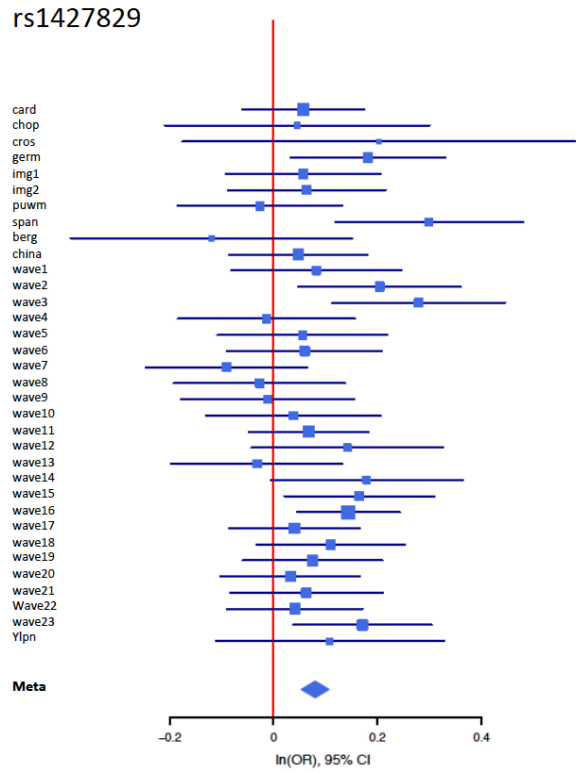

Figure 3.L1. Forest plot for rs1427829

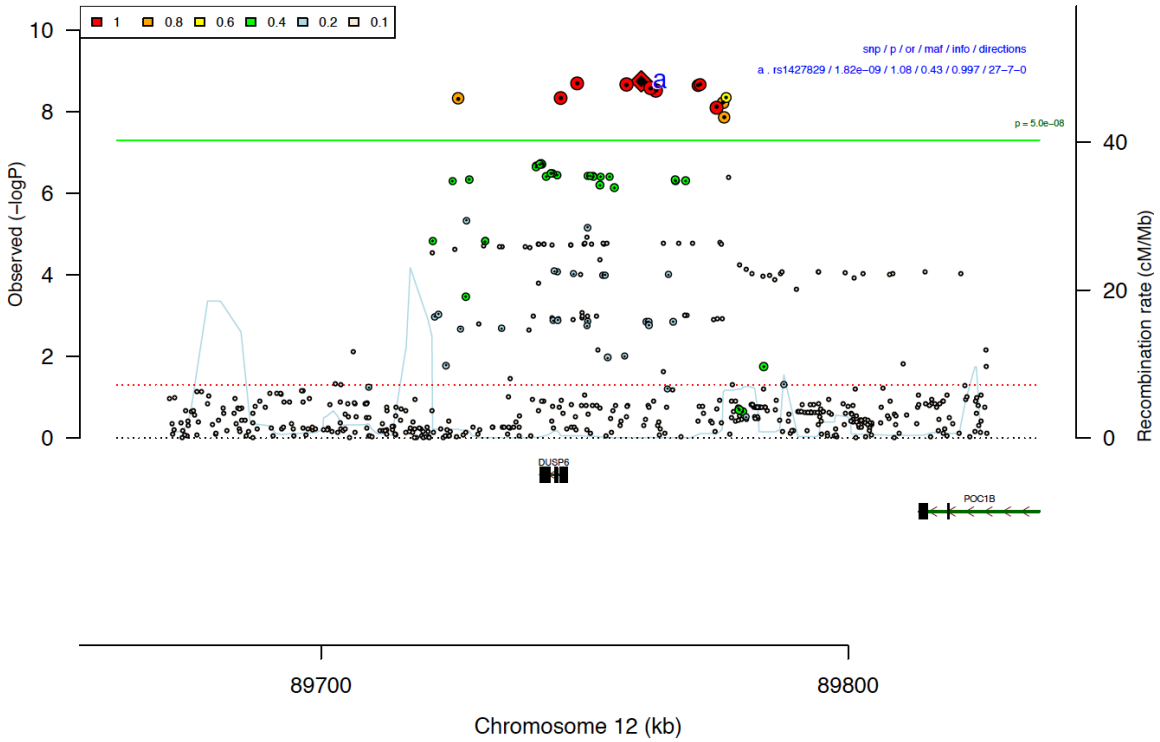

Figure 3.L2. Regional association plot for rs1427829

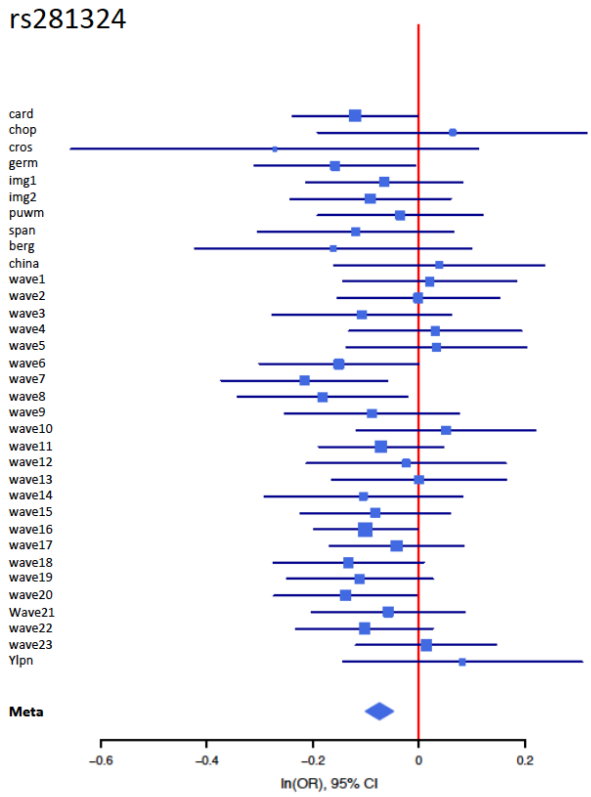

Figure 3.M1. Forest plot for rs281324

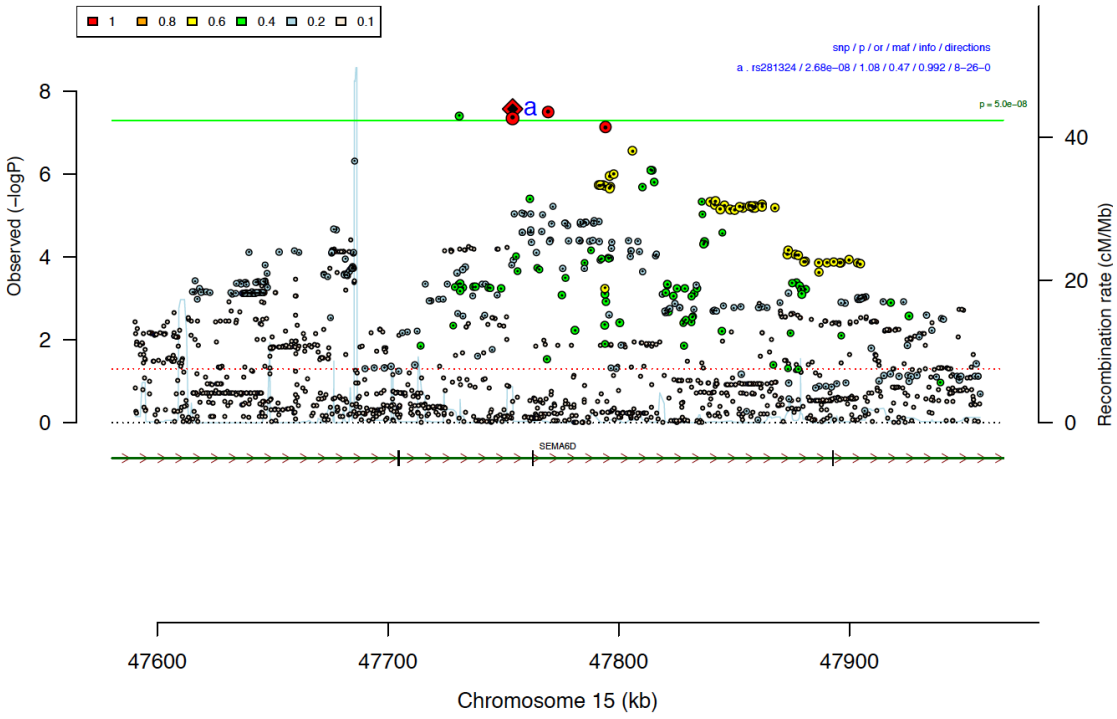

Figure 3.M2. Regional association plot for rs281324

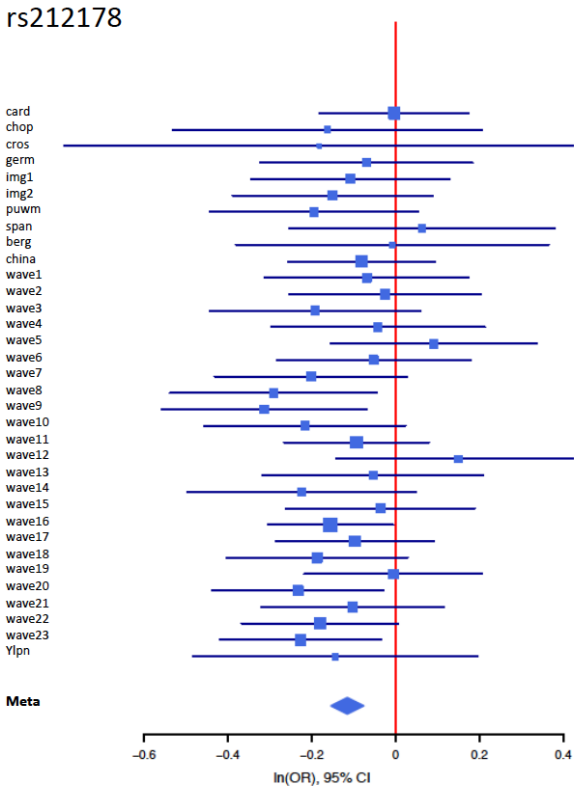

Figure 3.N1. Forest plot for rs212178

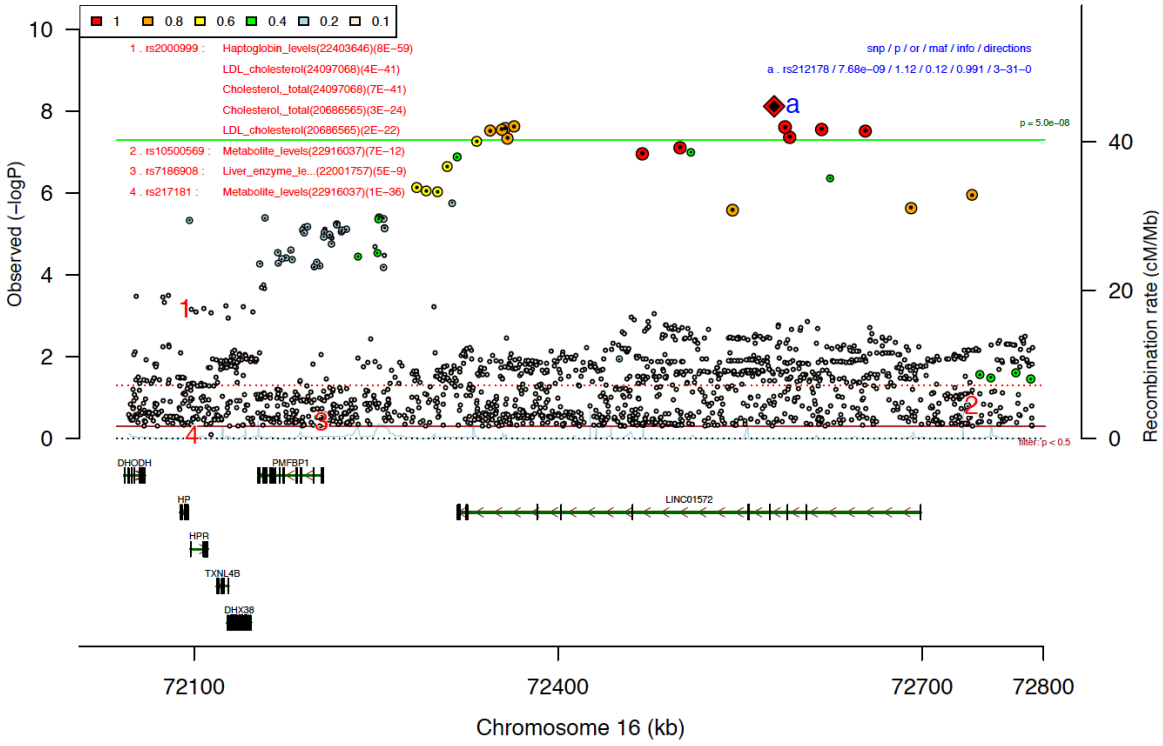

Figure 3.N2. Regional association plot for rs212178

Supplementary Figure 4.A – 4.D. Gene-based association, regional association plots

LD structure in the region around the four new genes (genes not overlapping with loci being gws in the single marker GWAS meta-analysis) significantly association with ADHD in the MAGMA gene-based association analysis.

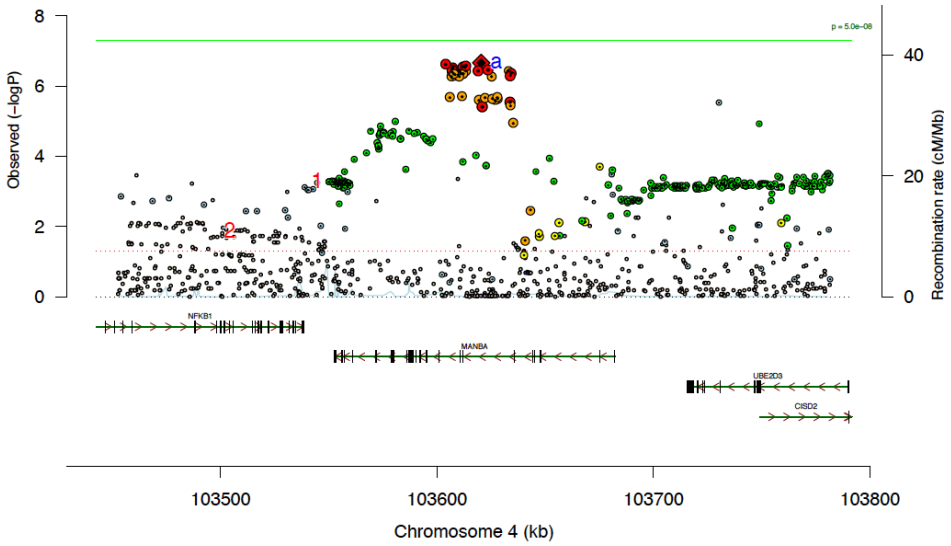

Supplementary Figure 4.A. Regional association plot for *MANBA* (+/- 100,000 bp up- and down stream the gene).

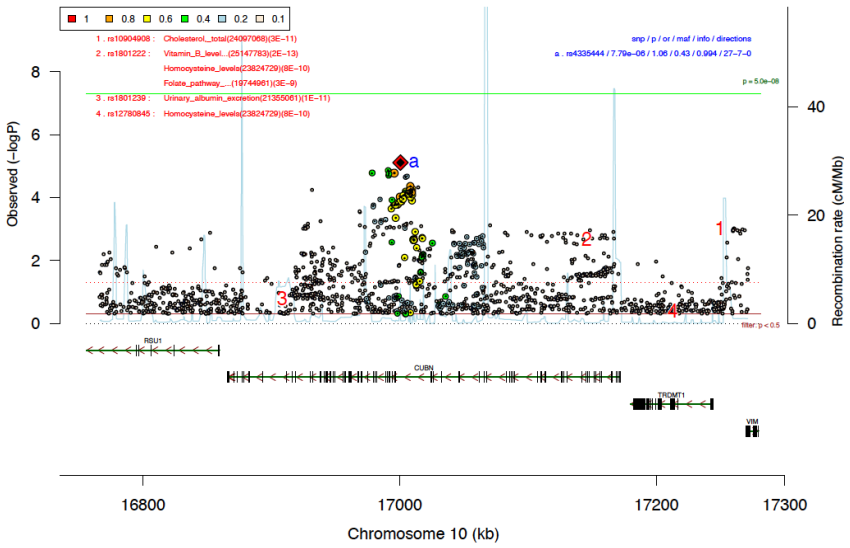

Supplementary Figure 4.B. Regional association plot for *CUBN* (+/- 100,000 bp up- and down stream the gene).

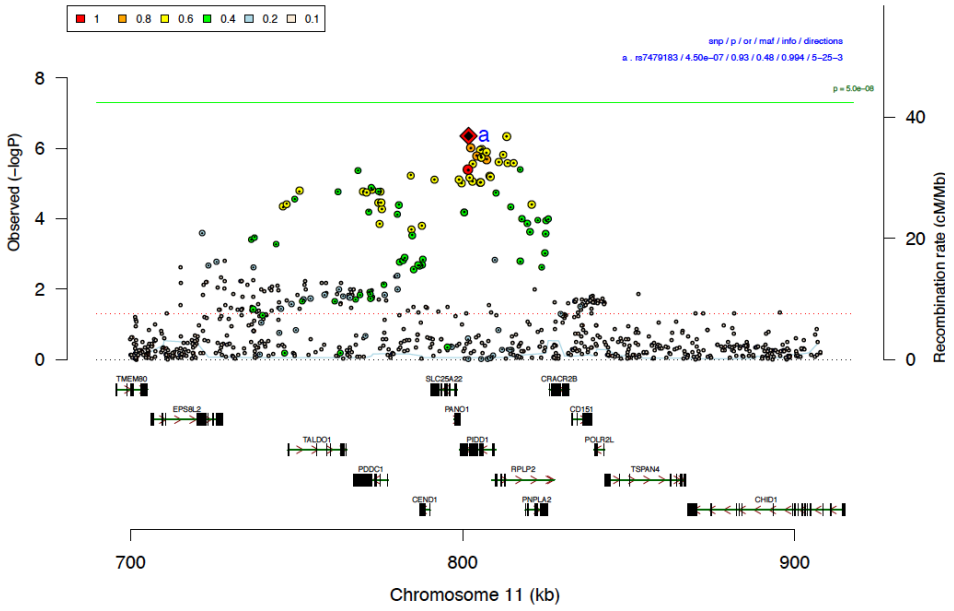

Supplementary Figure 4.C. Regional association plot for *PIDD1* (+/- 100,000 bp up- and down stream the gene).

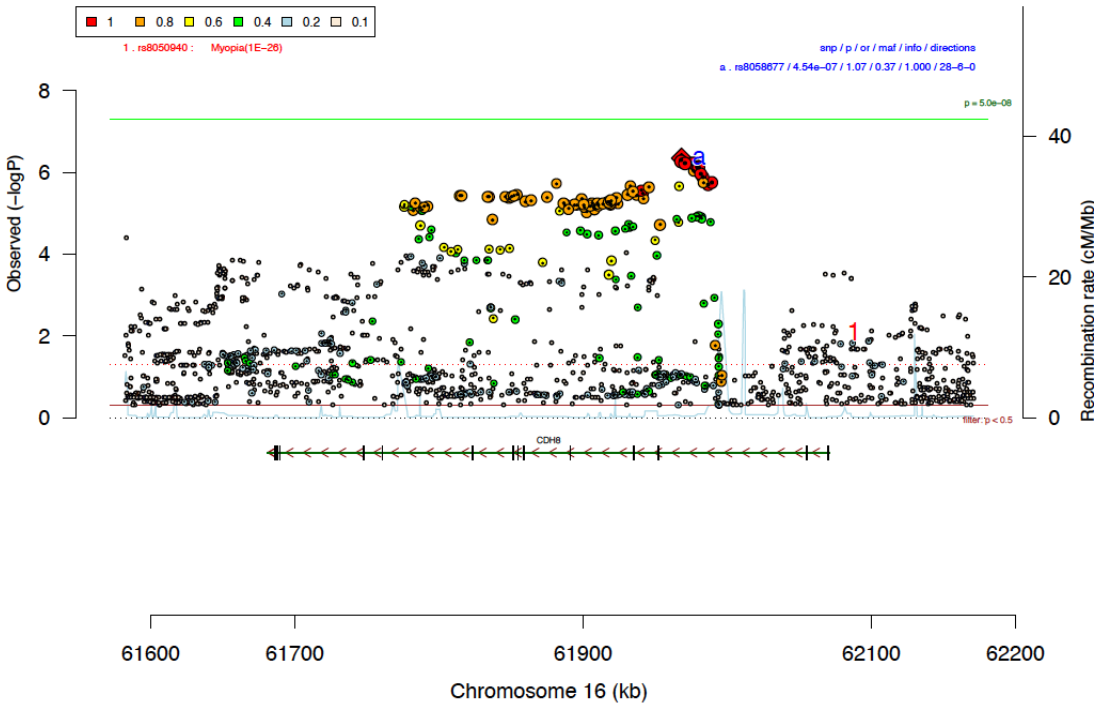

Supplementary Figure 4.D. Regional association plot for *CDH8* (+/- 100,000 bp up- and down stream the gene).

Supplementary Figure 5.A. – 5.B. Q-Q plot from GWAS meta-analyses

Quantile-quantile plot of the -log10 P-values from GWAS meta-analyses. PGCeur refers to analysis only including individuals with European ancestry.

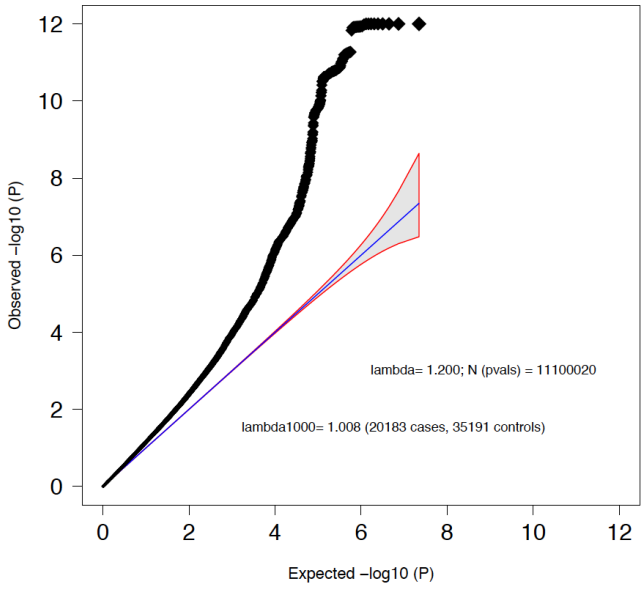

Supplementary Figure 5.A. Q-Q plot from GWAS meta-analysis

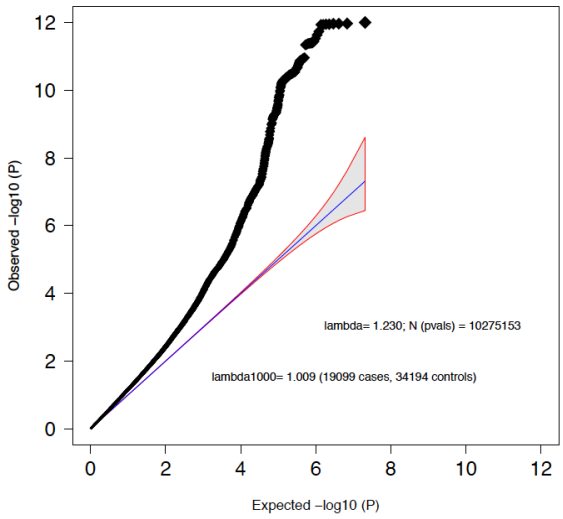

Supplementary Figure 5.B. Q-Q plot from European GWAS meta-analysis

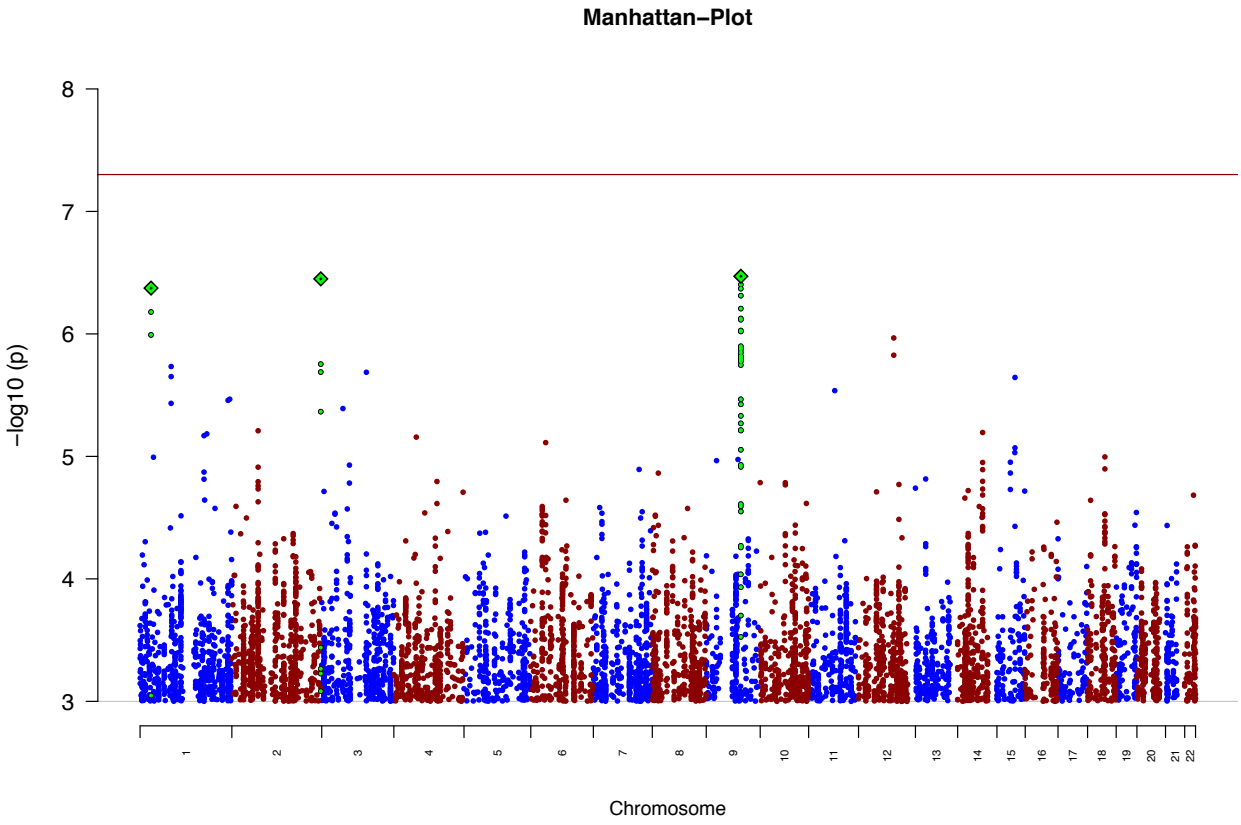

Supplementary Figure 6. Manhattan plot from test for heterogeneity between studies/waves in the ADHD GWAS meta-analysis

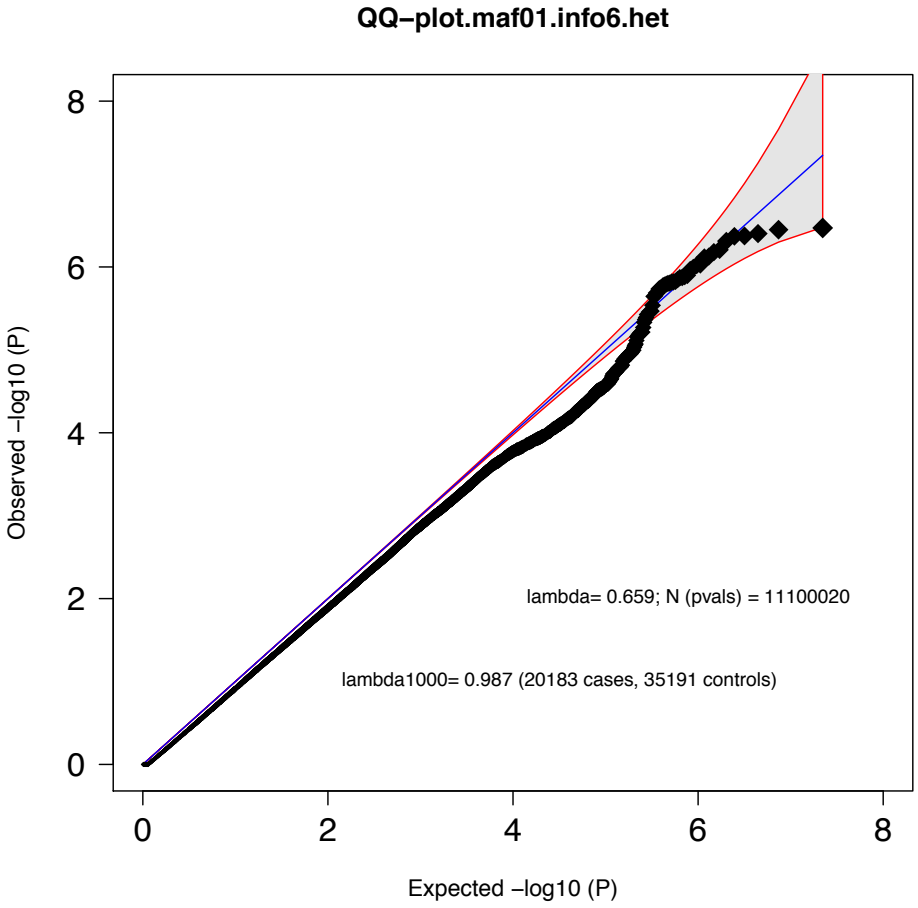

Supplementary Figure 7. Q-Q plot from test for heterogeneity between samples/waves in the ADHD GWAS meta-analysis

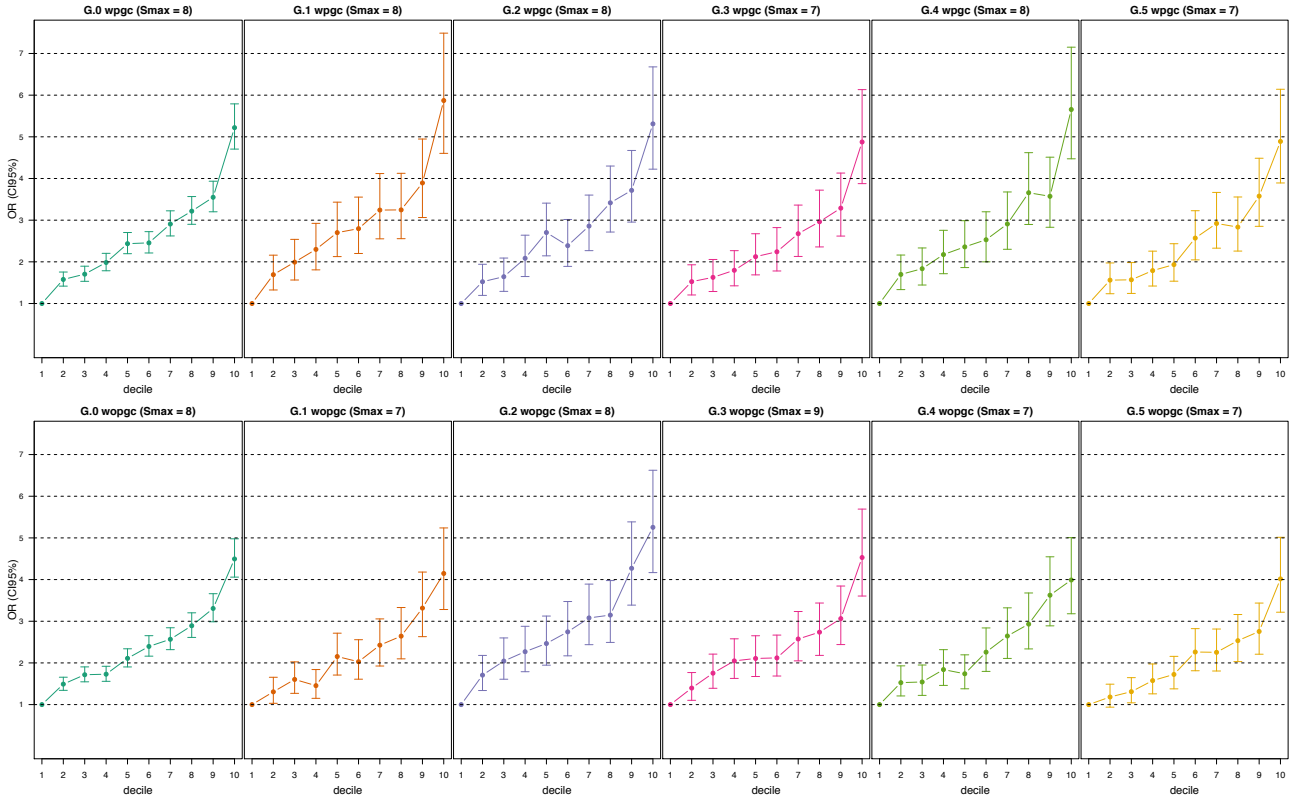

Supplementary Figure 8. Odds ratios by PRS within deciles in target groups

Odds ratio by PRS within each decile for each of the five target groups (G1-G5) and for the pooled (G0) analysis with (upper panels) and without (lower panels) PGC European samples included among the training data sets. Plots are shown for the P-value threshold with the highest Nagelkerke's R^2 (Smax). Error bars indicate 95% confidence limits.

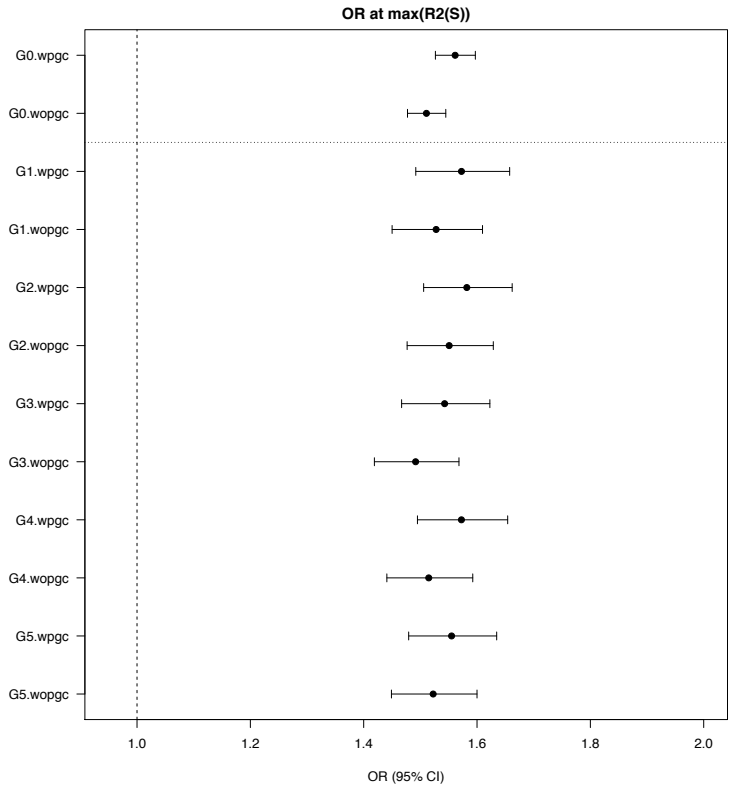

Supplementary Figure 9. Odds ratios within target groups in iPSYCH

PRS-based odds ratio and 95% confidence limits from logistic regression of continuous PRS (normalized by target group) for each target group considered separately (G1-G5) and pooled (G0). PRS estimated using iPSYCH waves alone as training sample (wopgc) or iPSYCH waves together with PGC European samples (wpgc).

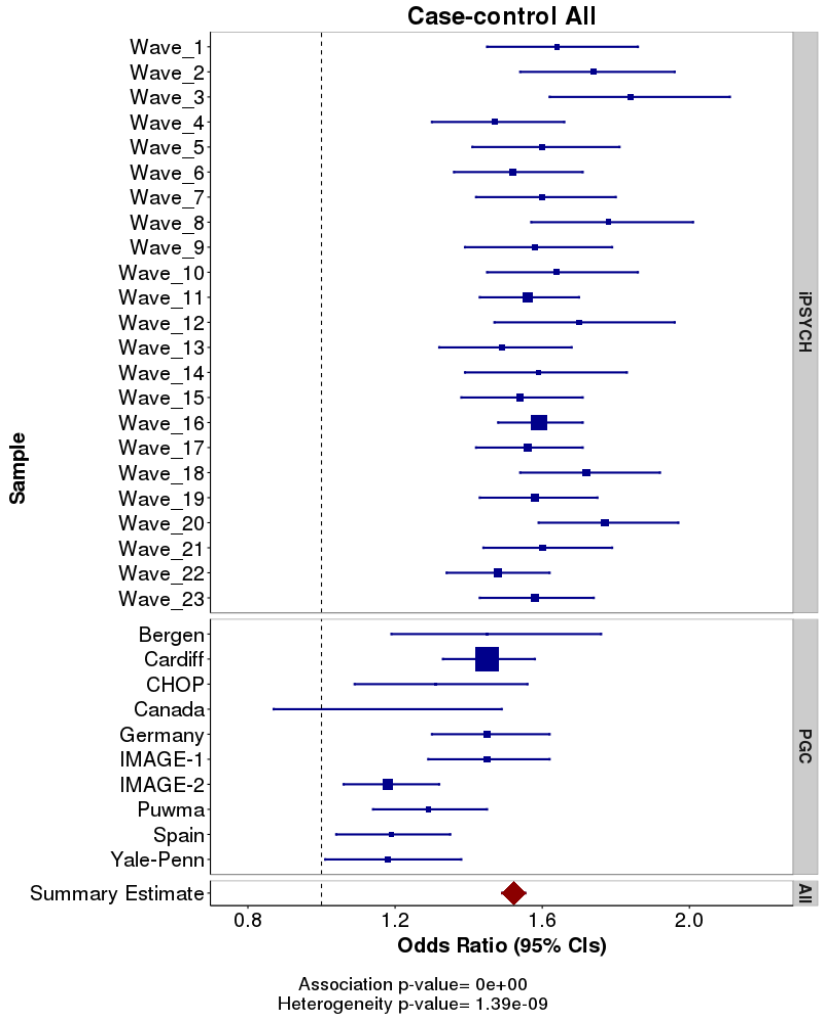

Supplementary Figure 10. PRS based odds ratios within each study/wave

PRS based Odds Ratio and 95% confidence limits from logistic regression of standardised PRS for each target study/wave.

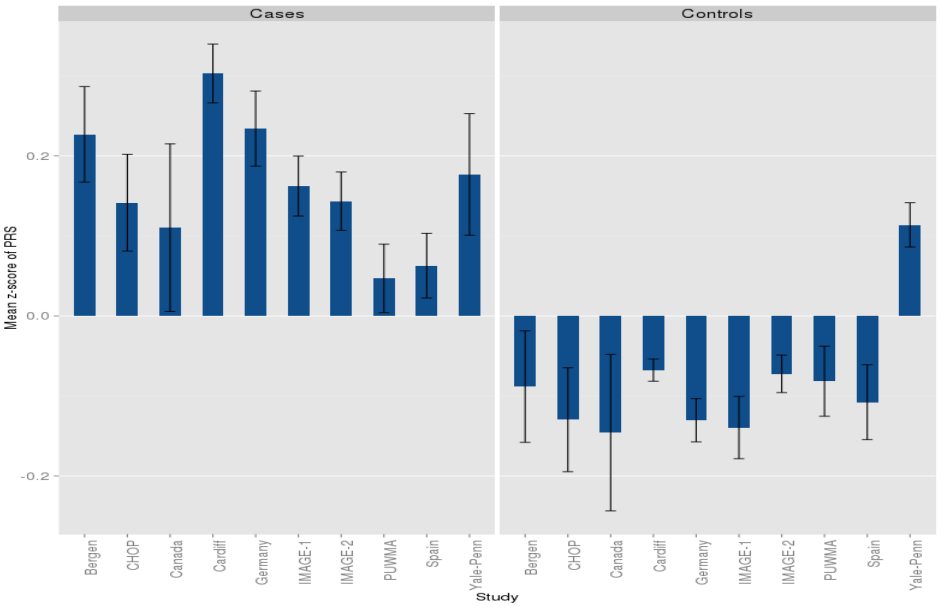

Supplementary Figure 11. ADHD PRS stratified by case-control status and PGC study

Mean PRS z-score (+/- standard error) plotted stratified by case status and PGC study.

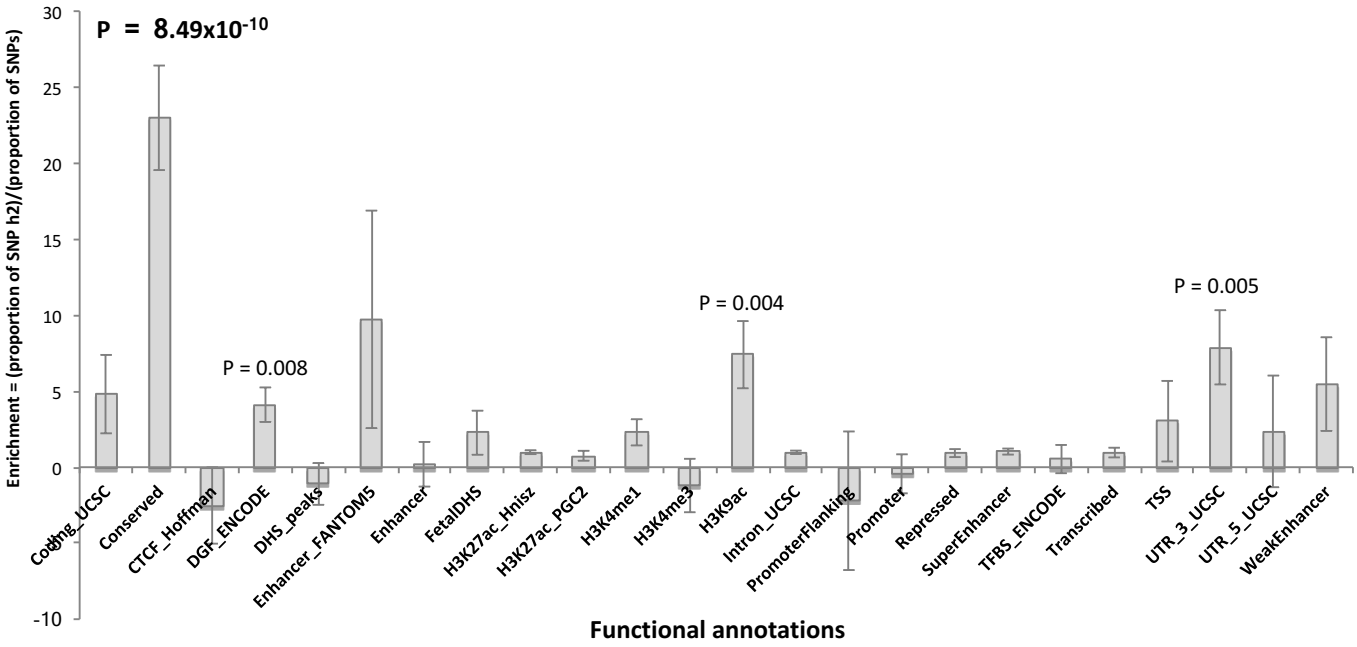

Supplementary Figure 12. Partitioning of h^2 by functional annotations

Enrichment of heritability per SNP in 24 functional annotations defined by Finucane et al.[64] Error bars represent 95% confidence intervals. P-values for annotation categories with nominal significant enrichment are shown and values on bold indicate significance after Bonferroni correction.

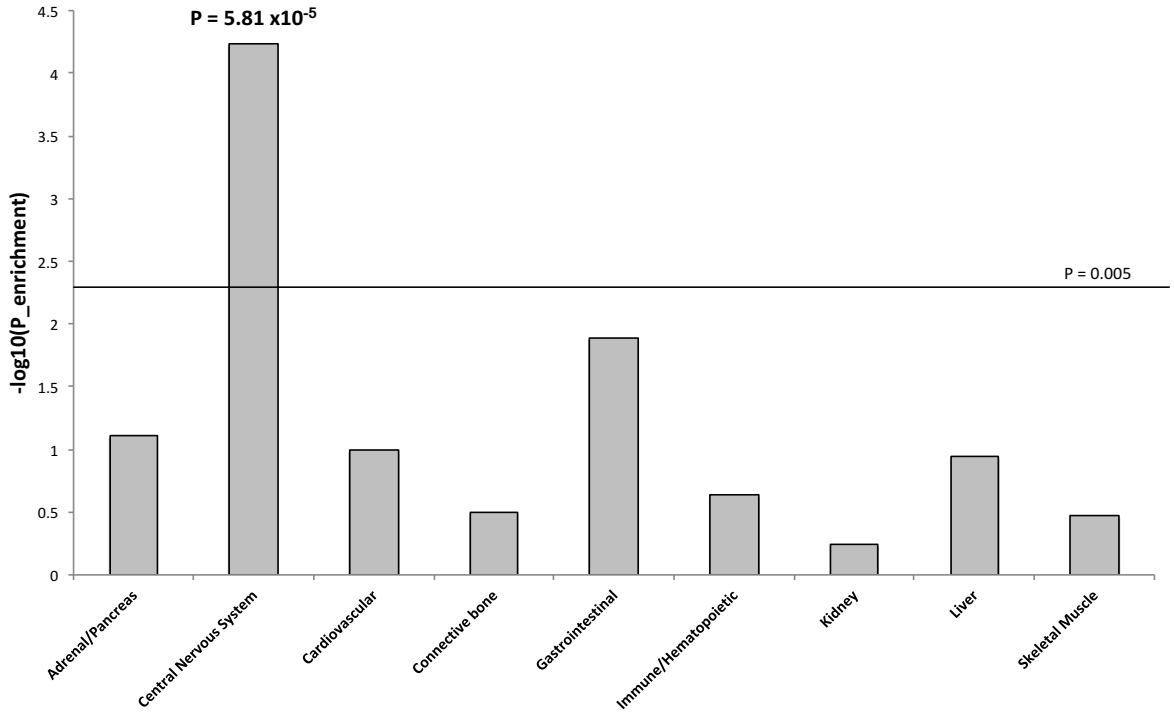

Supplementary Figure 13. Partitioning of h^2 by tissue-group annotations

Results from partitioning heritability by SNPs located in cell-group specific regulatory elements. The line indicate significance after Bonferroni correction (P = 0.005).

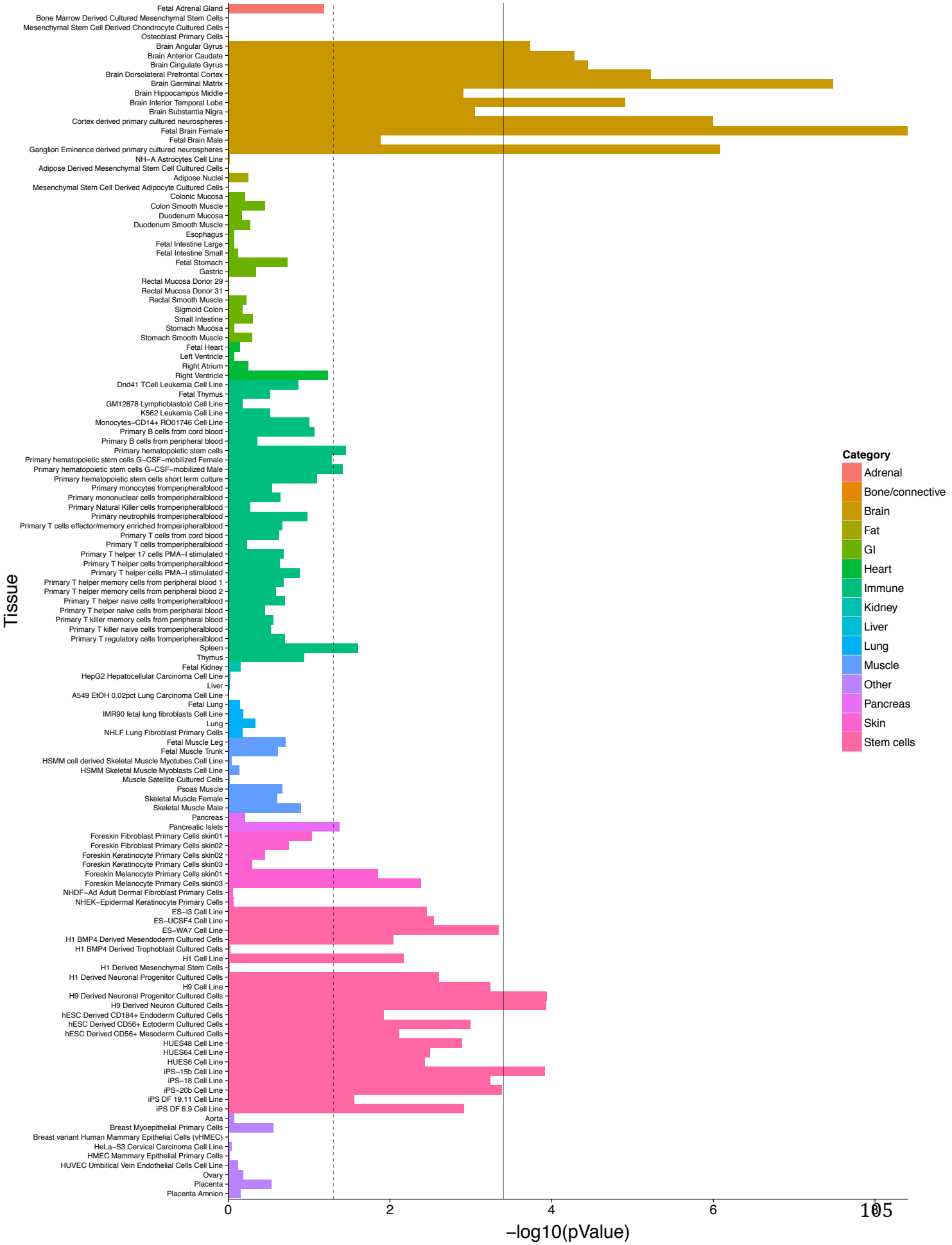
Fetal Adrenal Gland
Bone Marrow Derived Cultured Mesenchymal Stem Cells
Mesenchymal Stem Cell Derived Chondrocyte Cultured Cells
Osteoblast Primary Cells
Brain Angular Gyrus
Brain Anterior Caudate
Brain Cingulate Gyrus
Brain Dorsolateral Prefrontal Cortex
Brain Germinal Matrix
Brain Hippocampus Middle
Brain Inferior Temporal Lobe
Brain Substantia Nigra
Cortex derived primary cultured neurospheres
Fetal Brain Female
Fetal Brain Male
Ganglion Eminence derived primary cultured neurospheres
NH-A Astrocytes Cell Line
Adipose Derived Mesenchymal Stem Cell Cultured Cells
Adipose Nuclei
Mesenchymal Stem Cell Derived Adipocyte Cultured Cells
Colonic Mucosa
Colon Smooth Muscle
Duodenum Mucosa
Duodenum Smooth Muscle
Esophagus
Fetal Intestine Large
Fetal Intestine Small
Fetal Stomach
Gastric
Rectal Mucosa Donor 29
Rectal Mucosa Donor 31
Rectal Smooth Muscle
Sigmoid Colon
Small Intestine
Stomach Mucosa
Stomach Smooth Muscle
Fetal Heart
Left Ventricle
Right Atrium
Right Ventricle
Dnd41 TCell Leukemia Cell Line
Fetal Thymus
GM12878 Lymphoblastoid Cell Line
K562 Leukemia Cell Line
Monocytes-CD14+ RO01746 Cell Line
Primary B cells from cord blood
Primary B cells from peripheral blood
Primary hematopoietic stem cells
Primary hematopoietic stem cells G-CSF-mobilized Female
Primary hematopoietic stem cells G-CSF-mobilized Male
Primary hematopoietic stem cells short term culture
Primary monocytes fromperipheralblood
Primary mononuclear cells fromperipheralblood
Primary Natural Killer cells fromperipheralblood
Primary neutrophils fromperipheralblood
Primary T cells effector/memory enriched fromperipheralblood
Primary T cells from cord blood
Primary T cells fromperipheralblood
Primary T helper 17 cells PMA-I stimulated
Primary T helper cells fromperipheralblood
Primary T helper cells PMA-I stimulated
Primary T helper memory cells from peripheral blood 1
Primary T helper memory cells from peripheral blood 2
Primary T helper naive cells fromperipheralblood
Primary T helper naive cells from peripheral blood
Primary T killer memory cells from peripheral blood
Primary T killer naive cells fromperipheralblood
Primary T regulatory cells fromperipheralblood
Spleen
Thymus
Fetal Kidney
HepG2 Hepatocellular Carcinoma Cell Line
Liver
A549 EtOH 0.02pct Lung Carcinoma Cell Line
Fetal Lung
IMR90 fetal lung fibroblasts Cell Line
Lung
NHLF Lung Fibroblast Primary Cells
Fetal Muscle Leg
Fetal Muscle Trunk
HSMM cell derived Skeletal Muscle Myotubes Cell Line
HSMM Skeletal Muscle Myoblasts Cell Line
Muscle Satellite Cultured Cells
Psoas Muscle
Skeletal Muscle Female
Skeletal Muscle Male
Pancreas
Pancreatic Islets
Foreskin Fibroblast Primary Cells skin01
Foreskin Fibroblast Primary Cells skin02
Foreskin Keratinocyte Primary Cells skin02
Foreskin Keratinocyte Primary Cells skin03
Foreskin Melanocyte Primary Cells skin01
Foreskin Melanocyte Primary Cells skin03
NHDF-Ad Adult Dermal Fibroblast Primary Cells
NHEK-Epidermal Keratinocyte Primary Cells
ES-I3 Cell Line
ES-UCSF4 Cell Line
ES-WA7 Cell Line
H1 BMP4 Derived Mesendoderm Cultured Cells
H1 BMP4 Derived Trophoblast Cultured Cells
H1 Cell Line
H1 Derived Mesenchymal Stem Cells
H1 Derived Neuronal Progenitor Cultured Cells
H9 Cell Line
H9 Derived Neuronal Progenitor Cultured Cells
H9 Derived Neuron Cultured Cells
hESC Derived CD184+ Endoderm Cultured Cells
hESC Derived CD56+ Ectoderm Cultured Cells
hESC Derived CD56+ Mesoderm Cultured Cells
HUES48 Cell Line
HUES64 Cell Line
HUES6 Cell Line
iPS-15b Cell Line
iPS-18 Cell Line
iPS-20b Cell Line
iPS DF 19.11 Cell Line
iPS DF 6.9 Cell Line
Aorta
Breast Myoepithelial Primary Cells
Breast variant Human Mammary Epithelial Cells (vHMEC)
HeLa-S3 Cervical Carcinoma Cell Line
HMEC Mammary Epithelial Primary Cells
HUVEC Umbilical Vein Endothelial Cells Cell Line
Ovary
Placenta
Placenta Amnion
Tissue
0
2
4
6
10
−log10(pValue)
Category
Adrenal
Bone/connective
Brain
Fat
GI
Heart
Immune
Kidney
Liver
Lung
Muscle
Other
Pancreas
Skin
Stem cells

Supplementary Figure 14. Partitioning of h^2 by tissue-specific H3K4Me1 annotations

P-values for enrichment in the SNP heritability of ADHD by variants located within regulatory regions (H3K4Me1 peaks) of various cells and tissues (annotations from the Roadmap Epigenomics Mapping Consortium[67]). Dashed line: threshold for nominal significance. Full line: threshold for significance after Bonferonni correction.

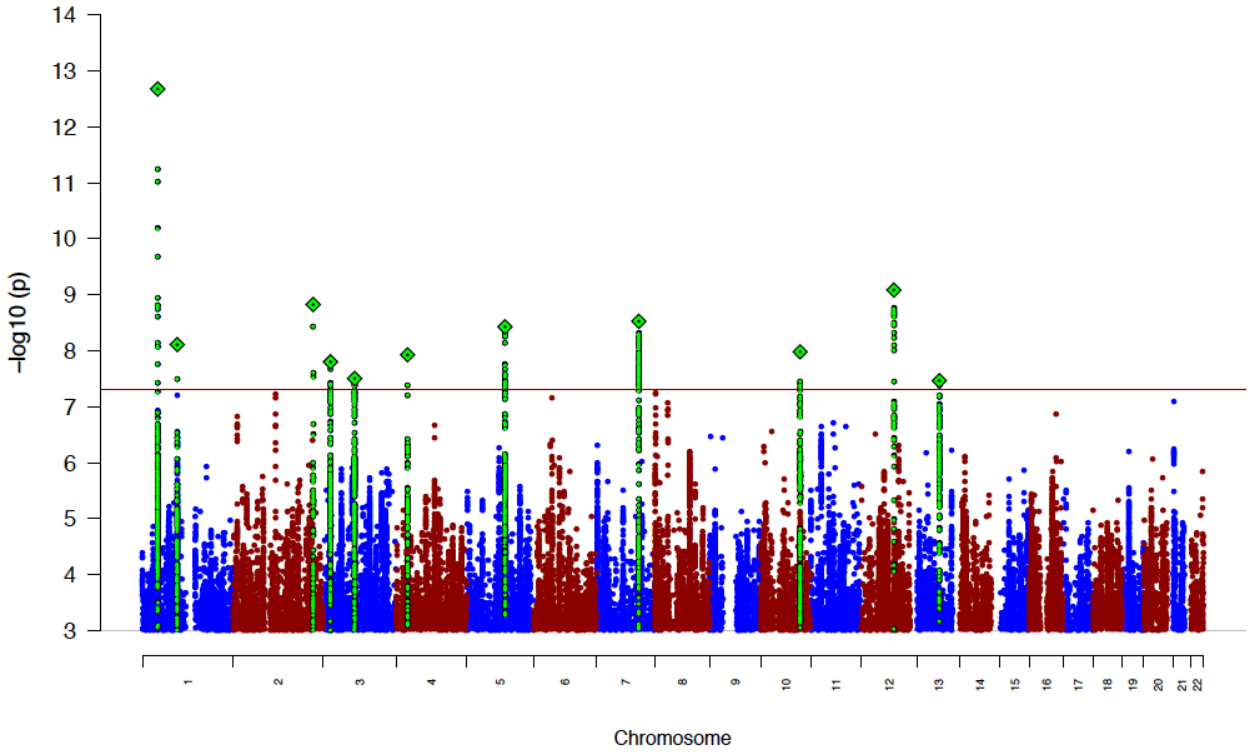

Supplementary Figure 15. Manhattan plot of results from meta-analysis of ADHD+23andMe

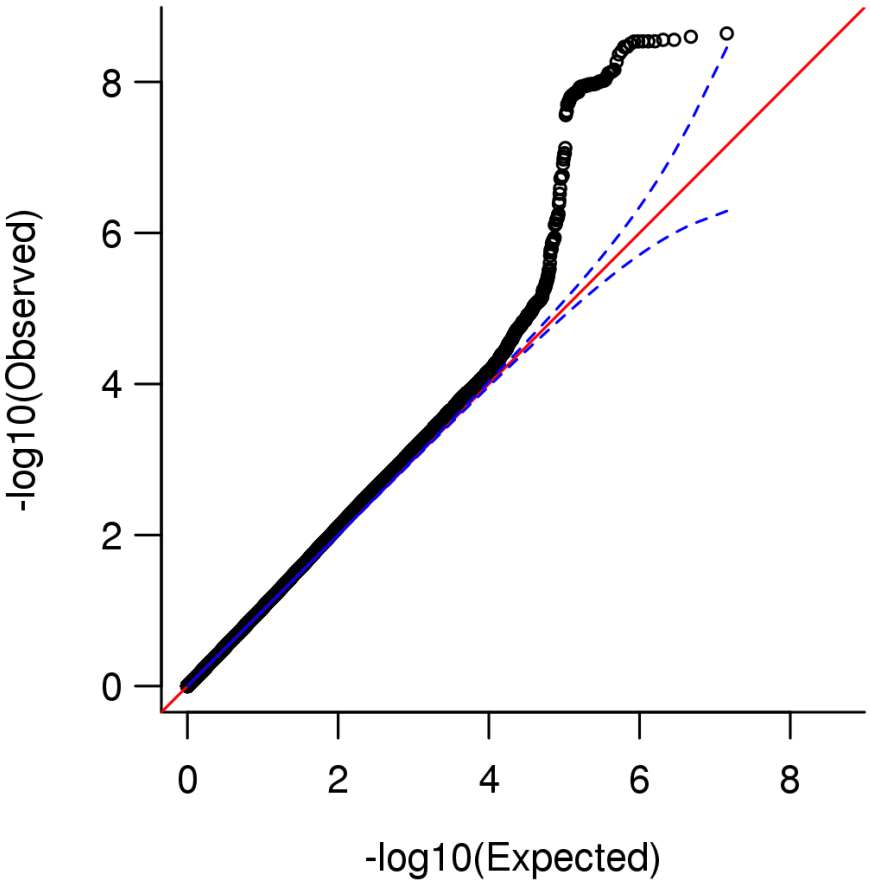

Supplementary Figure 16. Q-Q plot from test for heterogeneity between ADHD GWAS meta-analysis and 23andMe

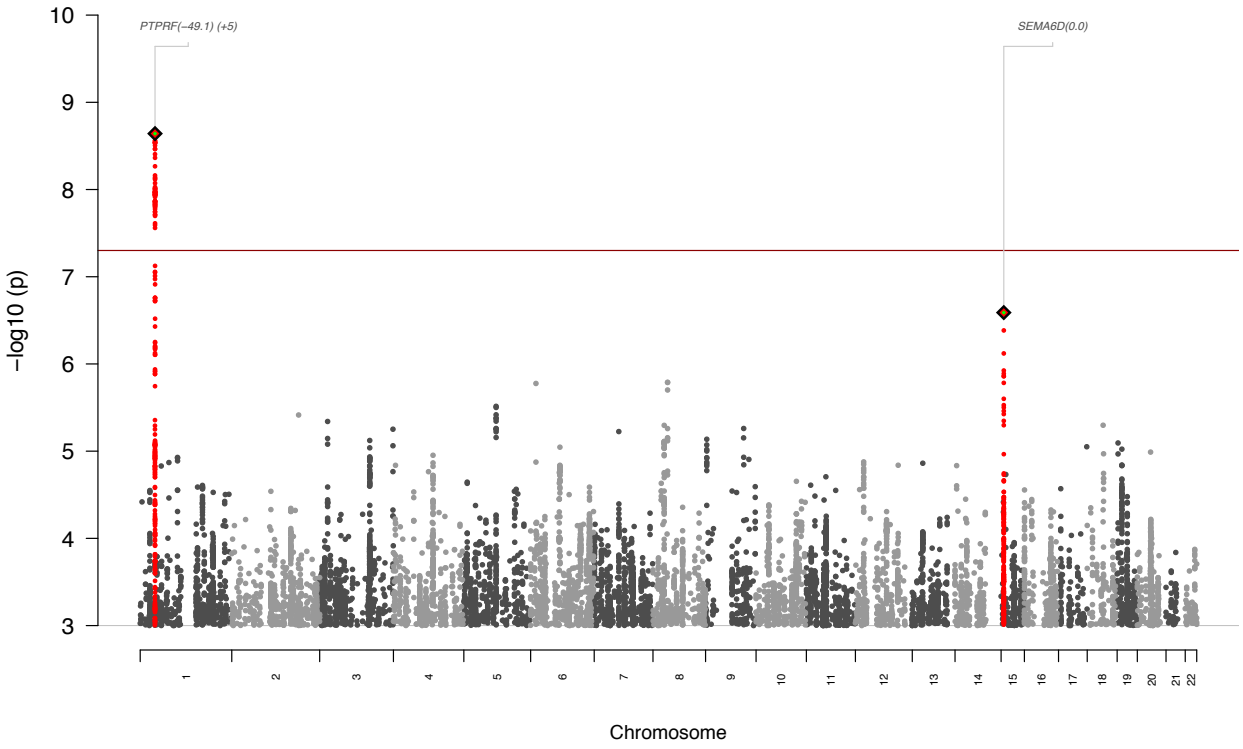

Supplementary Figure 17. Manhattan plot from test for heterogeneity between ADHD GWAS meta-analysis and 23andMe

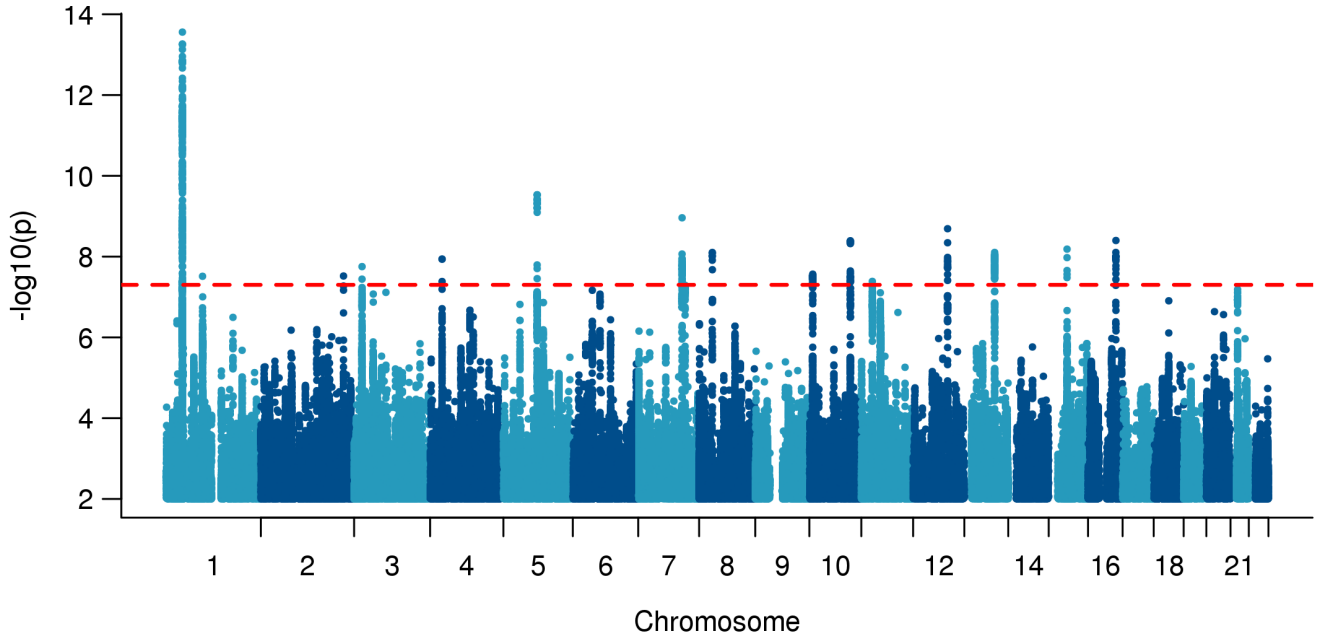

Supplementary Figure 18. Manhattan plot of results from meta-analysis of ADHD+EAGLE

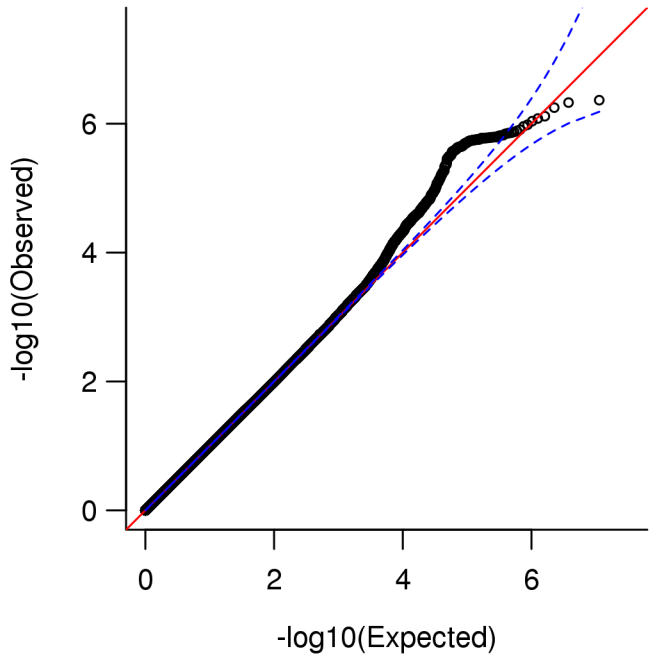

Supplementary Figure 19. Q-Q plot from test for heterogeneity between ADHD GWAS meta-analysis and EAGLE

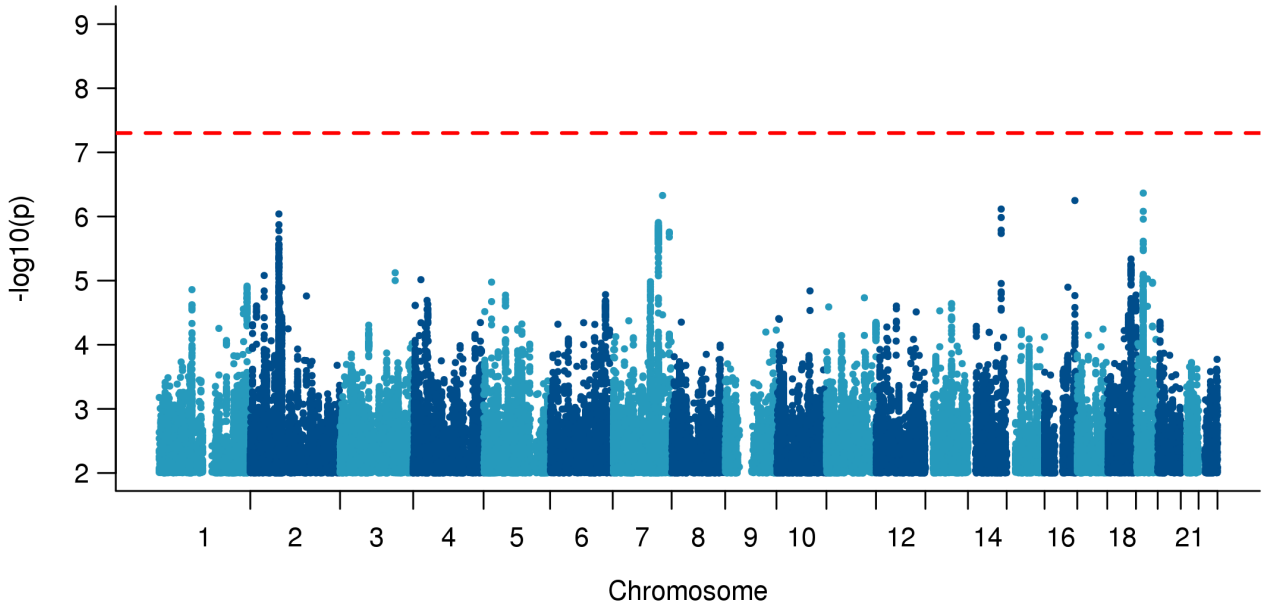

Supplementary Figure 20. Manhattan plot from test for heterogeneity between ADHD GWAS meta-analysis and EAGLE

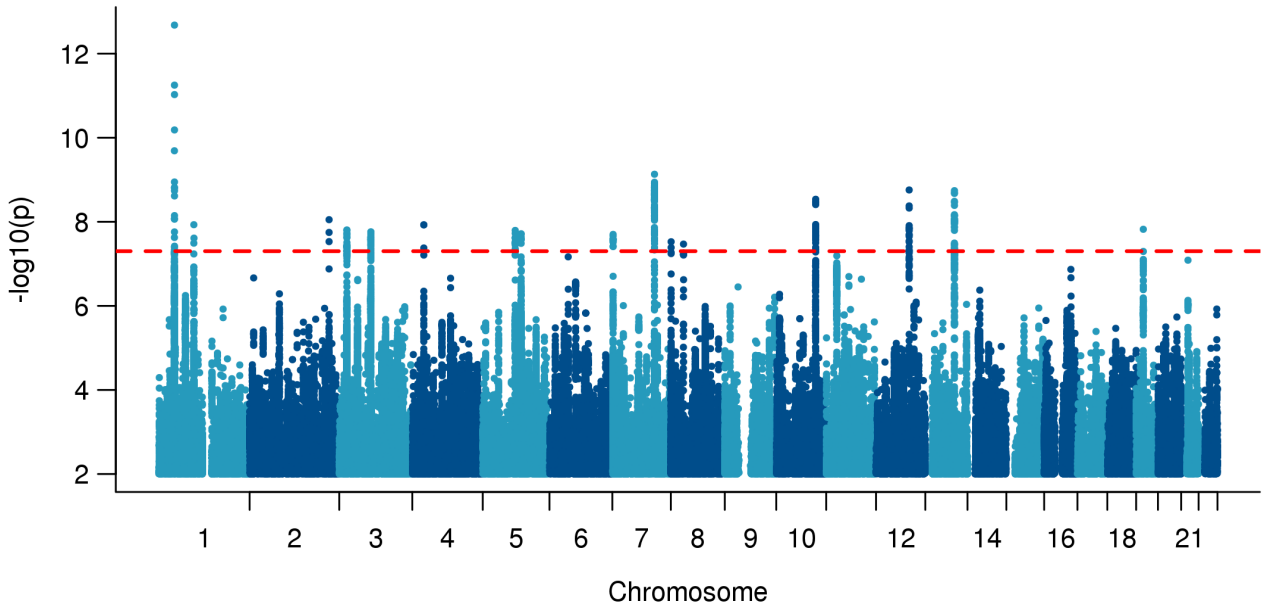

Supplementary Figure 21. Manhattan plot of results from meta-analysis of ADHD+23andMe+EAGLE

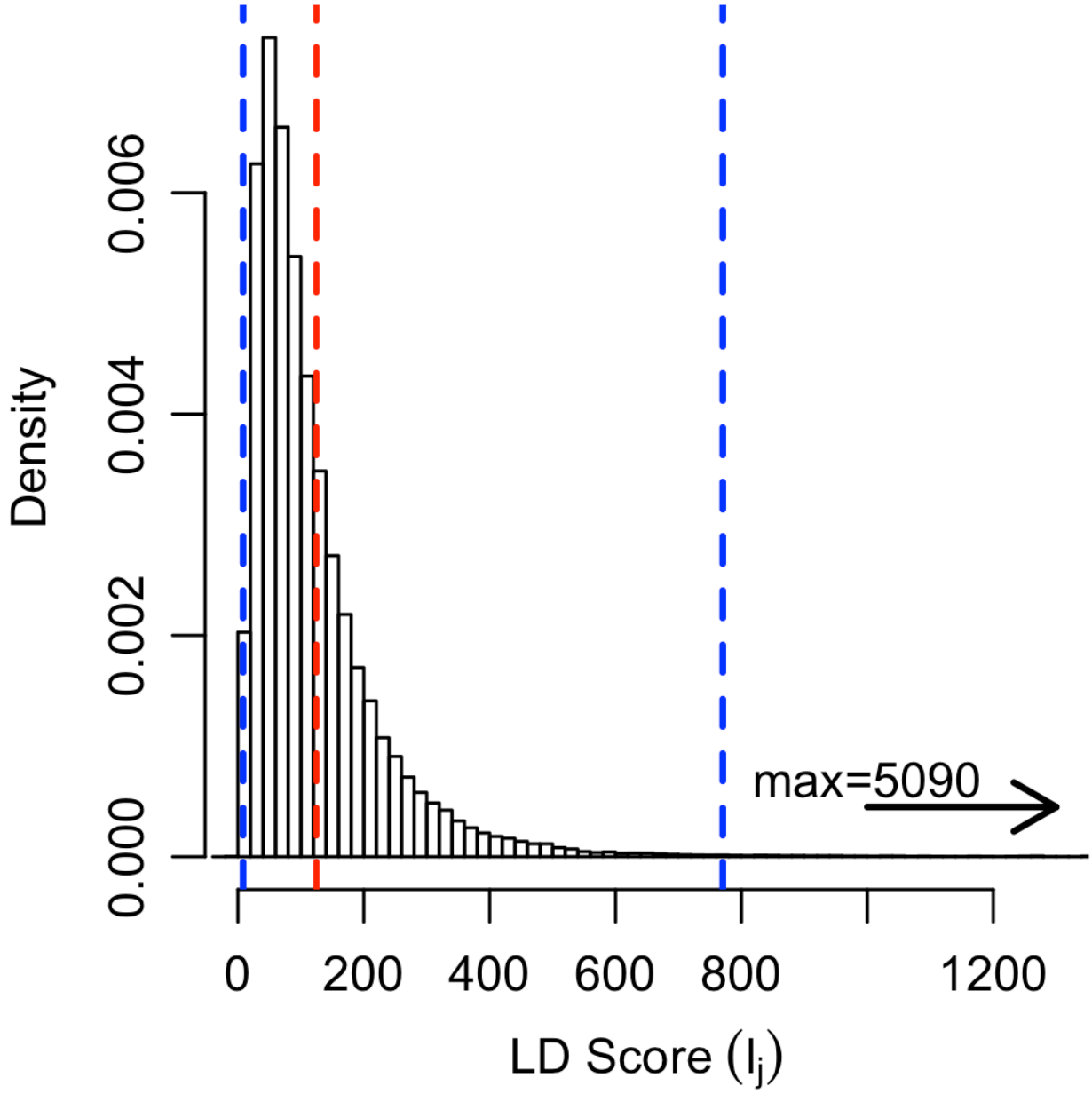

Supplementary Figure 22. Distribution of 1000 Genomes Phase 3 European LD Scores

Distribution of LD scores l_j for common HapMap3 SNPs estimated in 1000 Genomes Phase 3 data using individuals of European ancestry. LD scores downloaded from http://data.broadinstitute.org/alkesgroup/LDSCORE/. Red reference line indicates mean LD score. Blue reference lines indicate 0.5% and 99.5% quantiles of the distribution.

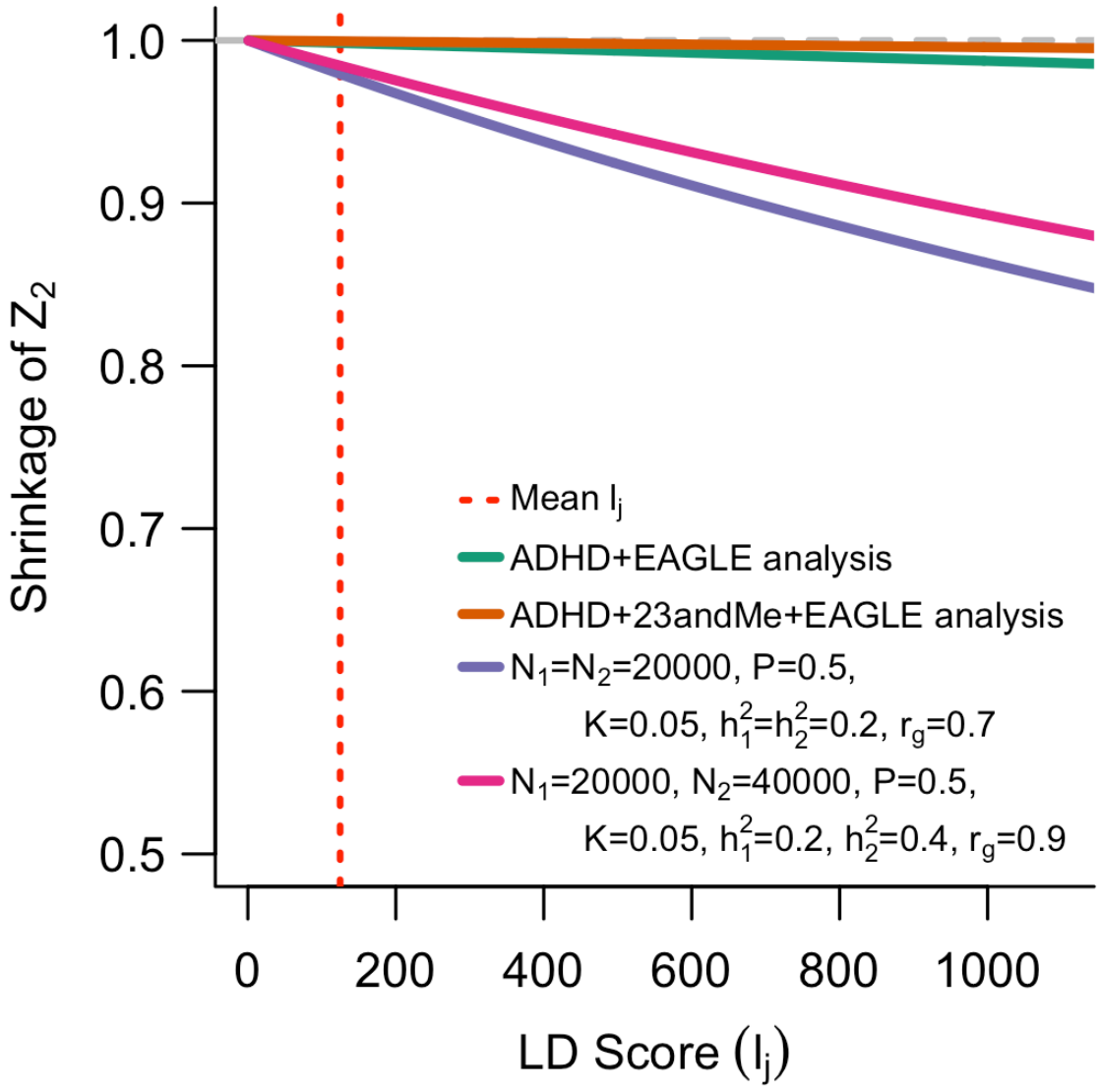

Supplementary Figure 23. Shrinkage factor for $\tilde{Z}_{2j}$ with varying l_j

Value of $1/\sqrt{1+(1-r_g^2)N_{2j}h_2^2\,l_j/M}$, the reduction in Z_{2j} to account for polygenic effects specific to the second phenotype, across the range of observed values for l_j. We compare the value of this term at the estimates of r_g^2, N_2, h_2^2, and M observed in the current study, as well as with example values for scenarios with lower r_g^2 or a more highly powered GWAS of the second phenotype (i.e. increased N_2 and h_2^2). The red reference line indicates the fixed value of $l_j = 124.718$ used for the current study.

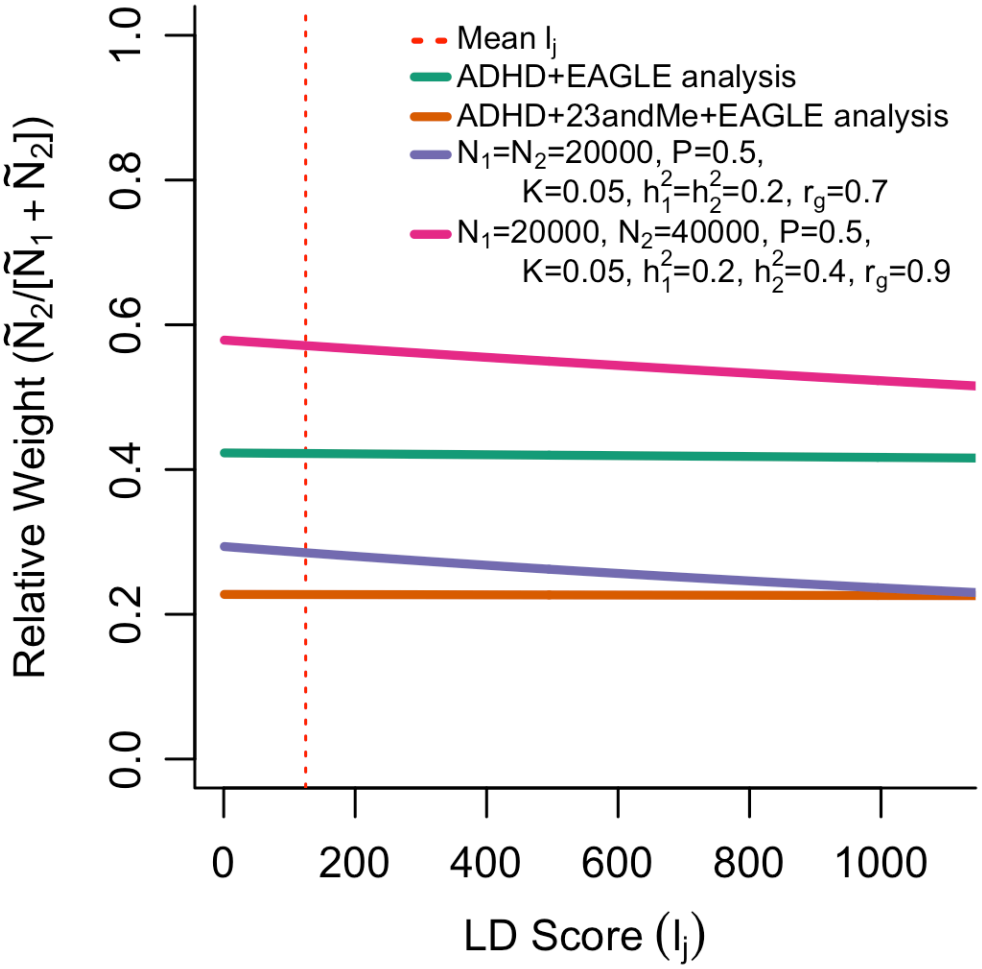

Supplementary Figure 24. Relative effective sample size $\tilde{N}_{2j}$ with varying l_j

Value of $\tilde{N}_{2j}/(\tilde{N}_{1j} + \tilde{N}_{2j})$, the relative effective sample size for the second phenotype, across the range of observed values for l_j. We compare the value of this term at the estimates of $N_1, N_2, r_g^2, h_1^2, h_2^2, K, P,$ and M observed in the current study, as well as with example values for scenarios with lower r_g^2 or a more highly powered GWAS of the second phenotype (i.e. increased N_2 and h_2^2). The red reference line indicates the fixed value of $l_j = 124.718$ used for the current study.

References

1 Pedersen, C. B., Gotzsche, H., Moller, J. O. & Mortensen, P. B. The Danish Civil Registration System. A cohort of eight million persons. *Danish Medical Bulletin* **53**, 441-449 (2006).

2 Mors, O., Perto, G. P. & Mortensen, P. B. The Danish Psychiatric Central Research Register. *Scand J Public Health* **39**, 54-57, doi:10.1177/1403494810395825 (2011).

3 Borglum, A. D. *et al.* Genome-wide study of association and interaction with maternal cytomegalovirus infection suggests new schizophrenia loci. *Molecular psychiatry* **19**, 325-333, doi:10.1038/mp.2013.2 (2014).

4 Hollegaard, M. V. *et al.* Robustness of genome-wide scanning using archived dried blood spot samples as a DNA source. *BMC Genet* **12**, 58, doi:10.1186/1471-2156-12-58 (2011).

5 Illumina. illumina GenCall Data Analysis Software. *Illumina Tech Note* (2005).

6 Korn, J. M. *et al.* Integrated genotype calling and association analysis of SNPs, common copy number polymorphisms and rare CNVs. *Nature genetics* **40**, 1253-1260, doi:10.1038/ng.237 (2008).

7 Goldstein, J. I. *et al.* zCall: a rare variant caller for array-based genotyping: genetics and population analysis. *Bioinformatics* **28**, 2543-2545, doi:10.1093/bioinformatics/bts479 (2012).

8 Elia, J. *et al.* Rare structural variants found in attention-deficit hyperactivity disorder are preferentially associated with neurodevelopmental genes. *Molecular psychiatry* **15**, 637-646, doi:10.1038/mp.2009.57 (2010).

9 Neale, B. M. *et al.* Genome-wide association scan of attention deficit hyperactivity disorder. *American journal of medical genetics. Part B, Neuropsychiatric genetics : the official publication of the International Society of Psychiatric Genetics* **147B**, 1337-1344, doi:10.1002/ajmg.b.30866 (2008).

10 Neale, B. M. *et al.* Meta-analysis of genome-wide association studies of attention-deficit/hyperactivity disorder. *Journal of the American Academy of Child and Adolescent Psychiatry* **49**, 884-897, doi:10.1016/j.jaac.2010.06.008 (2010).

11 Mick, E. *et al.* Family-based genome-wide association scan of attention-deficit/hyperactivity disorder. *Journal of the American Academy of Child and Adolescent Psychiatry* **49**, 898-905 e893, doi:10.1016/j.jaac.2010.02.014 (2010).

12 Lionel, A. C. *et al.* Rare copy number variation discovery and cross-disorder comparisons identify risk genes for ADHD. *Science translational medicine* **3**, 95ra75, doi:10.1126/scitranslmed.3002464 (2011).

13 Sanchez-Mora, C. *et al.* Case-control genome-wide association study of persistent attention-deficit hyperactivity disorder identifies FBXO33 as a novel susceptibility gene for the disorder. *Neuropsychopharmacology* **40**, 915-926, doi:10.1038/npp.2014.267 (2015).

14 Yang, L. *et al.* Polygenic transmission and complex neuro developmental network for attention deficit hyperactivity disorder: genome-wide association study of both common and rare variants. *American journal of medical genetics. Part B, Neuropsychiatric genetics : the official publication of the International Society of Psychiatric Genetics* **162B**, 419-430, doi:10.1002/ajmg.b.32169 (2013).

15 Zayats, T. *et al.* Genome-wide analysis of attention deficit hyperactivity disorder in Norway. *PloS one* **10**, e0122501, doi:10.1371/journal.pone.0122501 (2015).

16 Stergiakouli, E. *et al.* Investigating the contribution of common genetic variants to the risk and pathogenesis of ADHD. *The American journal of psychiatry* **169**, 186-194, doi:10.1176/appi.ajp.2011.11040551 (2012).
17 Hinney, A. *et al.* Genome-wide association study in German patients with attention deficit/hyperactivity disorder. *American journal of medical genetics. Part B, Neuropsychiatric genetics : the official publication of the International Society of Psychiatric Genetics* **156B**, 888-897, doi:10.1002/ajmg.b.31246 (2011).
18 Neale, B. M. *et al.* Case-control genome-wide association study of attention-deficit/hyperactivity disorder. *Journal of the American Academy of Child and Adolescent Psychiatry* **49**, 906-920, doi:10.1016/j.jaac.2010.06.007 (2010).
19 Bakker, S. C. *et al.* A whole-genome scan in 164 Dutch sib pairs with attention-deficit/hyperactivity disorder: suggestive evidence for linkage on chromosomes 7p and 15q. *American journal of human genetics* **72**, 1251-1260 (2003).
20 Myocardial Infarction Genetics, C. *et al.* Genome-wide association of early-onset myocardial infarction with single nucleotide polymorphisms and copy number variants. *Nature genetics* **41**, 334-341, doi:10.1038/ng.327 (2009).
21 Gelernter, J. *et al.* Genome-wide association study of alcohol dependence:significant findings in African- and European-Americans including novel risk loci. *Molecular psychiatry* **19**, 41-49, doi:10.1038/mp.2013.145 (2014).
22 Gelernter, J. *et al.* Genome-wide association study of opioid dependence: multiple associations mapped to calcium and potassium pathways. *Biological psychiatry* **76**, 66-74, doi:10.1016/j.biopsych.2013.08.034 (2014).
23 Gelernter, J. *et al.* Genome-wide association study of cocaine dependence and related traits: FAM53B identified as a risk gene. *Molecular psychiatry* **19**, 717-723, doi:10.1038/mp.2013.99 (2014).
24 Pappa, I. *et al.* A genome-wide approach to children's aggressive behavior: The EAGLE consortium. *American journal of medical genetics. Part B, Neuropsychiatric genetics : the official publication of the International Society of Psychiatric Genetics*, doi:10.1002/ajmg.b.32333 (2015).
25 Paternoster, L. *et al.* Meta-analysis of genome-wide association studies identifies three new risk loci for atopic dermatitis. *Nature genetics* **44**, 187-192, doi:10.1038/ng.1017 (2011).
26 van der Valk, R. J. *et al.* A novel common variant in DCST2 is associated with length in early life and height in adulthood. *Hum Mol Genet* **24**, 1155-1168, doi:10.1093/hmg/ddu510 (2015).
27 Middeldorp, C. M. *et al.* A Genome-Wide Association Meta-Analysis of Attention-Deficit/Hyperactivity Disorder Symptoms in Population-Based Pediatric Cohorts. *Journal of the American Academy of Child and Adolescent Psychiatry* **55**, 896-905 e896, doi:10.1016/j.jaac.2016.05.025 (2016).
28 Genomes Project, C. *et al.* An integrated map of genetic variation from 1,092 human genomes. *Nature* **491**, 56-65, doi:10.1038/nature11632 (2012).
29 Willer, C. J., Li, Y. & Abecasis, G. R. METAL: fast and efficient meta-analysis of genomewide association scans. *Bioinformatics* **26**, 2190-2191, doi:10.1093/bioinformatics/btq340 (2010).
30 Schizophrenia Working Group of the Psychiatric Genomics, C. Biological insights from 108 schizophrenia-associated genetic loci. *Nature* **511**, 421-427, doi:10.1038/nature13595 (2014).

31 Delaneau, O., Marchini, J. & Zagury, J. F. A linear complexity phasing method for thousands of genomes. *Nature methods* **9**, 179-181, doi:10.1038/nmeth.1785 (2011).
32 Howie, B., Marchini, J. & Stephens, M. Genotype imputation with thousands of genomes. *G3* **1**, 457-470, doi:10.1534/g3.111.001198 (2011).
33 Sudmant, P. H. *et al.* An integrated map of structural variation in 2,504 human genomes. *Nature* **526**, 75-81, doi:10.1038/nature15394 (2015).
34 Genomes Project, C. *et al.* A global reference for human genetic variation. *Nature* **526**, 68-74, doi:10.1038/nature15393 (2015).
35 Price, A. L. *et al.* Long-range LD can confound genome scans in admixed populations. *American journal of human genetics* **83**, 132-135; author reply 135-139, doi:10.1016/j.ajhg.2008.06.005 (2008).
36 Purcell, S. *et al.* PLINK: a tool set for whole-genome association and population-based linkage analyses. *American journal of human genetics* **81**, 559-575, doi:10.1086/519795 (2007).
37 Chang, C. C. *et al.* Second-generation PLINK: rising to the challenge of larger and richer datasets. *Gigascience* **4**, 7, doi:10.1186/s13742-015-0047-8 (2015).
38 Price, A. L. *et al.* Principal components analysis corrects for stratification in genome-wide association studies. *Nature genetics* **38**, 904-909, doi:10.1038/ng1847 (2006).
39 Winkler, T. W. *et al.* Quality control and conduct of genome-wide association meta-analyses. *Nat. Protocols* **9**, 1192-1212, doi:10.1038/nprot.2014.071 (2014).
40 Bulik-Sullivan, B. K. *et al.* LD Score regression distinguishes confounding from polygenicity in genome-wide association studies. *Nature genetics* **47**, 291-295, doi:10.1038/ng.3211 (2015).
41 de Leeuw, C. A., Mooij, J. M., Heskes, T. & Posthuma, D. MAGMA: generalized gene-set analysis of GWAS data. *PLoS Comput Biol* **11**, e1004219, doi:10.1371/journal.pcbi.1004219 (2015).
42 Wellcome Trust Case Control, C. *et al.* Bayesian refinement of association signals for 14 loci in 3 common diseases. *Nature genetics* **44**, 1294-1301, doi:10.1038/ng.2435 (2012).
43 Gormley, P. *et al.* Meta-analysis of 375,000 individuals identifies 38 susceptibility loci for migraine. *Nature genetics* **48**, 856-866, doi:10.1038/ng.3598 (2016).
44 McLaren, W. *et al.* The Ensembl Variant Effect Predictor. *Genome Biol* **17**, 122, doi:10.1186/s13059-016-0974-4 (2016).
45 Harrow, J. *et al.* GENCODE: the reference human genome annotation for The ENCODE Project. *Genome Res* **22**, 1760-1774, doi:10.1101/gr.135350.111 (2012).
46 Won, H. *et al.* Chromosome conformation elucidates regulatory relationships in developing human brain. *Nature* **538**, 523-527, doi:10.1038/nature19847 (2016).
47 Consortium, G. T. Human genomics. The Genotype-Tissue Expression (GTEx) pilot analysis: multitissue gene regulation in humans. *Science* **348**, 648-660, doi:10.1126/science.1262110 (2015).
48 Zhernakova, D. V. *et al.* Identification of context-dependent expression quantitative trait loci in whole blood. *Nature genetics* **49**, 139-145, doi:10.1038/ng.3737 (2017).
49 Roadmap Epigenomics, C. *et al.* Integrative analysis of 111 reference human epigenomes. *Nature* **518**, 317-330, doi:10.1038/nature14248 (2015).
50 Kircher, M. *et al.* A general framework for estimating the relative pathogenicity of human genetic variants. *Nature genetics* **46**, 310-315, doi:10.1038/ng.2892 (2014).

51 Hou, C. A simple approximation for the distribution of the weighted combination of non-independent or independent probabilities. *Statistics and Probabbility Letters* **73**, 179-187 (2005).
52 Farrell, M. S. *et al.* Evaluating historical candidate genes for schizophrenia. *Molecular psychiatry* **20**, 555-562, doi:10.1038/mp.2015.16 (2015).
53 Hawi, Z. *et al.* The molecular genetic architecture of attention deficit hyperactivity disorder. *Molecular psychiatry* **20**, 289-297, doi:10.1038/mp.2014.183 (2015).
54 Day, F. R. *et al.* Large-scale genomic analyses link reproductive aging to hypothalamic signaling, breast cancer susceptibility and BRCA1-mediated DNA repair. *Nature genetics* **47**, 1294-1303, doi:10.1038/ng.3412 (2015).
55 Subramanian, A. *et al.* Gene set enrichment analysis: a knowledge-based approach for interpreting genome-wide expression profiles. *Proceedings of the National Academy of Sciences of the United States of America* **102**, 15545-15550, doi:10.1073/pnas.0506580102 (2005).
56 Vernes, S. C. *et al.* Foxp2 regulates gene networks implicated in neurite outgrowth in the developing brain. *PLoS genetics* **7**, e1002145, doi:10.1371/journal.pgen.1002145 (2011).
57 Spiteri, E. *et al.* Identification of the transcriptional targets of FOXP2, a gene linked to speech and language, in developing human brain. *American journal of human genetics* **81**, 1144-1157, doi:10.1086/522237 (2007).
58 Lek, M. *et al.* Analysis of protein-coding genetic variation in 60,706 humans. *Nature* **536**, 285-291, doi:10.1038/nature19057 (2016).
59 Cross-Disorder Group of the Psychiatric Genomics, C. *et al.* Genetic relationship between five psychiatric disorders estimated from genome-wide SNPs. *Nature genetics* **45**, 984-994, doi:10.1038/ng.2711 (2013).
60 Yang, J., Lee, S. H., Goddard, M. E. & Visscher, P. M. GCTA: a tool for genome-wide complex trait analysis. *American journal of human genetics* **88**, 76-82, doi:10.1016/j.ajhg.2010.11.011 (2011).
61 Purcell, S. M. *et al.* Common polygenic variation contributes to risk of schizophrenia and bipolar disorder. *Nature* **460**, 748-752, doi:0.1038/nature08185 (2009).
62 Sherva, R. *et al.* Genome-wide Association Study of Cannabis Dependence Severity, Novel Risk Variants, and Shared Genetic Risks. *JAMA Psychiatry* **73**, 472-480, doi:10.1001/jamapsychiatry.2016.0036 (2016).
63 Polanczyk, G., de Lima, M. S., Horta, B. L., Biederman, J. & Rohde, L. A. The worldwide prevalence of ADHD: a systematic review and metaregression analysis. *The American journal of psychiatry* **164**, 942-948, doi:10.1176/ajp.2007.164.6.942 (2007).
64 Finucane, H. K. *et al.* Partitioning heritability by functional annotation using genome-wide association summary statistics. *Nature genetics* **47**, 1228-1235, doi:10.1038/ng.3404 (2015).
65 Finucane, H. K. *et al.* Partitioning heritability by functional annotation using genome-wide association summary statistics. *Nature genetics* **47**, 1228-1235 (2015).
66 Trynka, G. *et al.* Chromatin marks identify critical cell types for fine mapping complex trait variants. *Nature genetics* **45**, 124-130, doi:10.1038/ng.2504 (2013).
67 Kundaje, A. *et al.* Integrative analysis of 111 reference human epigenomes. *Nature* **518**, 317-330 (2015).
68 Ernst, J. & Kellis, M. Large-scale imputation of epigenomic datasets for systematic annotation of diverse human tissues. *Nature biotechnology* **33**, 364-376 (2015).

69 Bulik-Sullivan, B. *et al.* An atlas of genetic correlations across human diseases and traits. *Nature genetics* **47**, 1236-1241, doi:10.1038/ng.3406 (2015).
70 Yates, F. Contingency Tables Involving Small Numbers and the χ2 Test. *Supplement to the Journal of the Royal Statistical Society* **1**, 217-235, doi:10.2307/2983604 (1934).
71 R Core Team. *R: A language and environment for statistical computing.* , <http://www.r-project.org/> (2014).
72 Pearson K., L. A. On the inheritance of characters not capable of exact quantitative measurement. *Philosophical Transactions of the Royal Society of London* **Series A**, 79-150 (1901).
73 Cohen, J. The cost of dichotomization. *Applied Psychological Measurement* **7**, 249-253, doi:10.1177/014662168300700301 (1983).
74 Hunter, J. & Schmidt, F. Dichotomization of continuous variables: The implications for meta-analysis. *Journal of Applied Psychology* **75**, 334-349, doi:http://dx.doi.org/10.1037/0021-9010.75.3.334 (1990).
75 Hsieh, F. Y., Bloch, D. A. & Larsen, M. D. A simple method of sample size calculation for linear and logistic regression. *Stat Med* **17**, 1623-1634 (1998).
76 Lee, S. H., Wray, N. R., Goddard, M. E. & Visscher, P. M. Estimating missing heritability for disease from genome-wide association studies. *American journal of human genetics* **88**, 294-305, doi:10.1016/j.ajhg.2011.02.002 (2011).
77 Yang, J. *et al.* Common SNPs explain a large proportion of the heritability for human height. *Nature genetics* **42**, 565-569, doi:10.1038/ng.608 (2010).
78 Stouffer, S., DeVinney, L. & Suchmen, E. *The American soldier: Adjustment during army life.*, Vol. 1 (Princeton University Press, 1949).
79 Faraone, S. V. *et al.* Attention-deficit/hyperactivity disorder. *Nature Reviews Disease Primers*, 15020, doi:10.1038/nrdp.2015.20 (2015).
80 Ribases, M. *et al.* Exploration of 19 serotoninergic candidate genes in adults and children with attention-deficit/hyperactivity disorder identifies association for 5HT2A, DDC and MAOB. *Molecular psychiatry* **14**, 71-85, doi:10.1038/sj.mp.4002100 (2009).
81 Wang, B. Molecular mechanism underlying sialic acid as an essential nutrient for brain development and cognition. *Adv Nutr* **3**, 465S-472S, doi:10.3945/an.112.001875 (2012).
82 Yoo, S. W. *et al.* Sialylation regulates brain structure and function. *FASEB J* **29**, 3040-3053, doi:10.1096/fj.15-270983 (2015).
83 Hu, H. *et al.* ST3GAL3 mutations impair the development of higher cognitive functions. *American journal of human genetics* **89**, 407-414, doi:10.1016/j.ajhg.2011.08.008 (2011).
84 Sturgill, E. R. *et al.* Biosynthesis of the major brain gangliosides GD1a and GT1b. *Glycobiology* **22**, 1289-1301, doi:10.1093/glycob/cws103 (2012).
85 Ledeen, R. W. & Wu, G. Ganglioside function in calcium homeostasis and signaling. *Neurochemical research* **27**, 637-647 (2002).
86 Wu, G., Xie, X., Lu, Z. H. & Ledeen, R. W. Cerebellar neurons lacking complex gangliosides degenerate in the presence of depolarizing levels of potassium. *Proceedings of the National Academy of Sciences of the United States of America* **98**, 307-312, doi:10.1073/pnas.011523698 (2001).
87 Edvardson, S. *et al.* West syndrome caused by ST3Gal-III deficiency. *Epilepsia* **54**, e24-27, doi:10.1111/epi.12050 (2013).

88 Walton, E. *et al.* Epigenetic profiling of ADHD symptoms trajectories: a prospective, methylome-wide study. *Molecular psychiatry*, doi:10.1038/mp.2016.85 (2016).
89 Okbay, A. *et al.* Genome-wide association study identifies 74 loci associated with educational attainment. *Nature* **533**, 539-542, doi:10.1038/nature17671 (2016).
90 Woo, J. *et al.* Trans-synaptic adhesion between NGL-3 and LAR regulates the formation of excitatory synapses. *Nature neuroscience* **12**, 428-437, doi:10.1038/nn.2279 (2009).
91 Yang, T., Massa, S. M. & Longo, F. M. LAR protein tyrosine phosphatase receptor associates with TrkB and modulates neurotrophic signaling pathways. *J Neurobiol* **66**, 1420-1436, doi:10.1002/neu.20291 (2006).
92 Davies, G. *et al.* Genome-wide association study of cognitive functions and educational attainment in UK Biobank (N=112 151). *Molecular psychiatry* **21**, 758-767, doi:10.1038/mp.2016.45 (2016).
93 Zabolotny, J. M. *et al.* Overexpression of the LAR (leukocyte antigen-related) protein-tyrosine phosphatase in muscle causes insulin resistance. *Proceedings of the National Academy of Sciences of the United States of America* **98**, 5187-5192, doi:10.1073/pnas.071050398 (2001).
94 Zhang, Z. *et al.* A heterozygous mutation disrupting the SPAG16 gene results in biochemical instability of central apparatus components of the human sperm axoneme. *Biol Reprod* **77**, 864-871, doi:10.1095/biolreprod.107.063206 (2007).
95 Zhang, Z. *et al.* A sperm-associated WD repeat protein orthologous to Chlamydomonas PF20 associates with Spag6, the mammalian orthologue of Chlamydomonas PF16. *Mol Cell Biol* **22**, 7993-8004 (2002).
96 Somers, V. *et al.* Autoantibody profiling in multiple sclerosis reveals novel antigenic candidates. *J Immunol* **180**, 3957-3963 (2008).
97 de Bock, L. *et al.* Anti-SPAG16 antibodies in primary progressive multiple sclerosis are associated with an elevated progression index. *Eur J Neurol* **23**, 722-728, doi:10.1111/ene.12925 (2016).
98 Leung, L. C. *et al.* Coupling of NF-protocadherin signaling to axon guidance by cue-induced translation. *Nature neuroscience* **16**, 166-173, doi:10.1038/nn.3290 (2013).
99 Blevins, C. J., Emond, M. R., Biswas, S. & Jontes, J. D. Differential expression, alternative splicing, and adhesive properties of the zebrafish delta1-protocadherins. *Neuroscience* **199**, 523-534, doi:10.1016/j.neuroscience.2011.09.061 (2011).
100 Krishna, K. K., Hertel, N. & Redies, C. Cadherin expression in the somatosensory cortex: evidence for a combinatorial molecular code at the single-cell level. *Neuroscience* **175**, 37-48, doi:10.1016/j.neuroscience.2010.11.056 (2011).
101 Kim, S. Y., Chung, H. S., Sun, W. & Kim, H. Spatiotemporal expression pattern of non-clustered protocadherin family members in the developing rat brain. *Neuroscience* **147**, 996-1021, doi:10.1016/j.neuroscience.2007.03.052 (2007).
102 International League Against Epilepsy Consortium on Complex Epilepsies. Electronic address, e.-a. u. e. a. Genetic determinants of common epilepsies: a meta-analysis of genome-wide association studies. *Lancet Neurol* **13**, 893-903, doi:10.1016/S1474-4422(14)70171-1 (2014).
103 Miyake, K. *et al.* The protocadherins, PCDHB1 and PCDH7, are regulated by MeCP2 in neuronal cells and brain tissues: implication for pathogenesis of Rett syndrome. *BMC Neurosci* **12**, 81, doi:10.1186/1471-2202-12-81 (2011).

104 Oliver, P. L. *et al.* Disruption of Visc-2, a Brain-Expressed Conserved Long Noncoding RNA, Does Not Elicit an Overt Anatomical or Behavioral Phenotype. *Cereb Cortex* **25**, 3572-3585, doi:10.1093/cercor/bhu196 (2015).
105 Janson, C. G., Chen, Y., Li, Y. & Leifer, D. Functional regulatory regions of human transcription factor MEF2C. *Brain Res Mol Brain Res* **97**, 70-82 (2001).
106 Harrington, A. J. *et al.* MEF2C regulates cortical inhibitory and excitatory synapses and behaviors relevant to neurodevelopmental disorders. *Elife* **5**, doi:10.7554/eLife.20059 (2016).
107 Adachi, M., Lin, P. Y., Pranav, H. & Monteggia, L. M. Postnatal Loss of Mef2c Results in Dissociation of Effects on Synapse Number and Learning and Memory. *Biological psychiatry* **80**, 140-148, doi:10.1016/j.biopsych.2015.09.018 (2016).
108 Li, H. *et al.* Transcription factor MEF2C influences neural stem/progenitor cell differentiation and maturation in vivo. *Proceedings of the National Academy of Sciences of the United States of America* **105**, 9397-9402, doi:10.1073/pnas.0802876105 (2008).
109 Barbosa, A. C. *et al.* MEF2C, a transcription factor that facilitates learning and memory by negative regulation of synapse numbers and function. *Proceedings of the National Academy of Sciences of the United States of America* **105**, 9391-9396, doi:10.1073/pnas.0802679105 (2008).
110 Lambert, J. C. *et al.* Meta-analysis of 74,046 individuals identifies 11 new susceptibility loci for Alzheimer's disease. *Nature genetics* **45**, 1452-1458, doi:10.1038/ng.2802 (2013).
111 Hyde, C. L. *et al.* Identification of 15 genetic loci associated with risk of major depression in individuals of European descent. *Nature genetics* **48**, 1031-1036, doi:10.1038/ng.3623 (2016).
112 Novara, F. *et al.* Refining the phenotype associated with MEF2C haploinsufficiency. *Clin Genet* **78**, 471-477, doi:10.1111/j.1399-0004.2010.01413.x (2010).
113 Mikhail, F. M. *et al.* Clinically relevant single gene or intragenic deletions encompassing critical neurodevelopmental genes in patients with developmental delay, mental retardation, and/or autism spectrum disorders. *Am J Med Genet A* **155A**, 2386-2396, doi:10.1002/ajmg.a.34177 (2011).
114 Sia, G. M., Clem, R. L. & Huganir, R. L. The human language-associated gene SRPX2 regulates synapse formation and vocalization in mice. *Science* **342**, 987-991, doi:10.1126/science.1245079 (2013).
115 Tsui, D., Vessey, J. P., Tomita, H., Kaplan, D. R. & Miller, F. D. FoxP2 regulates neurogenesis during embryonic cortical development. *The Journal of neuroscience : the official journal of the Society for Neuroscience* **33**, 244-258, doi:10.1523/JNEUROSCI.1665-12.2013 (2013).
116 Schreiweis, C. *et al.* Humanized Foxp2 accelerates learning by enhancing transitions from declarative to procedural performance. *Proceedings of the National Academy of Sciences of the United States of America* **111**, 14253-14258, doi:10.1073/pnas.1414542111 (2014).
117 Vernes, S. C. *et al.* A functional genetic link between distinct developmental language disorders. *N Engl J Med* **359**, 2337-2345, doi:10.1056/NEJMoa0802828 (2008).
118 Lai, C. S., Gerrelli, D., Monaco, A. P., Fisher, S. E. & Copp, A. J. FOXP2 expression during brain development coincides with adult sites of pathology in a severe speech and language disorder. *Brain* **126**, 2455-2462, doi:10.1093/brain/awg247 (2003).

119 Wilcke, A. *et al.* Imaging genetics of FOXP2 in dyslexia. *Eur J Hum Genet* **20**, 224-229, doi:10.1038/ejhg.2011.160 (2012).
120 Lai, C. S., Fisher, S. E., Hurst, J. A., Vargha-Khadem, F. & Monaco, A. P. A forkhead-domain gene is mutated in a severe speech and language disorder. *Nature* **413**, 519-523, doi:10.1038/35097076 (2001).
121 Ribases, M. *et al.* An association study of sequence variants in the forkhead box P2 (FOXP2) gene and adulthood attention-deficit/hyperactivity disorder in two European samples. *Psychiatric genetics* **22**, 155-160, doi:10.1097/YPG.0b013e328353957e (2012).
122 Barban, N. *et al.* Genome-wide analysis identifies 12 loci influencing human reproductive behavior. *Nature genetics* **48**, 1462-1472, doi:10.1038/ng.3698 (2016).
123 Willnow, T. E., Petersen, C. M. & Nykjaer, A. VPS10P-domain receptors - regulators of neuronal viability and function. *Nature reviews. Neuroscience* **9**, 899-909, doi:10.1038/nrn2516 (2008).
124 Hermey, G. *et al.* The three sorCS genes are differentially expressed and regulated by synaptic activity. *J Neurochem* **88**, 1470-1476 (2004).
125 Breiderhoff, T. *et al.* Sortilin-related receptor SORCS3 is a postsynaptic modulator of synaptic depression and fear extinction. *PloS one* **8**, e75006, doi:10.1371/journal.pone.0075006 (2013).
126 Oetjen, S., Mahlke, C., Hermans-Borgmeyer, I. & Hermey, G. Spatiotemporal expression analysis of the growth factor receptor SorCS3. *J Comp Neurol* **522**, 3386-3402, doi:10.1002/cne.23606 (2014).
127 Reitz, C. *et al.* Independent and epistatic effects of variants in VPS10-d receptors on Alzheimer disease risk and processing of the amyloid precursor protein (APP). *Transl Psychiatry* **3**, e256, doi:10.1038/tp.2013.13 (2013).
128 Muda, M. *et al.* MKP-3, a novel cytosolic protein-tyrosine phosphatase that exemplifies a new class of mitogen-activated protein kinase phosphatase. *The Journal of biological chemistry* **271**, 4319-4326 (1996).
129 Caunt, C. J. & Keyse, S. M. Dual-specificity MAP kinase phosphatases (MKPs): shaping the outcome of MAP kinase signalling. *FEBS J* **280**, 489-504, doi:10.1111/j.1742-4658.2012.08716.x (2013).
130 Owens, D. M. & Keyse, S. M. Differential regulation of MAP kinase signalling by dual-specificity protein phosphatases. *Oncogene* **26**, 3203-3213, doi:10.1038/sj.onc.1210412 (2007).
131 Stewart, A. E., Dowd, S., Keyse, S. M. & McDonald, N. Q. Crystal structure of the MAPK phosphatase Pyst1 catalytic domain and implications for regulated activation. *Nat Struct Biol* **6**, 174-181, doi:10.1038/5861 (1999).
132 Bermudez, O., Pages, G. & Gimond, C. The dual-specificity MAP kinase phosphatases: critical roles in development and cancer. *Am J Physiol Cell Physiol* **299**, C189-202, doi:10.1152/ajpcell.00347.2009 (2010).
133 Dickinson, R. J., Eblaghie, M. C., Keyse, S. M. & Morriss-Kay, G. M. Expression of the ERK-specific MAP kinase phosphatase PYST1/MKP3 in mouse embryos during morphogenesis and early organogenesis. *Mech Dev* **113**, 193-196 (2002).
134 Li, C., Scott, D. A., Hatch, E., Tian, X. & Mansour, S. L. Dusp6 (Mkp3) is a negative feedback regulator of FGF-stimulated ERK signaling during mouse development. *Development* **134**, 167-176, doi:10.1242/dev.02701 (2007).

135 Mortensen, O. V. MKP3 eliminates depolarization-dependent neurotransmitter release through downregulation of L-type calcium channel Cav1.2 expression. *Cell Calcium* **53**, 224-230, doi:10.1016/j.ceca.2012.12.004 (2013).
136 Mortensen, O. V., Larsen, M. B., Prasad, B. M. & Amara, S. G. Genetic complementation screen identifies a mitogen-activated protein kinase phosphatase, MKP3, as a regulator of dopamine transporter trafficking. *Mol Biol Cell* **19**, 2818-2829, doi:10.1091/mbc.E07-09-0980 (2008).
137 Takaki, M. *et al.* Two kinds of mitogen-activated protein kinase phosphatases, MKP-1 and MKP-3, are differentially activated by acute and chronic methamphetamine treatment in the rat brain. *J Neurochem* **79**, 679-688 (2001).
138 Miraoui, H. *et al.* Mutations in FGF17, IL17RD, DUSP6, SPRY4, and FLRT3 are identified in individuals with congenital hypogonadotropic hypogonadism. *American journal of human genetics* **92**, 725-743, doi:10.1016/j.ajhg.2013.04.008 (2013).
139 Luo, Y. *et al.* Differential expression of FOXA1, DUSP6, and HA117 in colon segments of Hirschsprung's disease. *Int J Clin Exp Pathol* **8**, 3979-3986 (2015).
140 Banzhaf-Strathmann, J. *et al.* MicroRNA-125b induces tau hyperphosphorylation and cognitive deficits in Alzheimer's disease. *EMBO J* **33**, 1667-1680, doi:10.15252/embj.201387576 (2014).
141 Keyse, S. M. Dual-specificity MAP kinase phosphatases (MKPs) and cancer. *Cancer Metastasis Rev* **27**, 253-261, doi:10.1007/s10555-008-9123-1 (2008).
142 Kidger, A. M. & Keyse, S. M. The regulation of oncogenic Ras/ERK signalling by dual-specificity mitogen activated protein kinase phosphatases (MKPs). *Semin Cell Dev Biol* **50**, 125-132, doi:10.1016/j.semcdb.2016.01.009 (2016).
143 Qu, X. *et al.* Identification, characterization, and functional study of the two novel human members of the semaphorin gene family. *The Journal of biological chemistry* **277**, 35574-35585, doi:10.1074/jbc.M206451200 (2002).
144 Yoshida, Y., Han, B., Mendelsohn, M. & Jessell, T. M. PlexinA1 signaling directs the segregation of proprioceptive sensory axons in the developing spinal cord. *Neuron* **52**, 775-788, doi:10.1016/j.neuron.2006.10.032 (2006).
145 Toyofuku, T. *et al.* Dual roles of Sema6D in cardiac morphogenesis through region-specific association of its receptor, Plexin-A1, with off-track and vascular endothelial growth factor receptor type 2. *Genes Dev* **18**, 435-447, doi:10.1101/gad.1167304 (2004).
146 Toyofuku, T. *et al.* Guidance of myocardial patterning in cardiac development by Sema6D reverse signalling. *Nat Cell Biol* **6**, 1204-1211, doi:10.1038/ncb1193 (2004).
147 Benyamin, B. *et al.* Childhood intelligence is heritable, highly polygenic and associated with FNBP1L. *Molecular psychiatry* **19**, 253-258, doi:10.1038/mp.2012.184 (2014).
148 Rietveld, C. A. *et al.* GWAS of 126,559 individuals identifies genetic variants associated with educational attainment. *Science* **340**, 1467-1471, doi:10.1126/science.1235488 (2013).
149 Okbay, A. *et al.* Genetic variants associated with subjective well-being, depressive symptoms, and neuroticism identified through genome-wide analyses. *Nature genetics* **48**, 624-633, doi:10.1038/ng.3552 (2016).
150 Cross-Disorder Group of the Psychiatric Genomics, C. Identification of risk loci with shared effects on five major psychiatric disorders: a genome-wide analysis. *Lancet* **381**, 1371-1379, doi:10.1016/S0140-6736(12)62129-1 (2013).

151 Speliotes, E. K. *et al.* Association analyses of 249,796 individuals reveal 18 new loci associated with body mass index. *Nature genetics* **42**, 937-948, doi:10.1038/ng.686 (2010).
152 Berndt, S. I. *et al.* Genome-wide meta-analysis identifies 11 new loci for anthropometric traits and provides insights into genetic architecture. *Nature genetics* **45**, 501-512, doi:10.1038/ng.2606 (2013).
153 Shungin, D. *et al.* New genetic loci link adipose and insulin biology to body fat distribution. *Nature* **518**, 187-196, doi:10.1038/nature14132 (2015).
154 Bradfield, J. P. *et al.* A genome-wide association meta-analysis identifies new childhood obesity loci. *Nature genetics* **44**, 526-531, doi:10.1038/ng.2247 (2012).
155 Morris, A. P. *et al.* Large-scale association analysis provides insights into the genetic architecture and pathophysiology of type 2 diabetes. *Nature genetics* **44**, 981-990, doi:10.1038/ng.2383 (2012).
156 Teslovich, T. M. *et al.* Biological, clinical and population relevance of 95 loci for blood lipids. *Nature* **466**, 707-713, doi:10.1038/nature09270 (2010).
157 Tobacco & Genetics, C. Genome-wide meta-analyses identify multiple loci associated with smoking behavior. *Nature genetics* **42**, 441-447, doi:10.1038/ng.571 (2010).
158 Patel, Y. M. *et al.* Novel Association of Genetic Markers Affecting CYP2A6 Activity and Lung Cancer Risk. *Cancer Res* **76**, 5768-5776, doi:10.1158/0008-5472.CAN-16-0446 (2016).
159 Wang, Y. *et al.* Rare variants of large effect in BRCA2 and CHEK2 affect risk of lung cancer. *Nature genetics* **46**, 736-741, doi:10.1038/ng.3002 (2014).
160 Pilling, L. C. *et al.* Human longevity is influenced by many genetic variants: evidence from 75,000 UK Biobank participants. *Aging (Albany NY)* **8**, 547-560, doi:10.18632/aging.100930 (2016).
161 Okada, Y. *et al.* Genetics of rheumatoid arthritis contributes to biology and drug discovery. *Nature* **506**, 376-381, doi:10.1038/nature12873 (2014).